STATIC AND DYNAMIC MECHANICAL PROPERTIES OF AMORPHOUS RECYCLED POLY-(ETHYLENE TEREPTHALATE)

By

ARJUN RAJAKUTTY

Bachelor of Engineering in Mechanical Engineering

Anna University

Chennai, Tamil Nadu, India

2010

Submitted to the Faculty of the
Graduate College of the
Oklahoma State University
in partial fulfillment of
the requirements for
the Degree of
MASTER OF SCIENCE
July, 2012

STATIC AND DYNAMIC MECHANICAL PROPERTIES OF AMORPHOUS RECYCLED POLY-(ETHYLENE TEREPTHALATE)

Thesis Approved:

Dr. Jay C. Hanan

Thesis Adviser

Dr. Ranji Vaidyanathan

Dr. Kaan Kalkan

Dr. Sheryl A. Tucker

Dean of the Graduate College

TABLE OF CONTENTS

Chapter Page

LIST OF TABLES

Table Page

LIST OF FIGURES

Figure Page

CHAPTER I

1. INTRODUCTION

Polymers are widely used in today's world for a variety of applications. Polymers are basically long chains of molecules either combined with the same or different groups. Approximately 281 million tons of polymers were used in 2010 [1]. The last 25 years has seen synthetic polymer materials being used as efficient packaging material compared to other materials [2].

1.1. Poly (ethylene Terephthalate)

With good thermal, physical, mechanical properties, and comparatively low cost; Poly (ethylene Terephthalate) (PET) has been among the most widely used of polymer materials. It is estimated that PET has an 8% share in the world market [3] and more than 90% of plastic bottles are made from PET [4].

PET finds major applications as material for fibers, injection molded parts, and most importantly for blow molded bottles. PET is made from Terephthalatic Acid and Ethylene Glycol through the poly-condensation reaction of the monomers. PET production depends upon the chemical reaction between the monomers which are produced by esterification reactions.

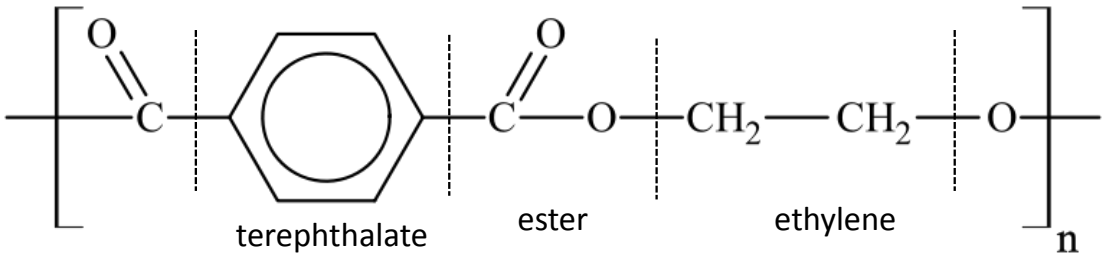

Figure 1: Poly (ethylene Terephthalate) molecular structure.[5]

The PET monomer contains two ester groups, one ethylene group and one terephthalate group as shown in Figure 1. PET is a linear thermoplastic that can be melted and molded on heating which makes it easier to reuse PET. Thermoset plastics on the other hand do not soften; they will break down at high temperatures. Thermoplastics have weak intermolecular forces whereas the thermosets have strong crosslinking between its bonds. Thermoset plastics are usually harder and more brittle [6]. The production of PET basically involves the esterification stage or trans-esterification stage where the raw materials Terephthalic Acid and Ethylene Glycol (esterification), and Dimethyl Terephthalate and Ethylene Glycol (trans-esterification) combine for the pre-polymerization reaction. This is followed by the melt condensation, which will provide a lower I.V. and low molecular weight resin. This process is followed by Solid State Polymerization (SSP), which is a very important technique of increasing the molecular weight and the intrinsic viscosity of the PET pellets before they are used for injection molding [7, 8]. It is very important to know the processing conditions for the polymers since they are highly sensitive to the molecular structure and macroscopic mechanical properties [9]. This will be discussed in detail, later in Section 1.1.2.

1.1.1 Properties of PET

The chemical composition and molecular structure plays an important role in determining the properties of PET and its copolymers. PET is generally considered as a strong, tough, flexible thermoplastic, which will crystallize and can be oriented into different molecular arrangements. Some common properties which favor usage of PET are its strength, temperature tolerance, wear resistance, toughness, low water absorbance, light weight, transparency i.e. clear amorphous state on cooling, wear resistance, corrosion resistance, design flexibility, chemical resistance, recyclability and long shelf life [2, 10]. PET after stretching still has properties of having a proper orientation, high stiffness, creep resistance, clarity, water vapor barrier, chemical and impact resistance. Several additives are mixed with PET to improve various properties before they are processed in manufacturing. While reducing the overall cost, fillers and modifiers are additives which improve the mechanical properties of polymers [11].

Among these properties, the molecular weight and the Intrinsic Viscosity (I.V.) are the two most common indicators, which will determine its end use. PET is made available in semi-crystalline pellet form to avoid sticking together during the drying process. In general, PET is classified based on its I.V. . The empirical expression which relates intrinsic viscosity to the molecular weight is given by Equation 1.1 which is known as the Mark Houwink equation.

$$[\eta]=K*M^{\alpha} \qquad (1.1)$$

Where η is the Intrinsic Viscosity (I.V.), M is the molecular weight, and K and 'α' are constants. The values of K and 'α' are determined based on different relationships

published in literature. The I.V. for PET usually ranges between 0.75 dL/g to 1.00 dL/g and the molecular weight is between 24000 g/mol to 36000 g/mol [2, 8, 9]. The end group is another important parameter, which affects PET properties. PET based polymers usually have both hydroxyl and carboxyl end groups. It is necessary to control these end groups in order to have the right processing. It is ensured that the level of carboxyl groups is around 30-40% of the total end group concentration for the melt processing stage and around 25-35% of the total end group concentration in the Solid State Polymerization (SSP) stage. These groups can help to catalyze hydrolysis reactions and can also benefit nucleation and crystallization. However if the content of carboxyl end groups is very high, it causes degradation which reduces the I.V. and molecular weight which in turn decreases the tensile strength thus weakening the container walls and may also cause blemishing [2]. To use PET for industrial applications, it is necessary for them to have good properties even after the processing stages. Usually for bottling applications; I.V. levels in the 0.72 dL/g -0.76 dL/g range are a required minimum. Similarly strapping requires around 0.74 dL/g I.V. and sheet applications require 0.7 dL/g I.V. [12]. The melt residence time should also be carefully chosen since it may decrease the I.V. if it is very high and based on this, the I.V. levels are also set for each application [13]. It is necessary to see that no external air comes into contact with the resin and affect its properties when it is residing inside the hopper.

Determining thermal properties such as glass transition temperature, crystallization and melting temperatures of PET will help tailor the processing methods as per the end use. Thermal properties are usually determined by Differential Scanning Calorimetery (DSC) experiments. A typical semi crystalline PET pellet is expected to

have a glass transition temperature of 80 ˚C, a crystallization temperature of around 160 ˚C and melting temperature around 250 ˚C [2].

Based on the PET synthesis methods, different grades of PET can be produced. Since PET is a semi-crystalline polymer, it will have both amorphous and crystalline phases and determining the amount of crystallinity in a polymer will help in estimating its mechanical behavior. Due to the presence of glycol linkages in PET, it can take two different rotational conformations, 'trans' which is the extended form and 'gauche', the relaxed form. Several studies have related trans conformations to crystalline phase and gauche formations to amorphous phase [8]. Figure 2 illustrates the behavior of a semi crystalline polymer upon stretching.

The crystallinity of PET is an important property to measure, as it influences the mechanical properties [14]. The initial crystallinity refers to the crystallinity level before the processing and the final crystallinity is the crystallinity level in the final product. The melt history, strain, glycol content, catalyst, stretching speed and temperature are all factors which affect the crystallinity. There might be a decrease in crystallinity from disruptions in structure whereas an increase would be from strain induced crystallization [8]. It was found that with increase in the initial crystallinity, the final crystallinity decreases [15]. Orientation of the molecules plays a role in affecting the final properties along with crystallinity. Tensile modulus and yield strength are directly related to the orientation and crystallinity in PET [8, 16, 17]. Usually hot fill bottles crystallize faster than cold fill bottles. The hot fill bottles need to have higher thermal stability to withstand the higher temperature applications [18].

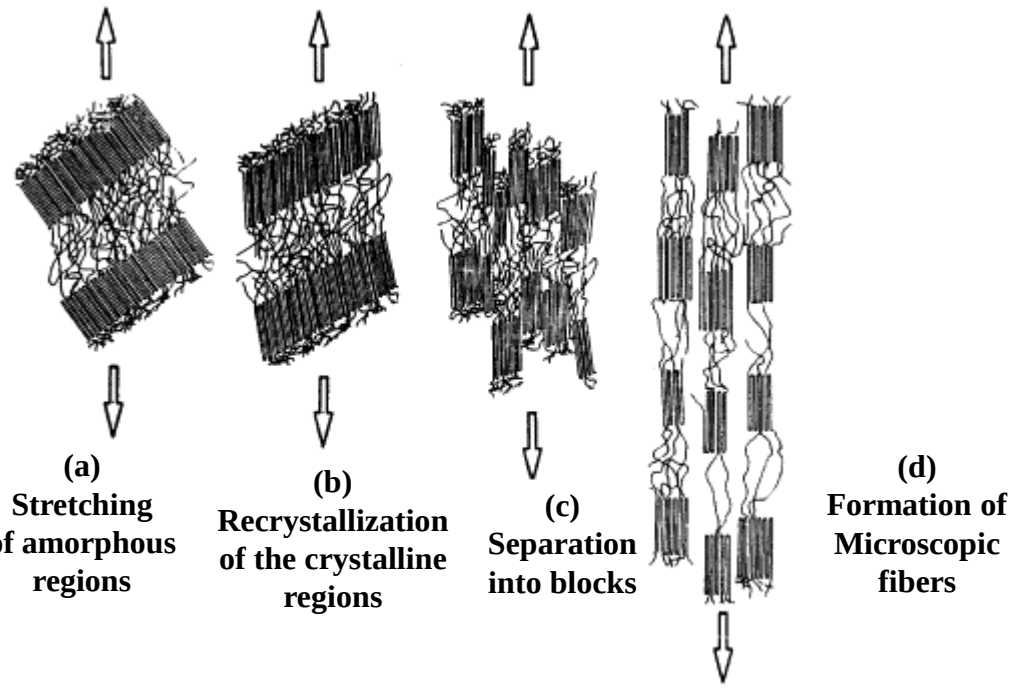

Figure 2: Plastic Deformation Stages of a Semi Crystalline Polymer [19].

1.1.2 Solid State Polymerization

Solid State Polymerization (SSP) is one of the most important steps in the processing of any polymer. SSP involves heating a polymer in an inert atmosphere or in vacuum at a temperature below the melting point of the material in order to increase the polymer chain length and to initiate and propagate the polymerization reactions [20, 21]. The polymerization reactions are governed by the temperature used, the pressure and the diffusion of particles from the inner to outer surface of the pellets. SSP is traditionally used to increase the molecular weight and the intrinsic viscosity of the polymer, which are very important factors affecting the mechanical properties. It is important to achieve an optimum molecular weight and intrinsic viscosity before the blow molding process begins in order to obtain the ideal blow molded article. Most of the reaction by-products

are removed by application of an inert gas and it is possible to attain the desired molecular weight and intrinsic viscosity by controlling the temperature and time used in the process. It is always preferred to have the temperature between the glass transition and melting temperatures.

The biggest advantages of SSP are that, it is a simple procedure, no complex equipment is required, heat damage can be controlled and is very less, it involves low operating temperatures and it is also environment friendly. Some of the disadvantages include solid state processability problems like formation of chunks and low reaction rates when compared to melt phase polymerization [22]. The solid state polymerization process involves treating the pellets after initial processing stages like drying and heat treatment. A vacuum pump is used to remove by-products and any signs of water in the pellets. After this step, nitrogen purging is carried out and temperature levels are maintained between glass transition and the melting temperatures. Also, the samples are taken from time to time to check its intrinsic viscosity and molecular weight; accordingly process parameters are adjusted to make optimum products [21]. SSP may be carried out in equipment like glass tubes, fluidized and fixed bed reactors, rotating flasks, tumbler dryers and liquid inert mediums, and vertical reactors with stirring blades. The primary advantage of using an inert gas during the SSP process is to remove the byproducts and promote oxidation without oxygen. The gas would help increase the nucleation sites and conversion rate [23]. Nitrogen, carbon dioxide, helium and steam are some of the commonly used gases in the SSP process.

Some important parameters affecting the SSP rate include the kinetics of the reaction, the diffusion of the reactive end groups and the interior and exterior diffusion of

the condensate with the mass surface [23-25]. The most important factor governing the SSP reaction is the temperature being used, since there should be chain growth but there should be no side reactions and sticking [22]. Other factors are the end group concentration regarded as the rate governing step since lower concentration of end groups will help increase the molecular weight [25], by-product diffusion and its dependence on particle size and inert gas flow rate. Crystallinity effects also influences SSP rates since it controls the reaction parameters and the extent of crystallization will help in ideal chain growth and packing [22].

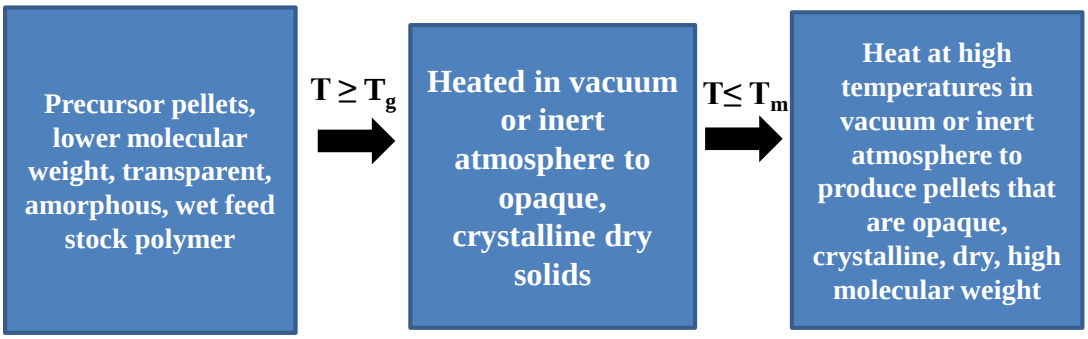

Figure 3: SSP Process [21].

Some of the disadvantages of SSP are overcome by using catalysts which help to increase reaction rates and prevent particles from sticking to each other. Katsikopoulos and Papaspyrides [26] observed that use of acid catalysts during solid state polyamidation of hexamethylenediammonium adipate increased reactions rates and also prevented agglomeration of particles. Karayannidis *et al.* [27] studied the effect of activated carbon black nanoparticles on solid state polymerization of PET. They observed that at temperatures of 210-220˚C, there were no significant effects, however at temperatures

close to 240˚C, there was an accelerated reaction and the I.V. value also increased. The carbon nanoparticles were found to disperse easily and acted as catalysts enhancing esterification. Agarwal *et al.* [28] studied influence of nitrogen sweep and high vacuum during SSP of PET. Their findings indicated that presence of vacuum increased the SSP reaction and there was also an increase in I.V. and molecular weight with temperature close to 270˚C. A new condensation reaction was observed with release of few by-products and it was found that using nitrogen decreased the speed of the SSP reaction but there was better control of the reaction and lesser degradation. Rodriguez *et al.* [29] looked into Solid State Polymerization and bulk crystalline behavior of PET. They found that high crystallinity levels gave rise to high molecular weights and that high reaction time and temperatures were needed to achieve such molecular weights. They also observed that using Antimony Trioxide increased the trans-esterification reaction rate. A lot of today's research is focused on studying role of catalysts in SSP. In 2005, Cruz and Zanin [30] investigated effects of Solid State polymerization process on recycled PET. While it was evident that the recycling process would cause a decline in molecular weight and essential mechanical properties, SSP was found to be an effective method of increasing the molecular weight of recycled PET and thus they concluded that this would help in developing efficient bottle to bottle recycling.

1.1.3 PET Bottle Manufacturing Process

The PET bottle manufacturing process is a highly automated process which operates at very high speed. The cycle time for the production of preforms from the injection molding machine and the production of bottles by the stretch-blow molding process is very low. The PET resin pellets are dried at temperatures around 165˚C in

order to reduce the moisture content in them before being used in the injection molding process. Drying time is usually around 6 hours. The resin is then melted and passed through the injection screw barrel. At this stage there is some shearing which occurs and may lead to breaking of the molecular chains. Now the molten PET is injected into the mold of the injection molding machine and then amorphous preforms are produced after cooling the preforms at high rates. It is important to note that there should be an optimum cycle time since a very low cycle time can result in the production of a defective part [8].

The injection molding and blow molding process can either be a single stage or a two stage process. In case of single stage process, the injection molding and blow molding is done on the same machine. After the production of the preforms, the preform temperature is adjusted to around 95-120˚C and the hot preform is placed in the mold and a stretch rod is inserted into it and it begins to stretch the preform. At the same time, high pressure air inflates the preform causing biaxial orientation. Now the bottle is obtained with a rigid neck as initiated in the injection molding process. In case of the two stage processing, the preforms are allowed to cool down and then reheated above the recrystallization temperature before the stretch blow molding process begins. The heated preforms are stretched and cold air is blown into the preforms to produce a biaxial orientation and finally the bottle is obtained. Care is taken to see that different sections of the preform are maintained at different temperatures and this is done by using heating lamps focused on different regions to ensure that the material distribution on the bottle takes place effectively [31].

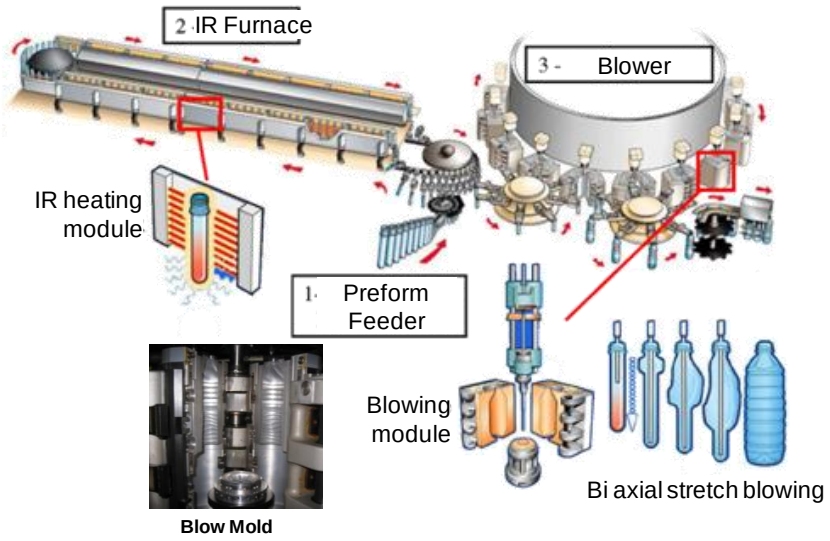

Figure 4: Injection Stretch Blow Molding Process.[32]

During this entire process, the orientation of the molecules will change in different stages. This is because different faces of the preform are subjected to different conditions, the outer regions will be at cold temperatures preserving the orientation, and the middle layers will have lower shear forces while the sub skin layers will have shear forces orienting molecules continuously [8]. It was found that along the thickness, there were three different layers in a slow crystallizing polymer; these were an amorphous skin layer, a crystalline intermediate layer and an amorphous core layer. The intermediate layer is produced as a result of shear forces [33]. The molecular orientation of the molecules changes in the injection molding process, the stretching process and the blowing process. This depends upon the cooling time and the mold temperature used [31]. Since the molecular orientation changes due to strain and the 'gauche' formations in the amorphous region transform to the 'trans' formations increasing the crystalline content, the process is called as strain induced crystallization [34]. During the blow molding process, the molecular chains will tend to relax and they try to resist the

crystallization. This is due to higher viscosity, which might produce excess crystallinity. The crystallinity will vary along the entire bottle and it also depends upon quality of material used apart from the processing techniques [8]. Sometimes, the final product may be reheated in order to increase its crystallinity. This is in the case of heat set resins. Such cases may arise due to increase in glass transition temperature with increase in the thermal stability of the product. [35].

1.2. Recycled PET

PET's major application in the packaging industry has been for plastic bottles. The need to reduce landfill consumption rates and drives to cut carbon emissions has brought about increased demand to recycle and reuse PET. PET is a thermoplastic basically meaning that it softens when heated and hardens again when it is cooled and hence it can be reused easily. PET is also among the most recycled polymers in the world. The first ever attempt at recycling PET was done in 1977 [36]. Over the years there has been an increase in PET recycling rates. In 2010, more than 1.5 billion pounds of PET bottles and containers were recycled and the recycling rate for PET in the United States reached 29%. Recycled PET (rPET) is used for applications in several areas like fiber for carpets, jackets, fillers, bottles, containers, films, sheets and strappings. Of the 1002 millions of pounds (MMlbs) rPET used in 2010, 70 % was used for fiber, sheet and film applications while 21% was used for food and beverage bottle applications [36].

It is estimated that around 4 % of the world's oil and gas production is used for production of plastic and another 3 % - 4 % is used in energy for their production. And most of these materials are being discarded within a year. Thus using plastics has not

been a sustainable option and recycling is more important than before especially keeping in mind the need to preserve and protect the environment [37]. From the PET that has been discarded in landfills, part of it goes to the reclaimers within the USA while the rest is purchased by exporters who send it to Asian countries where it is recycled and again reenters the USA in the form of pellets [36]. This is a cycle which keeps continuing unless recycling within the United States increases further. California is the single largest state in the USA handling PET recycling. Of the 395 million pounds of PET recycled in 2009, 56 million pounds was handled in California and the other 249 million pounds was exported [38]. Europe has a far higher recycling rate compared to the United States and this is attributed to the fact that their recovery system is much more systematic and advanced than in other parts of the world. In 2010, Europe had a combined recycling rate and energy recovery from plastic waste of 58 % [39]. The biggest driving factor for PET recycling has been its slow decomposition rate [40, 41]. Figure 5 shows the PET bottle recollection rates in the United States, the European Union, Brazil and Japan [42]. The European Union has the highest recycling efficiency. There are several factors which affect the PET recycling rate, these include the market demand, cheaper technologies, value addition and overall cost [41]. However, the process of bottle-to-bottle PET recycling may not be as easy as it seems since there is a need to ensure that the rPET has properties that are on par with virgin PET and also reduce contamination in PET.

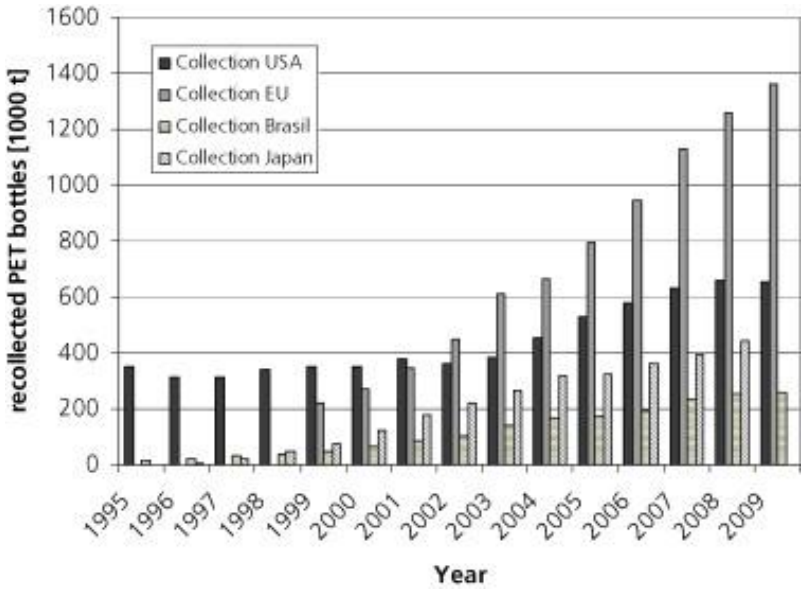

Figure 5: PET bottles recollection statistics for United State of America (USA), European Union (EU), Brazil and Japan.[42]

1.2.1 Recycled PET in the Market

With tones of PET being produced and used in the world every day, it is very important to recycle PET. However, there are some factors that influence the use of recycled PET (rPET) in the market the same manner virgin PET has been used. PET is a very valuable raw material (Market price of up to $1 /lb in 2011) and finding newer applications most importantly replacing traditional raw materials, metals and resins. rPET has a positive impact on the environment and reduces the impact on landfills, consumer waste, reduces emissions and helps in energy conservation. From a study by NgPlastics Corp. [43] , it was found that recycling PET reduced energy consumptions by 52.6 % and the recycling methods reduced carbon dioxide emissions by almost 54 %.

It is necessary to look at the concept of the 4R's; reduce, reuse, recycle and recover. The recovery part would primarily focus on energy. The concept of energy and

waste management needs to be constantly updated with advancement in technology and with more efforts to reach near zero wastage. The studies today are focused on the part of arriving at a stage where the gap between recycled and virgin resin usage has been closed significantly [37]. It would also be of greater significance to encourage bottle to bottle closed loop recycling as an efficient tool. Closed loop recycling involves using the material from used containers for new containers. However there are issues concerning the amount of content that can be reused and research is currently focused on processing techniques to increase amount of recyclable content that can be useful [44].

According to a study by Environmental Protection Agency (EPA), the energy required to produce products out of recycled plastic is 2/3 times lesser than that to produce products from virgin materials. A 23 % greenhouse gas reduction was reported in the plastic manufacturing process in 2010 [45]. The recycling of PET has resulted in a net reduction of emissions and energy usage based on comparison with manufacturing an equivalent amount of substance from virgin material, which consumed more energy and gave out more emissions [44]. One another very important factor, which would influence recycling of PET, would be the cost. Virgin plastics prices are influenced by the oil prices and the feedstock production. Since recovered plastic usually has properties lower than virgin material, the virgin material prices will directly impact the recovered plastic prices. But with higher oil prices also affecting the cost of collecting material, transportation and processing, recycling is being looked at as a more financially viable option today for several reasons [37]. Some important factors that might determine the introduction of rPET into the market would be producing the bottles and containers at conditions identical to virgin resins, using same cycle rates and process costs as virgin

resins, decontamination of the resin, storage ability identical to virgin resins, environmental concerns with respect to food grade applications, waste management, aesthetic appeal (yellowing), Acetaldehyde (AA) content and most importantly material properties [46].

PET is given a recycling code of "1" and is essentially among the most widely recycled polymer materials in the world. The chasing arrow symbol was used so that consumers would know that this material could be recycled. The recycling codes are assigned by the Society of Plastics Industry (SPI). The recycling codes are usually found at the bottom of the container.

1.2.1.1 Regulations on rPET

The United States Food and Drug Administration (USFDA) have set certain safety regulations with regard to using rPET for food applications. These are essential on transfer of contaminants to the foodstuff, using material not regulated for food contact and the presence of other material that may not comply with regulations. The FDA has set "Challenge Test" standards wherein all companies using rPET will have to achieve a level of removing contaminants from the material and see that the levels are negligible and do not harm consumers. A letter of non-objection will be issued to the company once it meets the FDA standards. Similarly there are regulations set by several European Union regulatory departments [47].

1.2.2 rPET in Composites

Besides having extensive applications in the packaging industry, rPET has also found applications in composite materials. Though polymer composites have been

around for a few years, using rPET in composite materials has been of interest only in the last decade. Rebeiz [48] was perhaps among the early researchers to investigate time-temperature properties of polymer concrete using rPET. rPET can be chemically modified to an unsaturated polyester which can be mixed with gravel and concrete to make polymer concrete (PC). This would enable reducing costs of PC products, while saving energy. White [49] investigated the properties of composite materials made from high lime fly ash and rPET and found that they had very good mechanical properties, low water absorption and low density. Ismail *et al.* [50] used rPET as fillers for natural rubber compounds and observed increase in the maximum torque, cure time, tensile modulus and an increase in the temperatures for Thermal degradation. Ronkay and Czigany [51] developed composites with rPET matrix and glass fibers and found them to have very high tensile and fracture toughness. Santos and Pezzin [52] investigated the properties of polypropylene reinforced with rPET fibers and concluded that using rPET in PP would improve its properties and offer better options for recycling. Bizarria *et al.* [53] studied the properties of rPET and organoclay nanocomposites which opened up a new field of application for rPET. Avila and Duarte [54] carried out a mechanical analysis on recycled PET/HDPE composites and found good performance for compression and machinability.

1.2.3 PET Recycling Processes

Traditionally there are two major processes used for recycling PET, they are chemical and mechanical recycling. Mechanical recycling is the most widely used method since its easier, faster and much more economical compared to chemical recycling.

The chemical recycling process involves depolymerization reactions into monomers or partial depolymerization into oligomers. Chemicals used in this process are water, methanol and ethylene glycol. The compounds arising from depolymerization reaction include terephthalic acid, dimethylterephthalate and bis-(hydroxyethyl)terephthalate [41]. This process of recycling PET is very costly, hence it is not considered as a viable option [55].

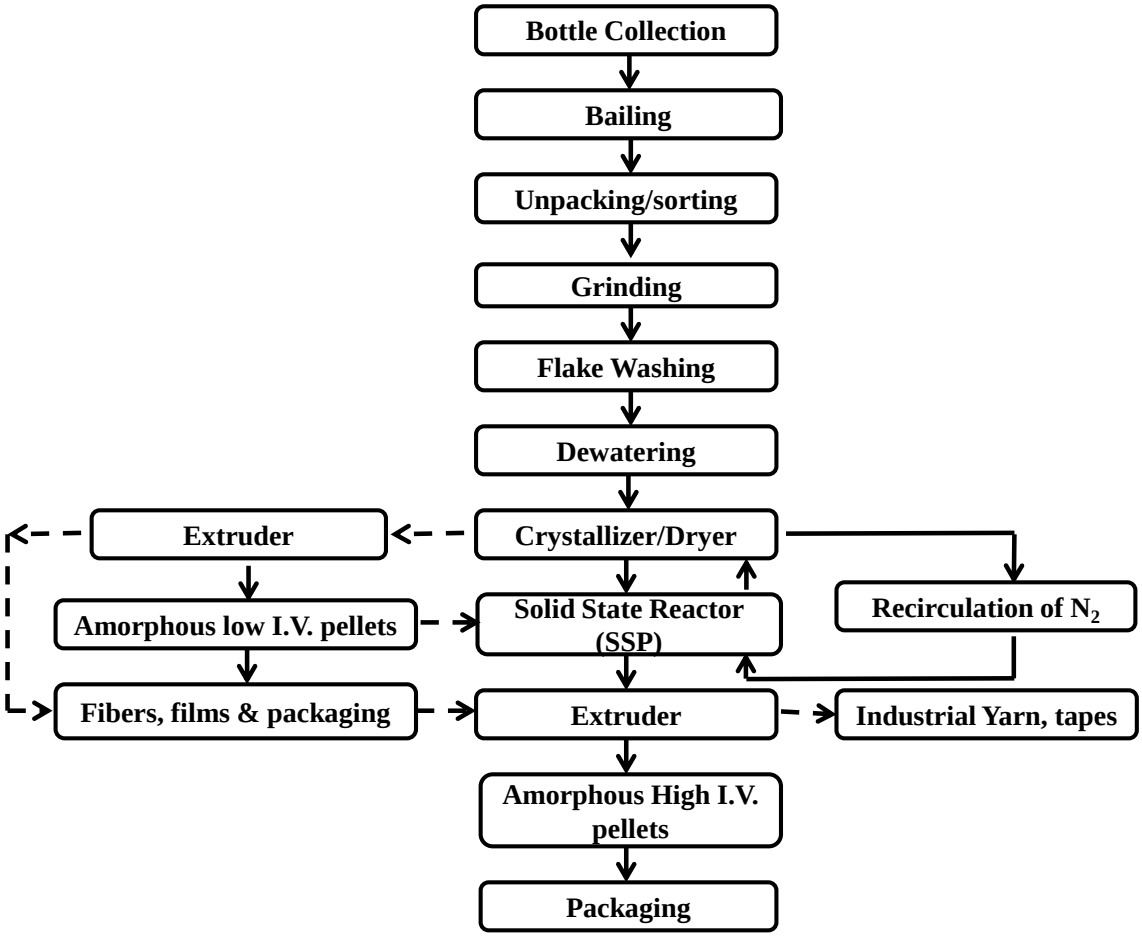

Figure 6: PET Recycling Process.[56]

The mechanical recycling process has several stages. Figure 6 gives an outline of the PET recycling process. The first stage involves collection of all bottles from curb

side or bottle recovery agencies from the government or private parties. These bottles are now compressed into compact bales and then made ready for shipment to various recycling agents. The first step at the recycling plant involves, unpacking all these bales and feeding the bottles into a bottle sorting section. Metal containers, PVC bottles, colored bottles, and glass containers are separated out. This is done either manually or with bottle sorting machines which are now advanced to work with lasers, infrared sensors, and color detection. The colorless PET bottles are now sent for size reduction and usually ground to flakes of around 8mm-10mm in size. The labels are also ground along with the bottles and they are later separated using pneumatic separators [56].

There are a large number of contaminants present in these flakes and they need to be removed. The flakes are washed with hot dilute alkaline water. This helps to remove the volatile and non-volatile contaminants on the surface since the surface gets hydrolyzed. The left over polyolefins from caps and labels are separated by floatation and rinsing the PET flakes with fresh water and spin drying them to remove moisture. These flakes can be directly sent to some manufactures for use in carpets, textiles and films [56]. Other methods to wash the flakes include washing with aqueous hot washing with 2 % Sodium Hydroxide (NaOH) solution and a detergent and then following up with cold wash. Also solvent washing can be done with tetrachloro ethylene (TCE) [41]. Several new super cleaning treatments have also been developed; these include high temperature treatments, inert gas treatments and surface treatments with nonhazardous chemicals. The super cleaning processes are also classified based on pellets and flakes [42].

Drying and conditioning is a very important step in the PET recycling process and this step helps in improving crystallinity and also in reducing the moisture levels. Usually drying conditions of around 140 ˚C -170 ˚C and a time of around 3 to 7 hours is considered optimum by manufacturers. No more than 50 ppm of water is to be present in the flakes [41]. The next step involves extrusion of the flakes into pellets or finished articles like fiber or films. The extrusion process produces granules but, due to contamination, these pellets have low molecular weight. They are acceptable for producing fibers, but need to be processed further to be used for bottling. The process of mechanical recycling of PET is advantageous due to the fact that it is environmentally friendly, requires lower investment, and is simple. The biggest disadvantage is that the process reduces the intrinsic viscosity and molecular weight of the resin pellet. The two most common degradation reactions of PET are hydrolysis and thermal degradation. The hydrolysis reaction leads to formation of carboxyl acid end groups and hydroxyl-ester end groups, while the thermal degradation reaction leads to the formation of carboxyl acid end groups and vinyl ester end groups [57]. Thermal degradation in PET usually begins to initiate at temperatures above 300 ˚C and takes full effect at 400 ˚C [58].

The presence of water and PVC enhances chain scission reactions. These hydrolysis reactions cause the formation of smaller chains with acid and hydroxyl groups. These degradation reactions give rise to byproducts which will end up acting as catalysts for degradation reactions and also suppress the molecular weight. Also they might increase the carboxyl content and decrease the thermal stability of PET [41]. In order to increase the IV and molecular weight, several new methods have been developed. One such method involves reprocessing under vacuum where all volatile substances and water

vapor are removed. Intensive drying systems with optimum temperatures are also being used [59]. There are also some stabilizers, usually metal based such as butyl tin mercaptide, antimony mercaptide and lead phthalate [60] added in order to reduce the contamination effects. Solid state polymerization is perhaps the most important processing step. As discussed earlier the pellets are heated to above their glass transition temperature and below their melting temperatures and over a period of time and with controlled temperature, this produces pellets with higher I.V. and molecular weight. Byproducts from SSP are removed quickly. The disadvantages of SSP include the slow speed and energy required for the process.

The mechanism of chain extension was first studied by Inata and Matsumura [61]. It is the process where a low molecular weight poly-functional material is reacted with PET hydroxyl and carboxyl groups in order to rejoin the broken chain resulting from PET chain scission mechanisms. They predicted that there were three types of reactions associated with the chain extension, a blocking reaction which involves a single molecule from the chain extender reacting with a molecule of PET, a coupling reaction where a molecule from chain extender joins with two PET chains and the third type would be no reaction at all. The chain extension process is affected by the end groups contents mainly the hydroxyl and carboxyl content as this would determine the increase or decrease in the molecular weight. It was generally found that an increase in carboxyl chain ends would increase the molecular weights. But it was also quoted that an equivalent amount of chain extension reactions should occur at the hydroxyl terminals of PET [62]. Cross linking reactions may also sometimes add to molecular weight where two radicals combine to increase the molecular weight [63]. The chain extenders are classified based

upon the PET functional end group they react with; this can be either hydroxyl end chain extenders or carboxyl end chain extenders. Some common types of chain extenders include diepoxides, bis-2-oxazolines and several other types of oxazolines. Chain extension was also found to increase the crystallinity in the samples [41].

Reactive extrusion is another process of improving properties of polymers and this is achieved by using an extruder as a reactor. It combines the extruder and reactor in one system. There are single screw and double screw extruder systems. One can adjust the die pressure, screw rotation rates, missing degree, residence time, heating rates, velocity of flow, viscosity and temperature to arrive at an optimum level for improving properties of PET [41].

1.2.4 rPET Decontamination

The process of recycling PET involves several stages. During these processing steps, the PET flakes or pellets are subjected to different temperatures and mechanical processing, which causes contamination, degradation and loss of properties. It is necessary to have high quality pellets and flakes in order to be considered for further use in commercial applications. Some of the common forms of contamination that is found in rPET flakes and pellets are explained in this section.

The most common acid contaminants found in rPET are acetic acid form poly vinyl acetate (PVA), rosin acid, abietic acid from adhesives, and hydrochloric acid from poly vinyl chloride (PVC) [41]. These acids usually end up causing chain scission reactions during the melt processing stage [55, 64, 65]. Water is another important contaminant and this causes reduction in the molecular weight via hydrolysis reactions.

It is recommended that the moisture content should be below 0.02 % in order to reduce the molecular weight reduction [55]. Coloring contaminations include those fragments from colored bottles or from labels. Improved processing techniques may reduce the level of removal of these contaminants [41]. Acetaldehyde is another contaminant which is a byproduct of PET degradation reactions. Stabilizers such as 4-aminobenzoic acid, diphenylamine and 4,5-dihydroxybenzoic acid are added to PET in order to minimize effects of acetaldehyde [66]. There may also be traces of pesticides, air borne contaminations, sand, fuel and detergents owing to use of PET in various environments [41].

Over the years, several methods have been devised in order to decontaminate rPET. Francis Schloss [67] developed a method of decontamination by steam distillation. The rPET flakes were reduced in size and steam distillation was performed at a temperature range from 150˚C-190˚C in order to remove the contaminants. The process was found to be very efficient in producing food grade rPET flakes for use in packaging material. Hayward and Deardurff [68] developed a method for optimization of rPET decontamination based on the accumulated thermal history. The method aimed at reducing the contamination that occurs in processing steps such as washing and drying. Common contaminants include pesticides, solvents, and hydrocarbons.

There is a specific thermal history associated with each stage of the processing and this data is analyzed in detail for optimization. It is important to meet the US Food and Drug Administration (FDA) regulations and thus the pellets or flakes should be free of contamination before they can be used for applications. The method also suggested that it was important that the drying temperature should be above the boiling point of

water but below the solid state temperature. Hayward *et al.* [69] suggested a method of decontamination of rPET through particle size reduction. This was suggested with an aim to reduce the contamination that occurred due to contaminants seeping through the polymer and matrix walls. They suggested that particle size should range from 0.005 inch to 0.1 inch in diameter. Hayward and Witham [70] published a method of treating r PET in order to reduce processing time and costs. This involved melting and thermally treating the rPET particles to avoid the repeated crushing, heat treatment and extrusion in order to achieve the particle size of 3/8 inches. Another method for recycling PET beverage bottles by treating with carbon dioxide via fluid extractions process was suggested by Al-Ghatta [71] in 1991. The method involved passing super critical Carbon dioxide through crushed bottles in order to remove contaminants.

1.2.5 PET Color Measurements

1.2.5.1 Introduction and Background of Color Systems

There are three major attributes to color: hue, chroma and value (lightness). When a color is described by these three attributes it makes it easier to be distinguished from others. Hue is related to how we perceive an object's color. Chroma depicts the dullness of a color, like how gray or pure it is. The luminous intensity of a color shows its degree or lightness or darkness. The first scale for measuring color was introduced in early 1905 by Albert H. Munsell. Three major things necessary to see a color are its source (illuminant), object (sample), and the observer (processor) [72]. The most widely accepted color measurement system today is given by the Internationale de l'Eclairge (translated as the International Commission on Illumination), which is the body responsible for photometry and colorimetry. They first developed a standardized system

to derive values for describing colors in 1931 [73]. The CIE color systems utilize three coordinates to locate a color in space, they are: “CIE XYZ”, “CIE L*a*b*” and “CIE L*C*h°”. The XYZ values are referred to as tristimulus values. These values however have limited use as color specifications because they correlate poorly with visual attributes. Y relates to lightness but X and Z do not relate to hue and chroma. Chromacity diagrams were developed with Yxy coordinate system where Y is the identifying value and xy is the coordinate system but it had limitations. Hence the CIELAB or CIE L*a*b* was developed in 1976 along with another system CIE L*C*h°. Instruments today have been developed to use any of these scales though most instruments use the CIELAB system. In the CIELAB system, the L* defines the lightness, a* denotes the red/green values and b* gives the yellow/blue values. The CIELAB color axis is shown below in the Figure 7.

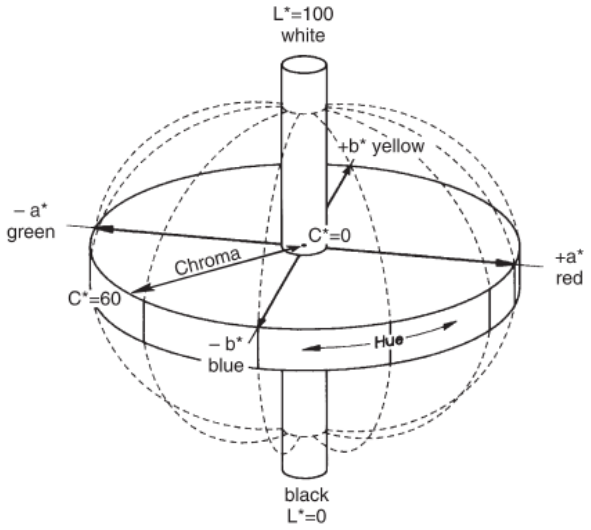

Figure 7: Three axis CIELAB representation.[72]

The ‘a*’ axis is from left to right and a shift in positive direction indicates increasing red, similarly for the b* axis, a shift in positive direction indicates yellowing.

Hence high b* values are related to yellowing effects [72]. Most equipment available in the market today is designed to give out the values of the essential parameters needed to calculate the yellowing index values, the percentage transmittance, absorbance and percentage reflectance and many more. The most commonly used color measuring instruments are Spectrophotometers and Tristimulus colorimeters.

1.2.5.2 Yellowing Definitions

For most color measurements in plastics, the degree of whiteness or yellowness are factors which are primarily studied. Whiteness is related to the quality of the substance and gives an indication of the impurities or defects [74]. Yellowness on the other hand may be related to scorching, soiling, and product degradation by light, chemical exposure and processing of the material [75]. Yellowness indices help to quantify these types of degradation with a single value [76]. ASTM has defined yellowness as "the attribute of color perception by which an object color is judged to depart from colorless or a preferred white towards yellow." Also their definition for Yellowness Index (YI) is given as "a number computed by a given procedure from calorimetric or spectrophotometric data that indicates the degree of departure of an object color from colorless or from a preferred white, towards yellow" [77].

1.2.5.3 Yellowing in PET

One of the primary reasons for yellowing in PET is because of the heat treatment procedures and the temperatures at which PET is processed, in particular, during the drying stage. Yellowing occurs because of oxidation and thermal degradation during this period. A slight yellowing in most cases cannot be ruled out while processing rPET.

However many industries today are working towards reducing the effect of yellowing which, over a period of time might increase sharply. While the yellowing effect makes it very easy to distinguish rPET during the recycling process and also while sorting, it is not considered beneficial otherwise. Phoenix Technologies suggests that dryer residence times should not exceed 8 hours to prevent yellowing of the resin [78].

CHAPTER II

2. STUDYING BEHAVIOR OF RECYCLED PET

2.1. Motivation

When PET is being used for packaging, it is subjected to different heating conditions, compression, severe shear, and tensile strain at high pressures and rates. Hence it is very important to study the properties of PET that would be relevant to its processing [79]. There are several concerns involving using recycled PET (rPET) along the same lines as virgin PET. Some questions to be answered;

- Does rPET have properties on par with virgin PET?
- Does rPET have properties that can allow for blow molding and production of bottles?
- Is rPET useful only for other non-bottling applications?

Apart from these, another factor in the packaging industry would be aesthetics, since on repeated processing, PET begins to yellow. Hence there is a need to study the color change effects in rPET.

The applications and mechanical behavior of rPET would need to be studied in order to come to a strong conclusion that rPET can indeed be considered for large scale applications and also to assert that its properties are similar to virgin PET or maybe in some cases even better. The behavior of PET in various heating conditions and the change in properties based on this treatment is also of interest. Studying the dynamic properties of rPET would help in understanding changes from recycling that might not be observed in static loading conditions. The effect of the differences in material properties on the structural performance of bottles is also be studied. Some other new parameters to be studied include friction from PET with an insight on industry applications. One important point to note is that rPET has typically been combined with other materials to create blends. It is thus important to study the differences in properties of PET and rPET blended.

2.2. Resin Ranking Parameters

There are a large number of PET resins available in the market classified based on their applications and properties. It is important to decide on the right resin to be used for the end applications. Hence there are several important resin ranking parameters. The most common resin ranking parameters include intrinsic viscosity and price per lb. Other parameters recently studied include: shear viscosity, energy savings, mechanical properties, and Molecular Weight. This study contrasts rPET to virgin PET based on these parameters so that even rPET can be ranked based on its performance [80]. This research also focusses on identifying various characterization techniques that help in arriving at the best indication and understanding of properties of rPET.

2.3. Mechanical and Thermal Properties

The mechanical and thermal properties of a polymer are important properties to determine the use. Typical thermal properties of interest for polymers are the glass transition temperature (T_g), the melting point, and the crystallization rate. These thermal properties help in deciding the optimum processing conditions. Young's modulus, yield strength, tensile strength, toughness, and the elongation at break are critical mechanical properties.

Robin *et al.* [81] compared properties of virgin and rPET before and after injection molding and found that rPET suffered thermo mechanical degradation during injection molding and exhibited a brittle behavior compared to virgin PET, which showed ductile behavior. On studying samples which had contaminants, it was found that the presence of impurities would decrease the intrinsic viscosity, molecular weight, and also affect crystallization. Samples from blow molded bottles were also studied and different thermal histories were observed. Galeski *et al.* [82] listed out characterization techniques that could be used for scrap poly(ethylene terephthalate) and recycled polymers in general. They characterized samples using several methods and suggested that using Thermogravimetric analysis (TGA), Differential Scanning Calorimetry (DSC), Fourier Transform Infrared Spectroscopy (FTIR), tensile testing, and rheometry to determine intrinsic viscosity and molecular weight were efficient methods to characterize samples. They have also concluded that if more than 50 ppm of contaminants like PVC were found in PET, it would make it worthless for advanced applications like film forming since it catalyzes the hydrolysis reactions and and reduces the strength of the material. A study carried out by Oromiehie and Mamizadeh [83] on a variety of PET and rPET samples

was aimed at recycling PET bottles and looking at means to improve their properties. It was found that the molecular weight and intrinsic viscosity decreased with increase in the content of rPET. Their inference was that this was due to shear degradation of the rPET. They also stressed the importance of the number of thermal cycles for recycling PET and its blends, since it would impact the crystallinity and mechanical properties. Zanin and Mancini [84] studied the effects of consecutive recycling steps on PET and its impact on mechanical properties and the changes in glass transition temperatures and crystallinity. They observed increases in the number of carboxyl end groups and the crystallinity. They also reported an increase in modulus but a decrease in ductility and impact resistance. Exposure to the atmosphere was also found to impact the properties.

Pattabiram *et al.* [85] studied the mechanical and thermal properties of rPET and their blends and used DSC and TGA for thermal analysis. They performed tensile tests at room temperature and elevated temperatures. Their findings showed differences in recrystallization behavior with regard to thermal properties and the strength of blends of rPET was lower than those of virgin PET. Kegal *et al.* [86] studied the effects of additives on processing and properties of rPET and found that additives like Titanium Dioxide (TiO_2) and Linear low-density polyethylene (LLDPE) wax in master batch compositions can improve processing capability and other properties of rPET. Peng *et al.* [87] studied effects of chain extenders on rPET blends and found that they improved mechanical properties significantly while broken polymer chains resulted in poor properties. Incarnato *et al.* [88] used pyromellitic dianhydride (PMDA) as a chain extender to successfully increase the molecular weight and the intrinsic viscosity of rPET. Some researchers also studied the effects of addition of glass fibers with rPET.

Kracalik *et al.* [89] studied the effects of mixing chopped glass fibers with PET in different proportions. They observed very good fiber dispersion of the fibers and also found that there was an increase in mechanical properties. A similar study was performed by Rezaeian *et al.* [90] using modified short glass fibers and they observed good mechanical properties and also shear thinning behavior at high shear rates and improved crystallinity. . Fraisse *et al.* [91] studied effects of PET blends with Polycarbonate (PC) and found that PC assisted the overall recycling process and also improved properties of rPET.

Intrinsic viscosity and molecular weight of the resin also help decide if one can use the resin for production. The temperature at which processing occurs is also important, since the I.V. will change with temperature and time. The I.V. change is directly proportional to temperature. After the SSP process, the intrinsic viscosity and molecular weight of the resin increases.

2.4. Dynamic Behavior of PET

Since PET is a time dependent polymer, it is very important to study the differences in properties over time. This would also help to explain its viscoelastic behavior better. While the behavior of PET at low strain rates and under static conditions has received attention widely over the years, its dynamic behavior needs to be studied to determine changes in properties due to processing conditions, manufacturing methods, and to understand the effect of higher strain rates. It would also help to relate to important dynamic events like drop tests, burst tests, transporting conditions and impact resistance. Traditionally drop tests are typically performed manually for quality assurance. Such

testing has been a time consuming process for introducing new designs. Finite Element Modeling is now being considered an effective tool to simulate drop tests. Also high strain rate testing is another useful indicator for a bottle's dynamic behavior [92]. Another aspect of studying dynamic properties relates to the process of stretch blow molding, which is a very important process in the production of PET bottles. It involves mechanical stretching of preforms at temperatures above its glass transition region. The processing stages with high temperature affects the degree of crystallinity and the physical properties of the polymer [93]. The preforms are heated to a high temperature of around 80 ˚C -120 ˚C, then stretched and blown in the mold to form the bottle. This process is very fast and today's industrial stretch rates are anywhere between 10 s^{-1} to 18 s^{-1}. The factors governing this process include the temperature, the speed of stretching, the draw rates, and the mode of deformation [94].

There have been numerous studies over the years on the effect of strain and drawing rates for PET. PET undergoes strain induced crystallization during stretching. This causes an increase in the stiffness, hardness, and provides better dimensional stability [95]. Ghanem and Porter [96] conducted solid state coextrusion on Poly ethylene Napthalate (PEN) near the Glass Transition Temperature (T_g) and studied Cold Crystallization Temperature (T_{cc}) effects. They concluded the percent crystallinity increased with increased draw rates and temperature. Guan *et al.* [97] however suggested that percent crystallinity reduced when the stretching temperature was increased in the biaxial stretching process. This was attributed to be the effect of thermal relaxation over chain orientation. These studies also arrived at conclusions that when the deformation was slow, crystallization effects were also very slow owing to molecular relaxation.

Buckley *et al.* [98] performed experiments on PET films at strain rates varying from 1 s^{-1} to 16 s^{-1} and found that the stress increased with strain rate, the hardening behavior was also dependent on temperature, and that it decreased with increasing temperature. Salem [99] suggested that crystallinity increased rapidly under high stress from his studies on drawing PET at strain rates from 0.01 s^{-1} to 2.1 s^{-1} and concluded that when the strain rate decreased the crystallinity also decreased. Morrison *et al.* [100] studied the mechanism of stress cracking for PET bottles and found that stress cracking was affected by the hardness of water and methods to prevent this would depend on water hardness and controlling alkalinity. Zaroulis and Boyce [101] performed experiments on PET at strain rates varying from 0.005 s^{-1} to 5 s^{-1} and observed a drop in modulus and yield stress with temperature. The DSC results on deformed and undeformed samples showed that cold the crystallization temperature decreased with strain and this was more prominent at higher temperatures. Boyce and Llana [95] observed that there was an increase in crystallinity with increasing strain rates and decreasing deformation temperatures. In their study on PET samples at strain rates varying from 0.005 s^{-1} to 2 s^{-1} over a temperature range of 90˚C to 105˚C. A more recent study by Menary *et al.* [94] on biaxial deformation in PET during stretch blow molding indicated that at very high strain rates, heat generated in the material owing to adiabatic heating would reduce strain hardening and could be related to crystallization. They observed that, at strain rates less than 8 s^{-1}, the stress required to stretch the material increased with decreasing temperature, increasing strain rate and molecular weight. At higher strain rates, the strain hardening reduced. They also observed differences in the curves based on orientation and crystallinity that was induced due to the stretching at high rate. Mahendrasingam *et*

al. [93] suggested the possibility of the existence of a transient structure as a precursor for strain induced crystallization. This was inferred from an increase in intensity of diffraction peaks related to crystallization.

Jabarin [102] made an interesting conclusion from his study that when stretching occurs at high speeds, there was a high degree of crystallinity and that stretching force or stress was not a significant factor in predicting crystallinity. Chaari *et al.* [103] investigated crystallization in PET using X-ray diffraction and they found that crystallinity was not significant at low strain rates, while for intermediate strain rates, crystallization occurred during the deformation process and for high rates, crystallization started right at the drawing stage and continued even after deformation. Gorlier *et al.* [104] also suggested that crystallization occurs first in the initial stage of deformation and actual crystallization occurs at relaxation steps later in the deformation process. All these studies indicated that an increase in strain rate would definitely impact crystallinity in PET as well as rPET and may cause changes in the values of some essential mechanical properties. The crystallinity is also dependent on the temperature at which the deformation is occurring.

2.4.1. Modeling for Dynamic Behavior

A major part of studying the dynamic behavior of PET would be to obtain mathematical models and other parameters that can be used for Finite Element Modeling (FEM) of the dynamic testing procedures such as drop tests, feel tests, and top load testing. In addition to Finite Element Modeling, these mathematical models would be useful to predict the dynamic properties of polymers for strain rates which were not tested

as well as for higher strain rates. Several models are available to study this behavior but it requires stress-strain data over a wide range of strain rates. Using FEM to model and simulate dynamic behavior will save time.

PET is known to exhibit viscoelastic behavior. For an isotropic material, the stress-strain relationship is linear in the low strain range and there is nonlinear plastic deformation for larger strain values. The linear portion is related to the Young's modulus, yield strength, and proportionality limit while the nonlinear deformation is related to strain hardening where there is very little change in the stress over a large strain zone. Learning about the strain behavior is necessary to study dynamic behavior of PET [92]. Most plastics exhibit behavior which can be classified either as viscoelastic or non-linear viscoelastic and the transition between the elastic-plastic zones is a very important region to study. It is difficult to obtain data over a wide range of strain rates owing to machine capability and accuracy of data at very high strain rates. Generally servo hydraulic machines and powerful extensometers can provide near accurate information for strain rates up to $1s^{-1}$. However, compliance corrections and errors need to be taken into account. Using mathematical models to study the strain behavior is very advantageous since it would minimize data requirement and allow prediction of material properties up to a certain limit. The effect of time and temperature would need to be studied in detail to predict behavior for higher strain rates. Read and Dean [105] explained the importance of using mathematical models to study the behavior of plastics under impact. They studied propylene-ethylene over a range of strain rates and observed changes in poisson's ratio and also stress-strain curves. They used the Eyring equation [106] in its simple form to model the rate dependent behavior.

$$\sigma_{y=} A+B \log \dot{\varepsilon}_p \quad (2.1)$$

Where A and B are temperature dependent parameters, $\dot{\varepsilon}_p$ is the strain rate and σ_y is the peak stress during a tensile test. Whereas for the strain hardening behavior, they developed a numerical function and fitted the values according to Equation 2.2.

$$\sigma = [\sigma_o + (\sigma_f - \sigma_o)(1-\exp-(\varepsilon_p/\varepsilon_{ps})^{\beta})](1-q\varepsilon_p) \quad (2.2)$$

Where, σ_o is the first yield stress, σ_f is the initial flow stress, ε_{ps} is the parameter representing the mean value of strain between the initial and flow stress. The parameter β affects the width of that range and q describes the decrease in stress with strain. They observed good correlation of experimental and calculated values.

One of the other most common models used to model strain behavior is the Cowper Symonds Model for yield stress;

$$\sigma_y/\sigma_{yo} = 1 + (\frac{\dot{\varepsilon}}{D})^{(1/p)} \quad (2.3)$$

Where σ_y is the yield stress, σ_{yo} is the initial yield stress, $\dot{\varepsilon}$ is the strain rate and D and p are constants from curve fitting the experimental data [92].

M. Abunawas [92] used n-power functions and the Cowper-Symonds equation to explain the stress strain relationship of PET over several strain rates and develop a suitable mathematical model for FEA drop test analysis. Q. Li *et al.* [107] developed a rate dependent constitutive model of PET for dynamic analysis and found increases in yield strength values with increasing strain rates. They suggested an improved model based on the Cowper-Symonds model for dynamic analysis. This model could be incorporated in performing Finite Element Analysis for impact resistance of bottles.

They also observed that the true stress values and the yield strength values increased with strain rate and thus strain rate has a significant effect on strain hardening behavior. The Cowper Symonds model is used to model for yield strength and has been used by researchers for low strain rates. Further the model is based on true stress and strain values.

2.5. PET Yellowing and Degradation

One major problem in using rPET is the yellowing imparted due to processing and recycling methods. This is a drawback in terms of aesthetic appeal. To minimize yellowing, optimum drying temperature and drying time must be used. Also coloring agents can be added to mitigate the yellow color. It is also a point to note that different types of rPET resins will have different levels of yellowness. Hence, in order to use the best resin that would cause the minimum yellowing, it is necessary to know the yellowness index values in different samples. The yellowness index would provide a good indicator of the color imparted in the samples; other parameters would include the percentage transmission and absorption for various types of samples and then compare the differences to arrive at best choice of resins and a final product that is attractive to the consumer.

The Waste & Resources Action Program (WRAP), a United Kingdom based organization developed a report along with Closed Loop Recycling, a leading recycling company in the United Kingdom (UK) which recycles High Density Polyethylene (HDPE) and PET into food grade rPET and rHDPE. They performed a detailed study on samples from “Marks & Spencer” and “Boots” and developed a report on feasibility of

using rPET in large scale packaging. Closed Loop Recycling used rPET mostly in their packaging and found that the yellowing did not hamper their packaging process in particular for thermoform packaging. The yellowing was significant in case of blow molded plastic bottles at the neck region but not significant in other portions of the bottle. Specialists from Vitembal and Reynolds believed that yellowing would not be an obstacle to the use of rPET. According to Closed Loop Recycling, they had fresh blended material dried for 6 hours and no yellowing effects were visible after blow molding. This indicated that having a proper drying period could reduce the yellowing. They also confirmed that though slight yellowing was visible in bottles which had 30% rPET in them, there was no unusual shrinkage or molding defects observed. Yellowing was more significant in 70% rPET stock. All products with different percentages of rPET in them were studied for 30 days and standard tests such as cap compatibility, stress cracking, yellowing effects, drop testing, and formulation stability were performed and observations revealed that that yellowing was not as significant as expected. All studies to measure yellowness were done through the London Metropolitan Polymer. They are in the process of studying this behavior further to come to a conclusion as to what should be an acceptable yellowness level [47]. A more recent report was released by the Union of European Beverages Association (UNESDA) and the European Federation of Bottled Waters (EFBW). The report listed out a design guide for PET bottle recyclability. They suggested that though some colorants can be used in order to mitigate the yellowing that occurs in rPET, it is necessary that these additions should be controlled or they may lead to other colors showing up. Also it was necessary to keep track of additives for barrier properties as these may also cause yellowing. The report also listed out procedures to

measure the yellowing index for PET, as prescribed by PET Container Recycling Europe (PETCORE) [108, 109].

In 2009, Singh *et al*. [110] studied methods to determine rPET content in PET sheets. They studied sheets with varying percentages of virgin PET and rPET. Ultra Violet Visible Light Spectroscopy was performed to determine the light transmission in sheets. For color measurements, a Hunter Lab LabScan XE colorimeter was used, and measurements were converted by the instrument to L*a*b* color scale values and the net color energy difference was calculated. It was found that the presence of rPET in sheets indicated a more green and yellow color in measurements with high b* values. Their inference was that during PET processing, the carboxyl end groups which are formed undergo oxidation and may be a reason for yellowing. Similarly Mortlock *et al*. [111] carried out a study to identify the luminescent species contributing to the yellowing of PET on degradation. They studied changes in the luminescence of PET degraded in the absence and presence of oxygen at different melt temperatures. It was found that species like hydroxylated terephthalate units, quinone and stilbene species arising from oxidation reactions contributed to yellowing. Fluorescence and phosphorence excitations were recorded on PET solutions using a Perkin-Elmer spectrometer.

Packer and James [112] studied the effect of PET process reaction time and determined that intermediate products formed during processing may lead to yellowing. This is mainly due to formation of Diethylene Glycol (DEG) end groups and the high temperature treatment stage where rapid yellowing occurs. This occurs at the polycondensation stage when reaction temperature is highest and molecular weight increases, leading to the formation of byproducts by polymer degradation. Measurements

were made using a Milton Roy Color Scan and values of a*, b* and L were noted. Fechine *et al*. [113] studied structural changes in PET due to photo degradation. Film samples were exposed for a long period under fluorescent lamps and after investigation, DSC data showed that exposed samples had a cold crystallization peak arising due to release of molecules into amorphous regions causing arrangement into crystalline phases. The value of b* was found to increase with total processing time and also with the processing temperature used [114].

It was also observed from X-ray analysis that crystalline orientation was lost and structural changes were significantly visible. Paci and Mantia [65] studied the competition between degradation and chain extension during processing of reclaiming PET. They said that apart from hydrolytic chain scission, which is the primary cause for PET degradation, repeated processing may induce some chemical reactions which can increase the polymer mass but may end up degrading the PET by forming other smaller by products. They found that among all degradation mechanisms, the ones due to air oxidation were most prominent. Hence it was necessary to have less humid conditions and proper drying in the processing steps. Spinace and Paoli characterized PET after multiple processing cycles and found that yellowing in PET increased with processing cycles. The PET first changes color from transparent to yellow and slowly degrades to darker colors. These changes were brought about by formation of carboxylic end groups which attribute to the degradation as well as due to chain scission which led to formation of chromophoric substances which absorb light near UV and visible range and slowly makes the material become opaque. This is because of a decrease in chain length which improves chain packing, increasing the crystallinity and crystal size. Mortlock *et al*.

[115] characterized species responsible for yellowing in melt degraded PET. This was mainly due to thermal oxidative degradation and formation of quinone.

2.6. Friction

There are a number of processes such as injection molding, stretch-blow molding, capping, labeling, packing and stacking involved in a bottling plant. During these processes, preforms and the bottles are transported between machines and stations by means of air conveyors, transfer fingers, or belt conveyors. With increases in the speed of operations, and the transportation between the different stations, the surface behavior for the preforms and bottles becomes increasingly important. There are issues related to bottle handling like the conveyor may get jammed from a bottle partially falling off, tripping in the rails, or bottles sticking to each other. From observations at the plant level concerning the motion of preforms or bottles after resin changes, changes in friction (Figure 8) are hypothesized to be a major factor causing these problems.

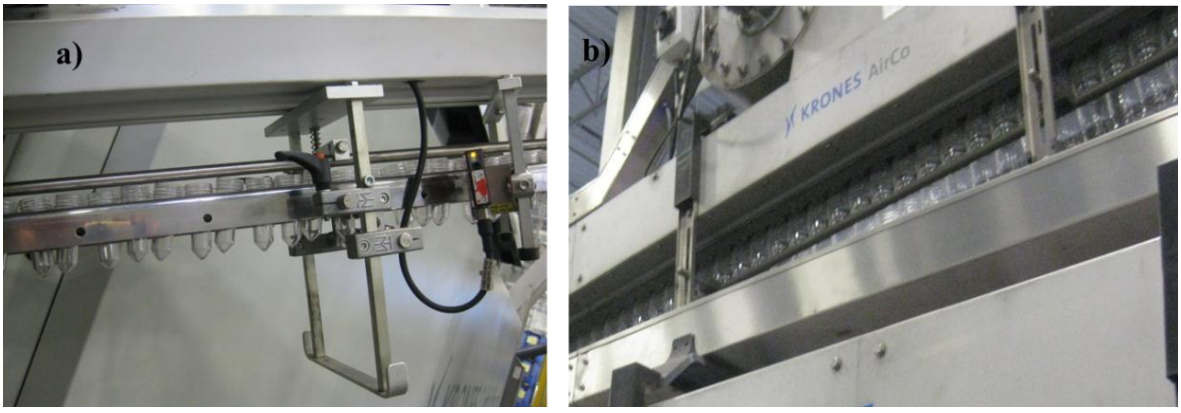

Figure 8: a) Preforms passing through conveyor to the blow molding machine b) Bottles passing through air conveyor towards filling stations.

Hence it would be informative to measure the friction between bottles or preforms. If significantly different between resins, this could be correlated to performance changes on the manufacturing line. Normally the coefficient of friction is a good indicator of the frictional forces. Several bottling companies are in the process of finding their own solutions to this problem. The American Society for Testing and Materials (ASTM) has set standards for measuring friction between thin plastic films; however no methods have been published for measurement between bottles. Contact locations on the bottles are limited based on its design and these would be areas which need to be studied in detail. It would also be interesting to study if the type of resin affects the frictional forces and if processing conditions play a role in changing these values. Here the focus is on any negative performance changes anticipated from increased friction by using rPET. As a new area of investigation, a new method of testing is also being developed and will be described in the methods section.

2.7. Finite Element Analysis (FEA)

There are several aspects of design and testing involved in production and testing of PET bottles. The dynamic behavior of PET needs to be studied in detail and some of the testing procedures are very time consuming and may not yield the accurate results due to errors in the test procedures and due to compliance. Using Finite Element Analysis to solve complex engineering problems and providing near accurate results would be the best option to save time and reduce costs. Finite element analysis finds applications in various fields where it solves engineering problems with a mathematical approach using a series of differential and integral equations. The finite element method (FEM) works on the principle of breaking up a larger continuum problem into several discrete problems.

The equations are generated based on boundary conditions, the loading conditions, and the stiffness matrix so generated and these would be solved to get required results [31]. Advanced software available today can solve these problems more efficiently and at faster speeds with a variety of applications and features.

The finite element method has played a significant role for research and analysis in the packaging industry over the years. Some of the core factors which the FEM addresses include machine design and plant design. FEM is well suited to the linear elastic materials involved. Recently FEM has been extended to aid in bottle design [31] and structural analysis. Reduction of costs is an important concern for any industry and with regard to the bottling industry, light weighting the bottles means reduction of material costs, but this would impact bottle design. This needs to be studied and FEA is a useful tool in such cases. When the bottles are stacked up and waiting for transportation in the bottling plant, they are subjected to different loading conditions, and again this behavior would need to be studied. Various conditions where FEA is used for bottles would be the top load, pressure, vacuum, hydrostatic deformation, squeeze test, drop test, conveyance, vending, seal closure, blow molding, and optimization of process [116].

An optimum bottle design would involve making a bottle which can withstand a considerable amount of top load. Bottle leaning and feel test for a bottle, which is done to measure the hoop stress effects is also of importance. Dynamic behavior of PET would be modeled with help of mathematical models and using FEM as an effective tool. To summarize, FEM finds applications in the packaging industry for modeling polymer behavior, for preform optimization, to simulate the stretch blow molding process, and most importantly for the structural performance [31]. One very important part of studying

the polymer behavior over various loading conditions would be to obtain the essential properties that are used as the input for the finite element procedure. Several mathematical models have been developed with regard to strain rate and loading behavior patterns on polymers. Colak and Dusunceli [117] studied the viscoelastic and viscoplastic behavior of HDPE and developed a model using viscoplasticity theory. Vigny *et al.* [118] studied the viscoplastic behavior of amorphous PET during plane strain tensile stretching process.

Preform optimization is essential for the bottle making process since the preform design and properties will impact the quality of the final bottle that is being blown. The heating of the preform is the most important stage since the temperature distribution over the preform will affect the distribution of material in the final blown bottle. Finite element simulations will help to understand the relation of preform thickness, material thinning and final wall thickness of the bottle [119]. Researchers have studied the process of blow molding in detail over the last decade. The amount of pressurized air used, the mold design, and the stretching required are essential parameters which will govern the properties and material distribution in the final bottle. Bagherzadeh *et al.* [120] used finite element simulation to perform a parameter study of the stretch blow molding process. A hyper elastic constitutive behavior was used for the simulations based on strain rate and temperatures. Menary *et al.* [121] validated the injection stretch blow molding process through free blow trials. They simulated the process using ABAQUS via two approaches; one was using free blow and the other was constant mass flow rate which gave them better results.

The final design and structural performance of the bottle is the most important aspect to be studied after preform optimization, blow molding simulation and material property determination [31]. Demirel and Daver [122] studied the effect of bottle base geometry on the properties of the PET bottles and the variations in top load, burst strength, and thermal stability. Van Dijk *et al.* [123] studied lateral deformation of plastic bottles with an emphasis on changing the vacuum resistance of a bottle for different top loads. Rowson *et al.* [124] used finite element analysis to model capping for 28 mm beverage bottles and analyzed possible defects under different loading conditions. Sumit Mukherjee [125] used an analytical approach to study top load and side load performance for oval containers. He observed that heating the preform played a very crucial role in the final material distribution and properties of the bottles. Preferential heating by changing lamp spacing based on design changes showed higher top load performance than those which used non preferential heating where common lamp spacing was used. We observe that structural performance of bottles has not received as much importance as it actually requires from researchers. The leaning of bottles, top load, and hoop strength are parameters to be studied in detail during the packing, storing and transportation of bottles. The effect of changing the material properties based on the type of resin used is also an important aspect to be studied using FEM.

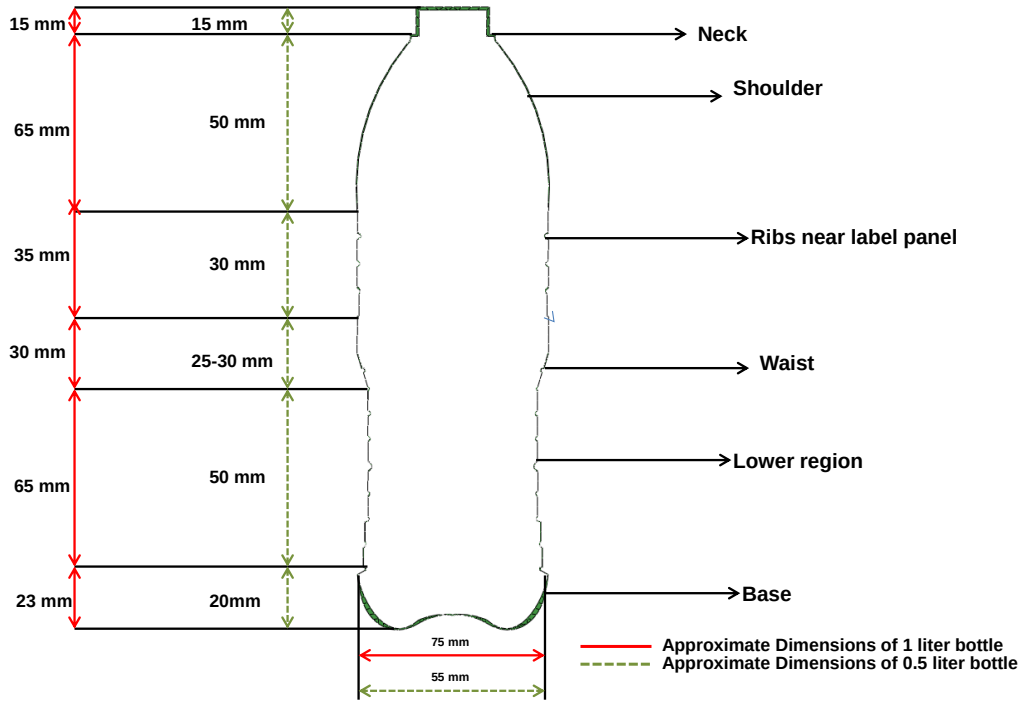

Figure 9: Bottle features and dimensions. [31]

It is evident from the literature [81-91] that the quasi-static properties of rPET have been studied in the past, but its dynamic behavior (at high strain rates) has not been studied. Additionally, the samples used were processed on lab scale which differs from the actual process. This work aims to answer those unanswered questions with respect to the use of rPET for large scale industrial processes. Yellowing in PET has been an issue for several years and finding ways to reduce it has been the focus of industry today. Besides studying the mechanical and thermal properties, understanding and correlating the mechanical behavior of the preforms as well as end product for different conditions would give broader range to compare rPET with virgin PET. The debate on how efficient rPET actually is with respect to energy savings and reducing the impact on environment is also to be validated.

CHAPTER III

3. MATERIALS AND METHODS

The materials and methods used in this research were selected in order to obtain data that can be correlated to several real time industrial processes. Further the samples used in this study were directly obtained from the industry scale machines such as injection molding rather than lab scale compression molding. This helps assure results relevant to industrial conditions. Several fixtures and new tests have been developed by the research team. Since there was no standard method for tensile testing of injection molding PET, a new fixture was designed and used [8]. Similarly fixtures were designed for hoop strength measurements [31], and friction tests [126]. A new method of CAD model generation using 3D scanning was used to generate models for input into FEM Analysis [31].

3.1. Materials

A large number of samples were required for the various tests performed in this study. Pellet samples were used for Differential Scanning Calorimetry (DSC) experiments. The rPET resin pellet had an I.V. of 0.76±0.02 dL/g and the virgin PET resin R_1 pellet had an I.V. of 0.76±0.02 dL/g.

The tensile preform samples were collected from a Husky HyPET 90 injection molding machine. The production preform samples were collected from a Husky HyPET 500 injection molding machine. Weight fractions of 100% virgin PET (R_1 resin with I.V. 0.76±0.02), 50% rPET (50% virgin PET R_1), and 100% rPET were used in this study. A 20% rPET (80 % virgin PET R_2 with I.V. 0.75±0.02 dL/g) preform sample was used in color measurements. The bottles used for friction testing and hoop strength measurements were all 0.5 L bottles, and the resin types were 20% rPET, virgin PET resins R_2 and R_1. The bottles were obtained from industrial blow molding machines operating at stretching rates of 12 to 18s^{-1}. The pellet samples were obtained in semi crystalline form, the preform samples were amorphous in nature and the bottles were of semi crystalline nature. The following characterization and test methods were used to determine the properties of the resins.

- Tensile testing
- Rheometry
- Differential Scanning Calorimetry (DSC)
- Color measurements
- Friction test
- Wall thickness measurements
- Hoop strength measurement (feel test)
- Top load test
- Density Measurements
- 3D scanning and model generation
- Finite Element Analysis (FEA)

3.2. Mechanical Testing

Mechanical Testing includes methods of determining properties such as the Young's modulus, tensile strength, yield strength, toughness, and percentage elongation till failure. Usually mechanical testing techniques include tensile testing, compression testing, fatigue testing, and nano-indentation. Tensile testing is well understood and gives bulk material properties, and hence it was chosen to determine the mechanical properties [8].

3.2.1. Tensile Testing

The tensile preform samples were tested on an INSTRON 5582 universal testing machine. The preform and its cross section CAD model are shown in Figure 10. The tensile preforms are designed with an extra bulged portion at the gate to be cut off in order to accommodate the fixture for tensile testing. Tensile testing was performed following ASTM D638 with an extension rate of 5 mm/min. Based on ASTM D638 "Standard Test Method for Tensile Properties of Plastics", the preform samples can be considered a rigid tube [127].

Figure 10: PET tensile preform sample and cross sectional view of CAD model.

3.2.2. Fixture Design

Normal preform geometry is such that it cannot be directly used for tensile testing in the INSTRON machine using standard grips. However, injection molding is one of the most consistent steps in the bottle manufacturing process. Preforms typically have less than 1% variation across millions of samples, which make them a good choice for testing. However, material testing benefits from testing on simple geometries. Hence it was necessary to design a custom fixture that would accommodate this particular preform. The present fixture design is a modification to an earlier design by Dr. Hanan as presented in S. Bandla's thesis [8]. The design of the tensile preform is well adapted for mechanical property testing. Several important modifications were done to this fixture, and the numbers of parts were reduced. The top portion of the fixture was designed in such a way that the shoulder of the preform would serve as a support on with the tapered portion near the neck providing a tight grip similar to "dog bone" tensile specimens. These "tensile" preforms have a gage length defined by the thin wall tube between the lower shelf where the pin rests and the upper shoulder below the finish. The final fixture design (Figure 11) consists of four major parts including the preform.

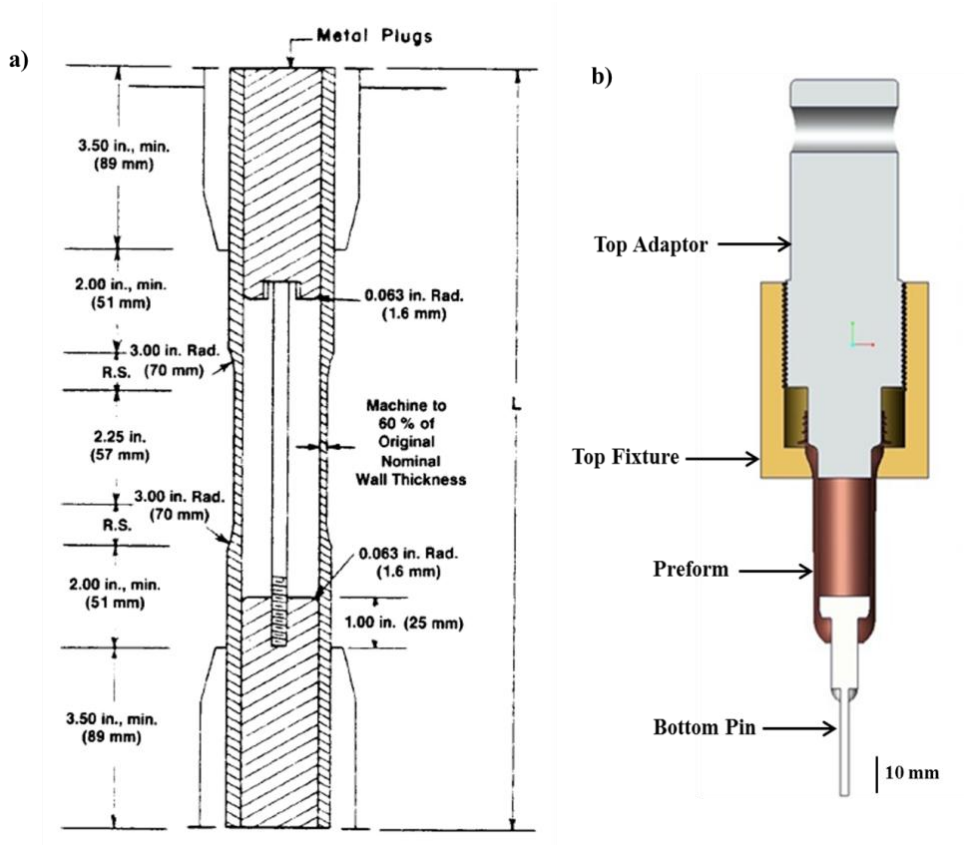

Figure 11: a) ASTM D638 Standard Test Setup Specifications[127] b) Cross Sectional CAD Model of Custom Fixture.

The top adaptor connects to the top platen of the tensile testing machine. This top adaptor screws into the top fixture part through which the preform drops inside and is held snug. Before dropping the preform into the top fixture, the nipple around the gate of the preform should be cut off and the bottom pin dropped into it. The bottom pin is held by the bottom grip of the INSTRON machine. All parts of the fixture were made of Stainless Steel (SS 304). The design of the fixture was made to have compatibility with the ASTM D638 test standards (Figure 11).

3.2.3. Tensile Testing Procedure

The preform samples for each type of resin were collected and their nipple was cut off to accommodate the preform inside the fixture. The fixture with the preform was set up on the Instron machine and tensile tests were performed.

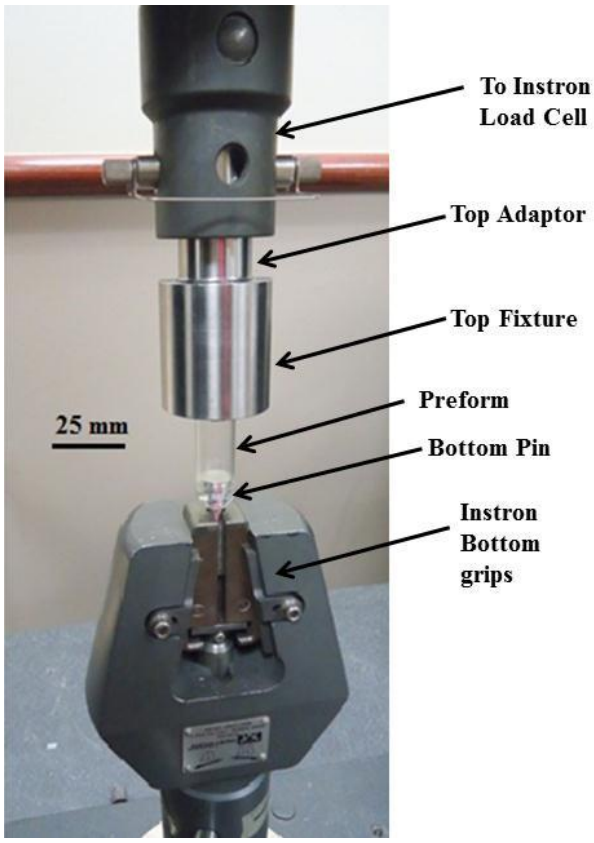

Figure 12: Fixture Setup on Machine.

An extension rate of 5 mm/min was chosen based on literature [8, 16, 128] which suggested that the drawing rate of PET is independent of the rate at or below 5 mm/min. The tests continue until sample failure. Sample failure usually occurs near the pin side of the gage section where the stretched sample breaks in the gage section. The average gage length for all the samples was around 30 mm as defined by reflectors placed on the physical gage section of the tensile preform. Care was taken to maintain this length as a

constant value. The inner diameter and external diameter of the preform was measured for all the samples. The average values for the inner diameter was 15.84 ±0.02 mm, while for the external diameter the value was 18.38 ±0.02 mm.

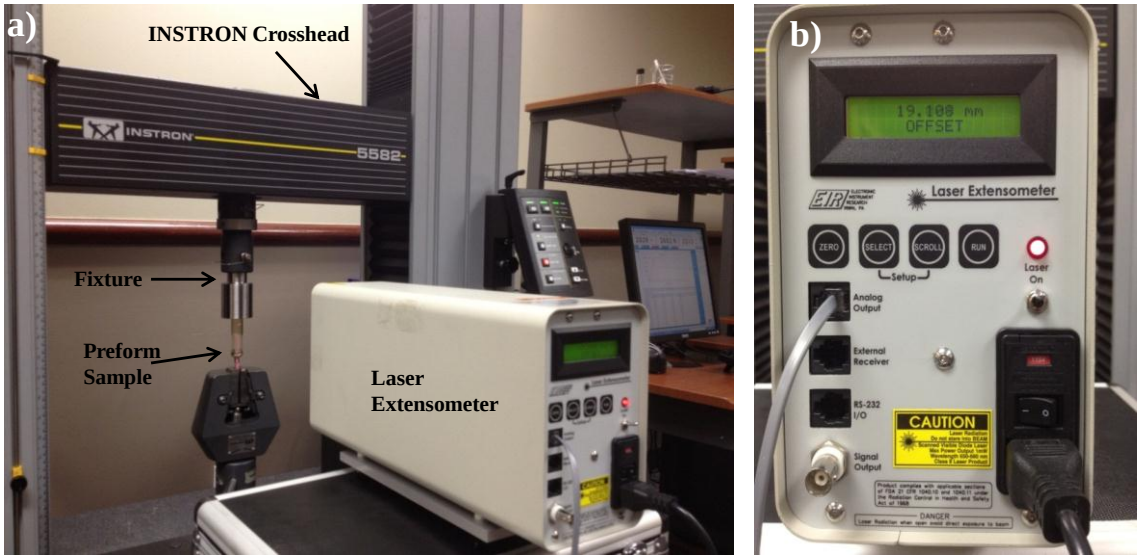

Figure 13: a) Test set up with laser extensometer b) Laser extensometer display.

During the testing process, there is compliance in the load-extension curve. This is from sample compliance, machine compliance, and fixture compliance. It is necessary to compensate all these loses and appropriate compliance correction on all data. To avoid this problem and to have better accuracy of results, extensometers can be used to obtain more accurate values and to measure the readings to the particular gage length required. For this work, a Laser Extensometer model LE-05 from Electronic Instrument Research was used for strain measurements. The full scale reading was set to 10 mm, with a target distance at 380 mm and an average of 64 scans for a data set. The maximum resolution was 0.001 mm and measurement range is from 8 mm to 130 mm. Two self-reflecting glass tab stickers were placed on the preform samples with separation of approximately

30 mm which was taken as the average gage length. The entire test setup along with the laser extensometer is shown in Figure 13.

3.2.4. Dynamic Testing

In order to determine the dynamic behavior of resins, preform samples were tested at a wide range of strain rates (Table 1). The samples were tested at eight different extension rates. As per ASTM E8 [129], the rate of deformation is governed by the rate of straining, rate of stressing, rate of crosshead separation, elapsed time and the free-running cross head speed. Conventional quasi-static strain rates lie between 10^{-5} s^{-1} to 10^{-1} s^{-1} whereas the dynamic tensile testing range would be from 10^{-1} s^{-1} and greater. The test speeds chosen must be such that it allows accurate determination of the loads and strains. And another important factor governing choosing test speed is that the time for completion of the test should not be very high. [130] Since plastics are time dependent materials, the testing time is of great importance.

Table 1: List of Extension Rates and Strain Rates Tested.

S.No	Extension Rate	Strain Rate
	mm/min	per sec
1	5	0.0028
2	10	0.0056
3	50	0.0278
4	100	0.0556
5	200	0.1111
6	300	0.1667
7	400	0.2222
8	500	0.2778

No modifications were done to the test setup and only the extension rates were changed on the machine. Care was taken to maintain the average gage length to

approximately 30 mm. The tests were done from the minimum rate chosen (5 mm/min) up to the maximum extension rate (500 mm/min) capability of the hydraulic Instron machine. The strain rates ranged from 10^{-3} s^{-1} to 10^{-1} s^{-1}.

3.2.5. Defective Sample Study: Polariscope Imaging

In some cases, samples might fail prematurely, even before yielding reached the gage section or it might also fail half way during the stretching deformation. Such cases of brittle failure were observed in only a few samples and were associated to sample defects. The 50% rPET samples showed more cases of brittle failure. To study these defects, a poloriscope was used to study the fringe patterns in the preform samples. A defective sample would have an uneven distribution of fringes or in some cases; the fringes would even be absent or blurred.

3.3. Rheometry

Rheology has been a very effective tool to study the molecular behavior especially with respect to flow behavior. It is of great application in polymers since it helps to study the relation between flow and deformation patterns from the molecular structure [131]. In the polymer industry, studying the zero shear viscosity also known as the melt viscosity is of prime importance since it helps to understand the ease of processability of the resin as well as its properties in the molten state [79].

Measurement of the shear viscosity is done using a rheometer which measures the flow and deformation under a shear force. Rheometry measurements were done at Niagara Bottling LLC. Before the measurements, drying time for the pellets was at least one hour at ambient pressure and a temperature of 177°C. This particular temperature of

177°C was chosen since this is the typical drying temperature in the hopper of the injection molding machine. Characterization was done using a rotational rheometer AR-2000ex (TA Instruments) at 1% strain under a nitrogen atmosphere to delay degradation of the resins. Samples were prepared by melt pressing pellets directly on the rheometer platens at 260°C.

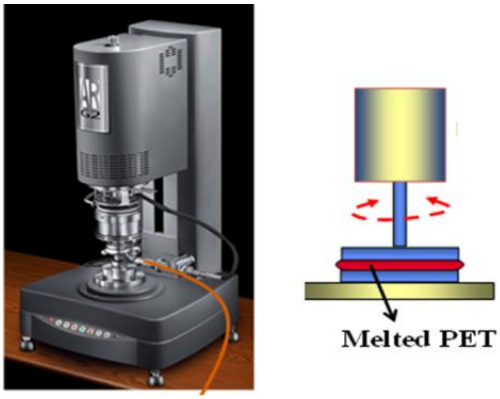

Figure 14: Rheometer Test Setup[132].

Three minutes of equilibration was performed in all measurements. A parallel-plate configuration was used with a plate diameter of 25 mm. For dynamic melt rheology measurements, the Linear Viscoelastic Region (LVR) was determined by oscillatory strain sweeps at a frequency of 1 Hz. A time sweep was performed to verify the sample stability. Frequency sweeps were then carried out at 1% strain [132].

3.4. Crystallinity Measurement: Differential Scanning Calorimetry (DSC)

Crystallinity is considered one of the most important properties for a semi crystalline thermo plastic. It helps in determining the mechanical properties of a polymer such as brittleness, toughness, modulus, clarity, creep and barrier properties [14]. Thermal analysis using Differential Scanning Calorimetry (DSC) is considered a very

effective method of determining the crystallinity content in polymers. Thermal analysis helps to determine properties of the material as a function of temperature [133]. DSC helps us to determine the percentage of crystallinity content as well as the amorphous content in a polymer. Today we also have new methods of DSC analysis such as Modulated Temperature DSC which allows us to study temperature changes over small heating cycles and also with varying temperatures; however this process is time consuming.

In general a crystalline material has molecules arranged in a particular order or pattern whereas an amorphous phase consists of molecules in a random arrangement. PET undergoes two types of crystallization; spherical "cold" crystallization producing a white color during heating and stress induced crystallization, which is transparent and is obtained by stretching [134]. A differential scanning calorimeter measures the heat in and out of a sample and also measures heat of the sample with respect to a reference. It can heat or cool the sample based on the input parameters given and is ideally used to measure the transition temperatures such as the glass transition temperature, melting temperature, crystallization temperature and also the heat capacity. One can observe endothermic and exothermic peaks in the DSC thermogram.

For all the DSC measurements, samples weighing approximately 10 mg were cut from the test specimens and placed in aluminum pans and closed with lids. Pellet samples from 100% rPET resin and virgin PET resin R_1 were tested. Preform samples were tested from six different regions on each preform (100% rPET, 50% rPET, and virgin PET R_1) to study crystallinity along the length of the preform. The tests were performed using a DSC Q2000 from TA Instruments. The tests were started at room

temperature and raised in steps of 10˚C per minute up to 280˚C, and then held for 5 minutes. After this, the samples were cooled down to room temperature at 10^{o}C per minute. For the pellet samples and the preform finish samples, a second heating cycle was also performed. All other samples had single heating and single cooling cycles. Based on the sample's thermal history, we may or may not find a cold crystallization peak. The percentage crystallinity is calculated using the formula in Equation 3.1.

$$\% \text{ Crystallinity} = \frac{\Delta Hm - \Delta Hc}{\Delta Hmo} * 100 \quad (3.1)$$

Where ΔH_m is the heat of melting, ΔH_c is the heat of cold crystallization and ΔH_{mo} is the standard heat of melting of 100 % crystalline PET which is taken as 140 J/g. During stretch blow molding, different regions of the bottle will have different levels of crystallinity. Low values of crystallinity reduce barrier and creep properties. High crystallinity reduces impact and clarity. In order to ensure one gets favorable properties, blown bottles might be held at temperature between glass transition and melting temperatures to stabilize. The preforms are also preheated in this temperature range [14].

The heats of melting ΔH_m and cold crystallization ΔH_c are determined by calculating the area under the crystallization and melting peaks respectively. The units for the heats of melting and crystallization are in J/g. The glass transition temperature can be determined by the drop in the curve during the first heating cycle. As temperature is increased above T_g, molecular mobility increases rapidly. This permits the molecules to align with their neighbors and crystallize as seen in the exothermic peak. Although the baseline appears to stabilize between a certain temperature range, there is an ongoing

process of crystallization and crystal perfection over that temperature range. The term "crystal perfection" is used to describe the process where small, less perfect crystals melt and then re-crystallize into larger, more perfect crystals that will melt again at a higher temperature [135].

A typical thermogram for quench cooled PET is shown in Figure 15. This should be completely amorphous and have no initial crystallinity. Both the cold crystallization and the melting peaks are present. The region between the two peaks is not heat capacity basely; and as mentioned earlier, it is still a process of ongoing crystallization and crystal perfection; hence it was not advisable to integrate the cold crystallization and melting endotherms separately. As a result, it is impossible to get a true area measurement by integrating the peak separately. Hence the crystallinity measurements in this study were obtained by integrating the entire region from the onset of cold crystallization till the end of melting. The glass transition for PET on the second heat will depend on the rate of cooling. If the PET was quenched after heating, a large fraction of amorphous material and a large T_g can be observed. If it was cooled more slowly, then there would be higher crystallinity. The second heating cycle will not tell us anything about the initial crystallinity because the melt erases the thermal history [135].

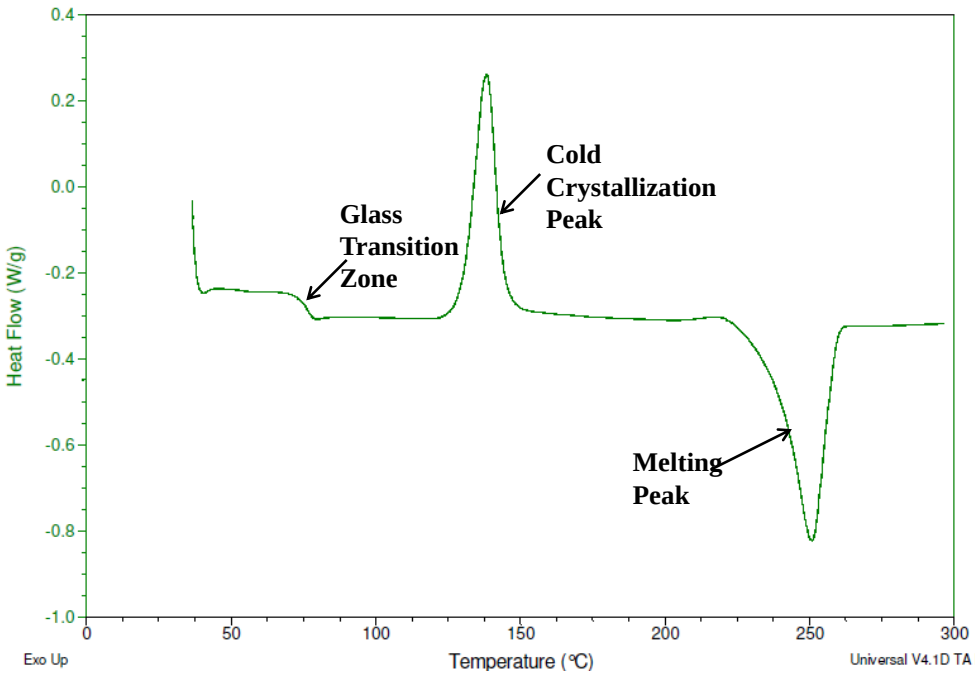

Figure 15: Typical thermogram for quench cooled PET. [133]

3.5. Color Measurements

The color measurements on the preforms were done at Hunter Labs in Virginia [136]. Eight different preform samples were used for the measurements. The color measurements were done on an UltraScan PRO instrument (Figure 17). The instrument can measure color transmission, reflectance, and absorbance from the visible wavelength to the near Infra-Red (IR) range from 350nm-1150nm. Samples were held using custom preform holders (Figure 17). The instrument was standardized in Total Transmission (TTRAN) Mode with medium area view.

Figure 16: Preform samples used for color measurements.

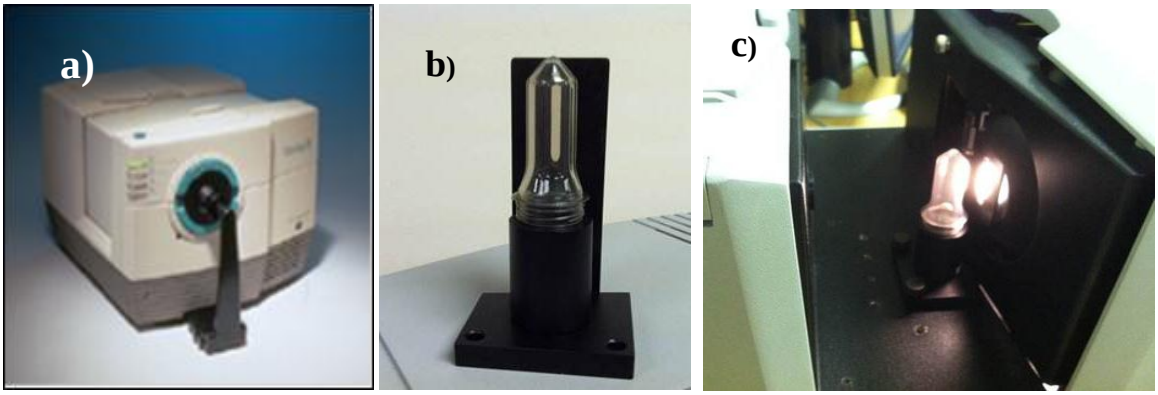

Figure 17: a) Ultrascan PRO Instrument b) Preform Holder c) Sample in Instrument.[136]

- Measurement data is reported in illuminant D65 and the 10 degree observer in CIE L*, a*, b*, Y Transmission (D65/10), and Yellowness Index (YI) E313 (D65/10).
- A total of 3 readings were taken for each sample (with replacement) for repeatability.

Each measurement took about 1 second. Cycle time (including the measurement and time to display) is approximately 3 seconds. The whole process of placing the sample and taking the measurement might take 30 seconds to a minute. The EasyMatch QC software which comes with the machine was used to analyze and receive the data. It

has an available ASCII export feature that allows the export of color data to a CSV file. The heat damage by yellowing could be measured with the b* values or the Yellowness Index (YI) values. All 8 samples were measured in transmission to obtain % Transmission and % Absorption [136]. The data was normalized based on the preform wall thickness values.

3.6. Friction Measurement

The friction measurements were done at Oklahoma State University using a special set up designed at the university [126]. The test set up is designed to hold two bottles; one would be stationary while the other rotates. The set up (Figure 18) consists of a stand, which would hold one bottle horizontally with the neck of the bottle held inside a bottle chuck, which is attached to a motor which rotates the bottle. The other end of the bottle is attached to an adjustable cast Nylon 6 tail stock. The other stationary bottle is placed on top of the already fixed bottle and is attached to an adjustable grip. This grip is attached to a meter arm which holds the force gauge and resists the deflection of the arm, thus converting this deflection into an electric signal which would be sent as force input to the force gauge by the load. A Mark-10 series 5 force gauge with accuracy of ± 0.1 % of full scale with resolution of 1/5000 and 7000 Hz sampling rate was used for the setup. There would be no source of any extraneous friction since all measurements are done directly using the force gauge installed on the beam holding the stationary bottle. This would avoid errors arising from measurements using torque which is a function of radius. Bottles of different length can be accommodated since the tail stock and chuck can be adjusted. The stainless steel rods, PVC grip, 6061-T4 aluminum alloy and cast nylon-6 materials were chosen to avoid corrosion, for light weight and also to

enable the setup to be used over a long period in several environments [126]. The friction between the bottles and preforms is considered as sliding friction and hence the test setup was designed as such. After placing the bottles in the grips, the lever arm is balanced so that there is no force exerted on the stationary bottle. After this, a normal force in the form of standard weight block is applied on the grip holding the stationary bottle. The power output was adjusted to 12V for the motor and the test was started.

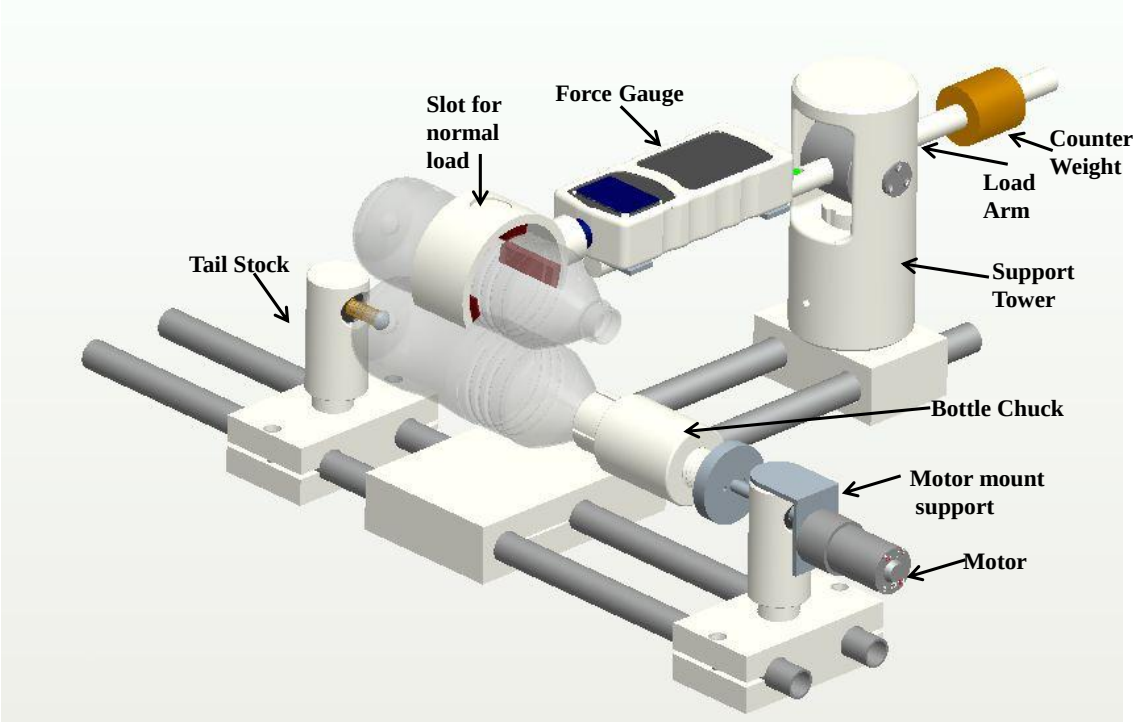

Figure 18: CAD Model of Friction testing setup. [126]

After a period of 60 seconds, the averaged normal force reading would be displayed on the load cell and the test was stopped. The maximum compression peak value and the maximum tensile peak value are displayed on the top right corner of the force gauge and these values are also noted. The standard weights used were 200g and 100g respectively. The friction measurement tests were performed on virgin PET resin

R_1 bottles from weighing 7.5g and on 8.5g virgin PET resin R_2 bottles as well as on 20 % rPET bottles weighing approximately 9.3g. Preform samples of virgin PET resin R_1, R_2, R_5, 50 % rPET and 100 % rPET were also tested. The coefficient of friction was calculated using the formula,

$$F_r = \mu * N \tag{3.2}$$

Where F_r is the frictional force (reaction force), N is the normal force applied and μ is the coefficient of friction. Care was taken to ensure that the force gauge readings were set to zero before start of each test and also to ensure that all the units were homogenous. The tests were run for 30 seconds for preforms and 60 seconds for bottles and the values were recorded for every second using the interface software 'MESURLITE' between the force gauge and the computer. The first reading at the instant the test began was used to calculate the value of static friction and the corresponding readings average give the value of the coefficient of dynamic friction.

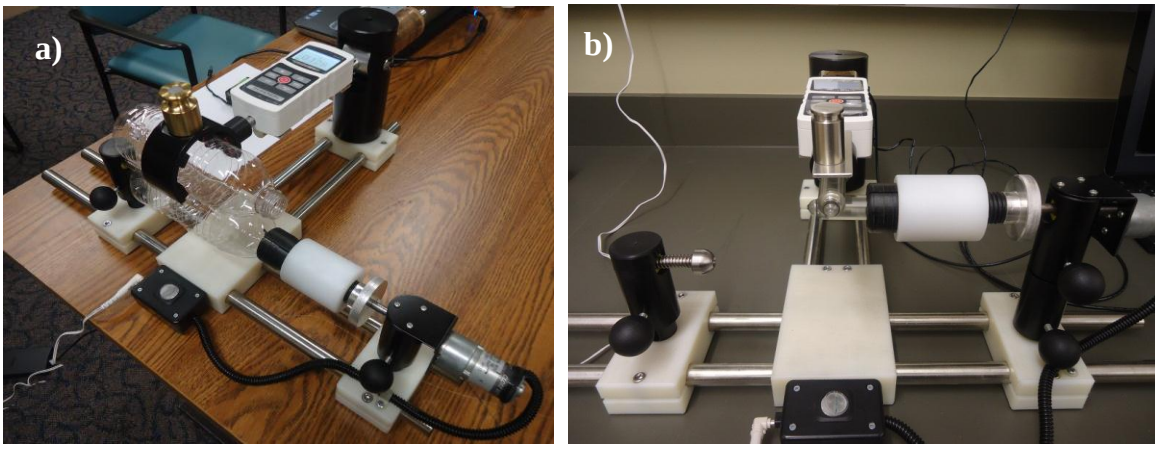

Figure 19: Friction testing setup for a) Bottles b) Preforms.

3.7. Wall Thickness Measurements

The wall thickness measurements for the preforms and the bottles were done using two techniques. The first method involved using the Magna Mike instrument and the other was using the AGR Gawis instrument. Wall thickness is a very important parameter to be calculated for measurements relating to carbon dioxide retention, oxygen permeation, barrier properties, color measurements, finite element simulations, CAD model generation, and for other important property determination. The magna mike works on the principle of the Hall Effect. A metal ball is placed inside the bottle and the wand is dragged along the bottle wall. The attraction between the ball and the wand will give us the value of the wall thickness. There are several sizes of the ball diameters available and the highest diameter is usually preferred for the maximum accuracy.

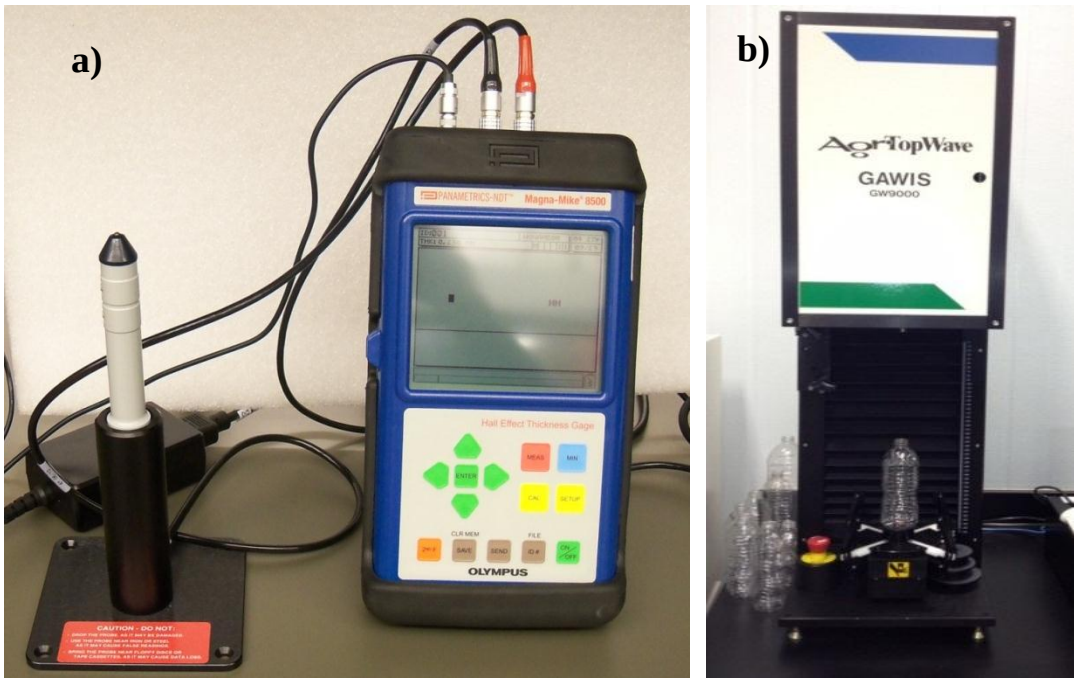

Figure 20: a) Magna Mike apparatus for wall thickness measurements. b) GAWIS wall thickness measuring test setup.

The AGR GAWIS is a more advanced wall thickness measuring instrument which includes auto feed options and also has multiple angles of measurement. The wall thickness measurements for the 20 % rPET bottles were done on a GAWIS GW9000 instrument at Niagara Bottling LLC. [137] . Thickness measurements were done at different heights measured from the top and at various angles.

3.8. 3D Scanning and CAD Model Generation

It is very difficult to obtain a perfect CAD model of the bottle that can be used as input for the finite element analysis. Further the bottle designs keep changing often and the blow molding machine will require changing the mold design. However to obtain an accurate real time model of the exact blow molded bottle would be tough since existing CAD software would take lot of time to generate an exact model and they might contain some errors. To overcome this problem, 3D scanning is a very efficient technique of obtaining real time CAD models.

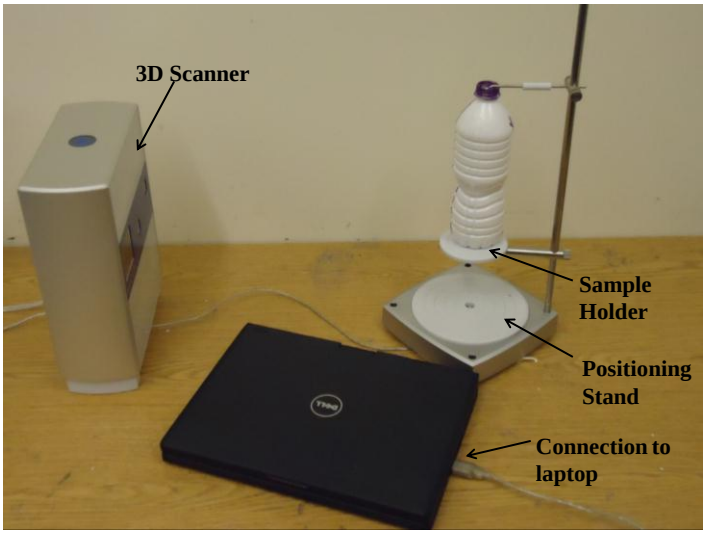

Figure 21: 3D Scanning setup.

The 3D scanning technique uses color, shape and size to analyze an object. The scanner emits laser rays which will identify the object from reflection and then builds the image. The scanner collects a series of images and then combines them to generate the complete model.

A Next Engine 3D scanner was used to scan the bottle which was used for the finite element simulations. The scanner is equipped with two 3.0 mega pixel cameras and four lasers. It has both macro and wide precisions. It has an accuracy of 0.1 mm and the object should be able to fit into a 76 x 127mm area. Wide precision gives accuracy of 0.3nmm and object should fit an area of 254 x 330mm. A 360˚ angle scan was used to obtain the images so that the entire bottle geometry could be covered [31].

In order to obtain the perfect scan, surface preparation of the sample is needed. The bottles were sprayed with white Rustoleum paint and were marked at strategic points in order to merge the horizontal and vertical scan images. Rough surfaces are not preferred for scanning. After the bottle was allowed to dry for a 12 hour period, it was placed in the holder and then the scan was started. The room is required to be dark in order to prevent other images from interfering with the scan and to obtain the best possible scan. The number of divisions was selected as 16 for the highest accuracy which would be HD 17K points/inch^2. After the scan image has been obtained, it needs to be corrected to remove unnecessary scan images and needs to be fused. The trim option is used to cut out unwanted areas from the scan. The alignment tool is used to align the multiple scan images which have been obtained with the help of aligning pins. The fusing option is very important to fuse holes, merge, re mesh holes and correct the image. The polish option can also be used to fill holes and clean defects [31].

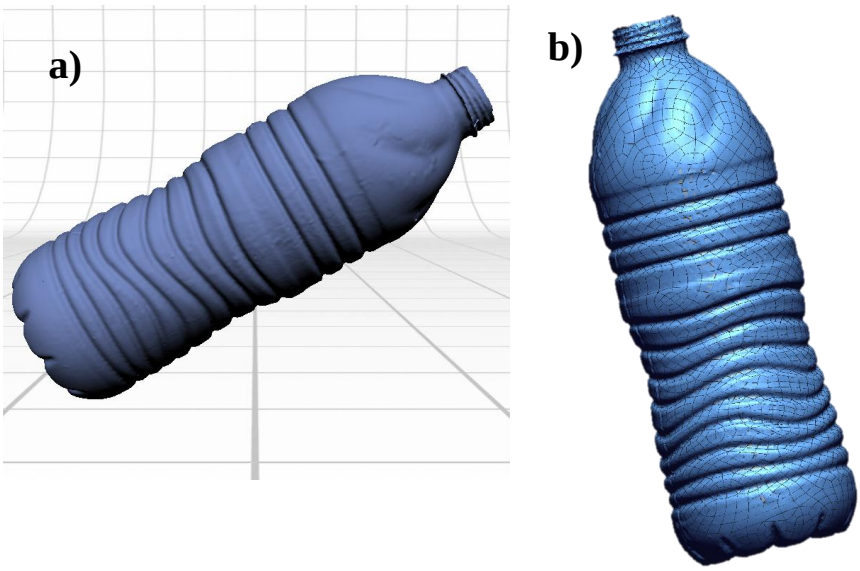

Figure 22: a) Scanned Image b) CAD Model after mesh buildup.

After the scanned image has been generated, the output file will have an extension .scn, this file cannot be directly used as input for the finite element analysis. Hence it would need to be converted into an .IGS or .STP file for input into ABAQUS. The scanned image file is opened in Rapidworks software which will allow us to build up a mesh and then convert the scanned image into a CAD model. Trimming, cleaning and polishing can also be done using rapid works. After deleting the unwanted data, a tight mesh is to be generated on the raw scan model. A poly vertices noisy cluster value of 100 was chosen and then a single mesh was created. Mesh density can be chosen as intermediate to speed up the process of model generation. The next step is the solidify option, which will create surfaces on the model and convert the scanned image into a CAD model. By now choosing the export option, we can export the file to the required CAD model format, usually it is converted to .IGS or .STP format since ABAQUS accepts these formats as input [31].

3.9. Hoop Strength Measurement: Feel Test Setup for bottle stiffness

The feel test for measurement of the bottle stiffness (hoop strength) of the bottle was very important since this would help in understanding how the bottle undergoes deformation. A standard test set up was developed at Oklahoma State University [31]. The setup was designed considering the bottle as similar to a thin walled pressure vessel or cylindrical structure. The fixture was made compatible to fit on an Instron machine so that controlled force could be applied over a time period.

Figure 23: Feel test set up on INSTRON machine.

The set up (Figure 23) was bolted to the Instron machine using bolts, and the bottle was placed on the base plate. There were different plates for different bottles and its height could also be adjusted. One end of the rope which connects to the belt was attached to the INSTRON machine while the other end was fixed on the fixture. Two

small thick cylindrical tubes 0.4” in diameter and 1’ long were connected to the Kevlar band around the bottle to concentrate the force on two points similar to real life force application on a bottle. The bottles were tested at the waist location (Figure 24). The tests were performed at an extension rate of 10 mm/min and the test was stopped when the load reached around 45 N which is approximately 10 lbf. The loads vs. extension curves were obtained and the stiffness values were calculated.

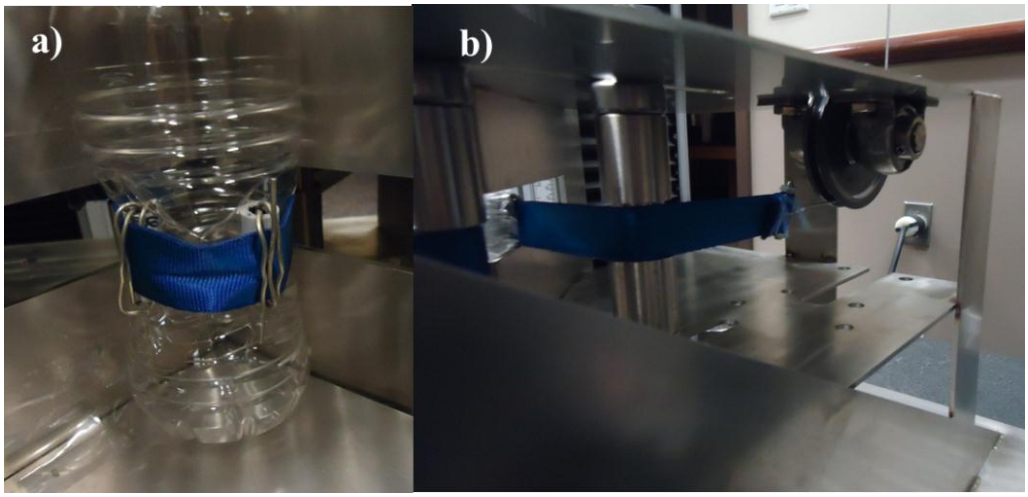

Figure 24: a) The Kevlar band around the bottle. b) Interior of fixture.

3.10. Top Load Testing

Determination of top load is another very important design parameter for PET bottles. The top load test procedure involves placing a filled PET bottle in the test setup and applying a steadily increasing load until the bottle deforms. The same test would be performed for an empty bottle to determine the empty bottle top load. Determining the top load would help us to understand the load that the bottle can withstand in axial direction before it begins to deform. The point where there is a sudden drop in load is noted and this is the top load capacity of the bottle. This is of great benefit especially

when bottles are stacked up in pallets in the bottling plant awaiting shipment. One can prevent damage to bottles by appropriately stacking the bottles based on the top load. The top load tests were performed at Niagara Bottling LLC. with a Dillon GTS-1000 digital control motorized test stand on 0.5 L Eco 3 bottles for 20 % rPET and virgin PET resin R_1. The machine was set in auto reverse mode and a compression speed of 100 mm/min was given. The height travelled by the platen was set between 5 mm to 10 mm. The top compression platen begins to move down and deform the bottle and the values are noted on the scale right above. A target of 70-80 lbf is considered efficient top load for a bottle [138].

Figure 25: Top load testing setup [138].

3.11. Finite Element Analysis

Once the properties for the rPET were determined, the next step was to implement these properties into finite element simulations. Finite element analysis was done on one particular bottle design. The goal of the finite element analysis was to study the effect of

change in essential material properties on the overall performance of the bottle keeping the design constant. Top load performance and lean test analysis were performed on the bottle. The boundary conditions would be similar for the simulations but the material properties would be changed accordingly for virgin PET material and rPET material. The bottle was scanned using a Next Engine 3D scanner and then the model was generated using rapid works software. The model was imported into ABAQUS 6.10 as an .IGS file. The model was described as a deformable shell part. Eulerian parts could be used for modeling liquids in Eulerian and Legrangian-Eulerian analysis [31].

The next part involves assigning the material properties to the model. The material properties for the simulations are assigned in four sections: general properties, elastic properties, plastic properties, and creep properties. The general properties included assigning the density value; this value was assigned based on the density measurements done on different samples. The elasticity properties would be those determined from the stress strain curves. The value of young's modulus was input based on data from the elastic portion of the stress strain curve. The elastic properties were considered isotropic. The values for the plasticity were given based on output from virtual prototyping software. The creep properties were assigned using the plasticity sub option; 'potential' as resistance values. These values were also taken from the virtual prototyping software [31]. After assigning the material properties, the wall thickness values are to be given. Before assigning the thickness values, we would need to create sections on the bottle. Hence 18 different sections were created on the bottle and the thickness values were given. However the section assignment is done after the meshing is completed.

The most important step in finite element analysis would be the meshing of the model. The meshing is done using the mesh module. The fineness and density of the mesh is very important in order to obtain an accurate result. The Free Meshing technique was used to mesh the part. This was done after first seeding the part. The shell element type was used in meshing. Conventional shell elements were used since the thickness of these sections is less than the other dimensions. Since the bottle does not have uniform thickness in all sections, section assignments would need to be given and then the thickness values for each section would be assigned. This was done by assigning nodal sections. The sections were assigned by manually selecting the regions from the bottle from the view port. 18 different sections were already created and thickness values were specified and hence now the sections were assigned to the respective locations [31].

Based on the complexity of the problem, the type of analysis is chosen and this is specified in the step module. Dynamic explicit analysis is chosen since the transient response of the bottle is required with time. This step is in addition to the default step where all the boundary conditions would need to be specified. The values for the step time, increment time and the mass scaling factor are defined here. A high value for the mass scaling factor helps to arrive at the solution faster. Contact properties are also to be created since the bottle would involve interaction with rigid bodies. The General Contact option was used, and surfaces were defined on the rigid plates used in the top load analysis. Frictional contact was specified for tangential behavior and hard contact was specified for normal behavior in the case of interaction properties [31].

The last step before actually submitting the job and starting the analysis would be assigning the loading and boundary conditions. The bottle base was fully fixed and a

displacement load was given to the bottle top in case of lean test. While for the top load test, the bottle was fixed to the bottom plate and a displacement load is given to the top plate. Specifying the accurate boundary conditions is very important to obtain the right result. For dynamic explicit analysis, it is necessary to specify the amplitude values before giving the displacement values since this would help in ramped up loading rather than direct impact loading [139, 140].

3.11.1. Material Parameters for Simulations

The part is input into ABAQUS in .IGS format. The plates are modeled as analytical rigid. The Deformable Shell part type was selected for the bottle. The meshing was done choosing the explicit shell option and the shell element was S4R. The plates did not require meshing since it was a rigid part and there is no deformation to the plates. The membrane intersection layer was modeled using M3D8R elements and it was assumed that it could stretch infinitely. The other material properties were assigned with minor modifications based on change in bottle design to the values used by Vaidya [31]. The most significant material properties that would require change would be the values of density, the young's modulus, and the wall thickness values. The impact of these changes on the values would be investigated.

General Properties:

Density:

This value would vary based on the resin that is used in the bottle, typically virgin PET resin R_1 would have a value of 1325 kg/m^3 , resin R_6 would have value of 1335 kg/m^3 , resin R_3 would have 1310 kg/m^3 and 100 % rPET would have 1330 kg/m^3.

Elastic Properties:

Young's modulus

Virgin PET resin R_1= 2520 MPa, Virgin PET resin R_6= 2700 MPa, Virgin PET resin R_3= 2105 MPa and for 100 % rPET= 2490 MPa.

Poisson ratio= 0.4.

Plasticity Properties:

Table 2: Plasticity properties.

Yield stress (MPa)	Plastic Strain
80.24	0
159.84	0.867

Creep Properties:

Table 3: Creep properties.

R_{11}	R_{22}	R_{33}	R_{12}	R_{13}	R_{23}
1.75	1	1.75	1	1.75	1

The membrane properties which would be the layer of intersection for air and water were given the following properties; Density: 1.189 kg/$m^{3;}$ Bulk Modulus=1.42 x 10^5 Pa; Poisson's ratio =0.5

The step module included specifying dynamic explicit analysis with time period of 2 seconds and mass scaling factor of 20000.

For the case of the bending (lean test), the material properties remained the same. The boundary conditions did not require the rigid plates. Instead a horizontal

displacement was applied to the top node of the bottle and also the bottom of the bottle was fixed (Figure 26). This horizontal displacement value was based on a bending of 3 degrees. Hence the height of the bottle would be multiplied by sine of 3 degrees and this would be the displacement value.

For the top load test, the contact formulations were given by creating surfaces on the plates for regions in contact with the bottle. This was defined as general contact. The boundary conditions included fixing the bottom plate and applying a downward displacement to the top plate (See Appendix G Figure 71). This would be similar conditions to the actual testing set up. Also a pressure of 0.1 MPa was given to the bottle internal surface to account for water pressure.

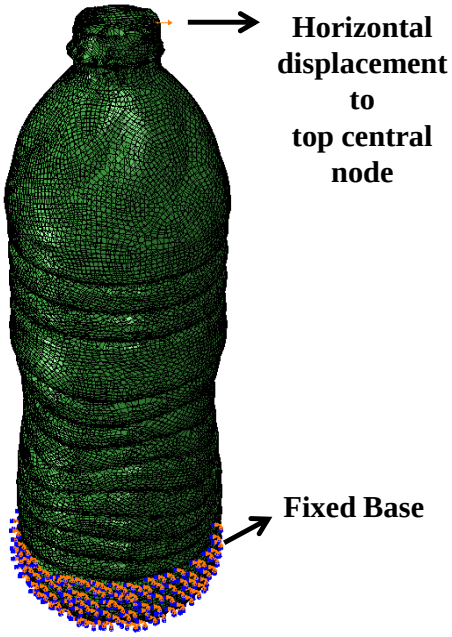

Figure 26: Boundary conditions for lean test simulation.

CHAPTER IV

RESULTS

4.1. Tensile Test Results

Tensile testing of amorphous preforms was carried out to determine the bulk mechanical properties; Young's modulus, yield strength, tensile strength, toughness, and percentage elongation till failure of the PET resins. A set of 5 samples were tested for each resin type. The load-extension curve of a typical PET preform sample consists of the following; elastic zone, yielding zone, plastic zone, hardening zone, and failure zone, as illustrated in Figure 27. Strain values were recorded using a Laser extensometer. The Young's modulus is calculated from the slope of the elastic region of the engineering stress-strain curve. The yield stress values are calculated by using the 0.2 % strain offset method. The method involves determination of the yield strength from the point of intersection of the line drawn parallel to the slope of the elastic region with the engineering stress-strain curve. The Young's modulus and the yield strength values are presented in Figure 28 for 8 different resin types (See Appendix A for resin classification). The resins were ranked according to increasing values of Young's modulus as shown in Figure 28.

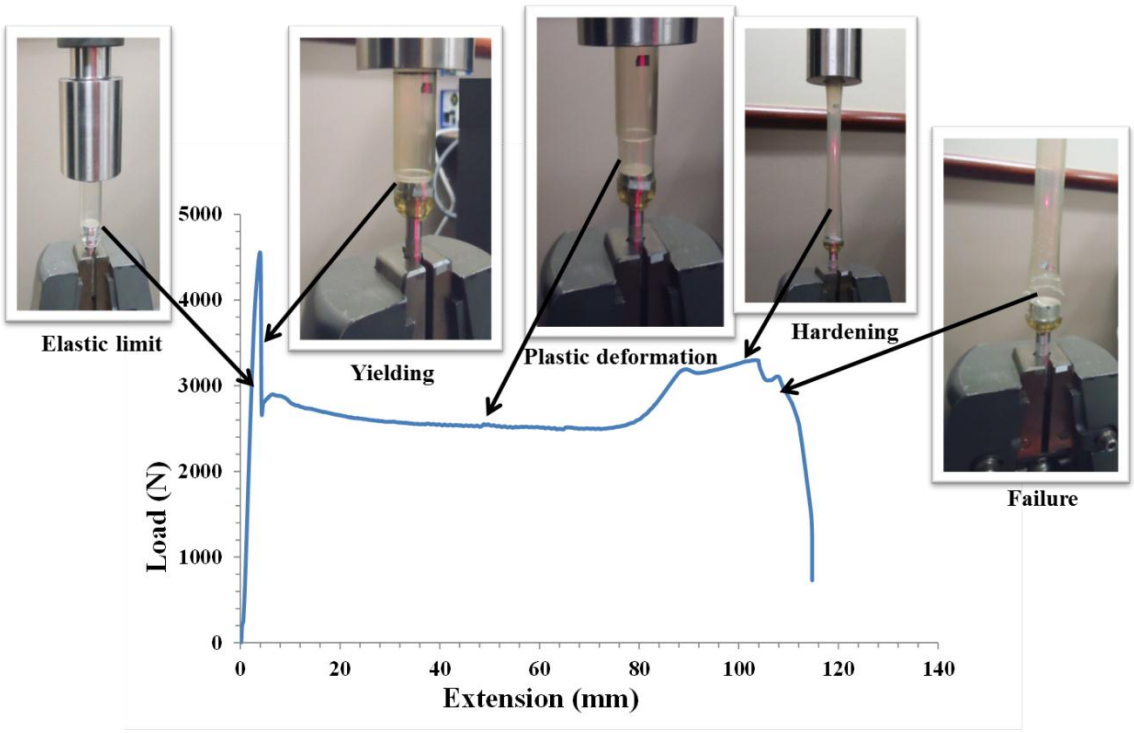

Figure 27: Typical stages of PET sample behavior on load extension curve.

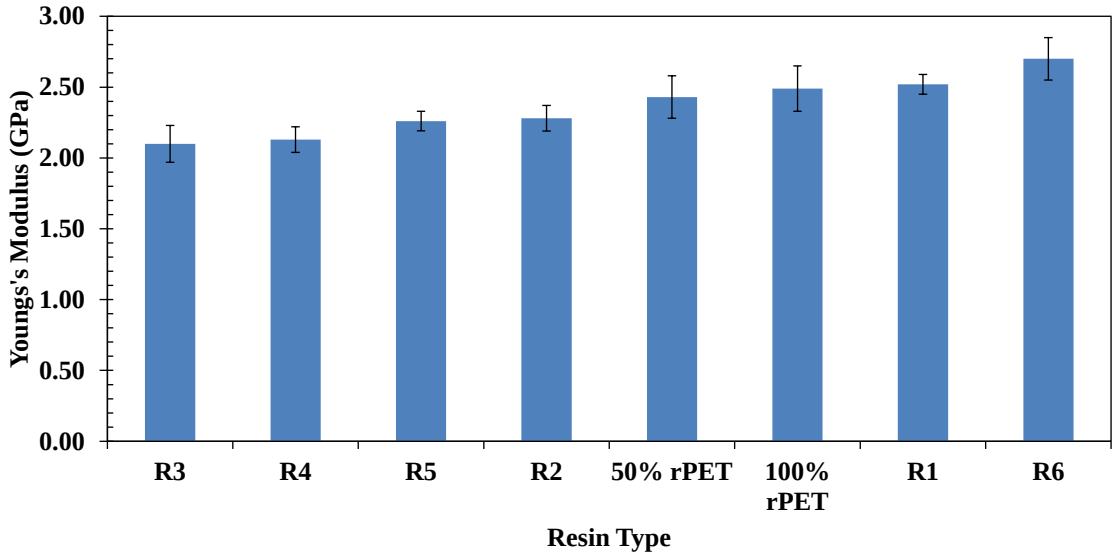

Figure 28: PET Resins ranked based on lowest to highest values of Young's modulus.

From Figure 28, it is evident that the value of Young's modulus for the virgin PET resin R_6 is the highest while the virgin PET resin R_3 with 0.82 I.V. has the least Young's modulus. The percentage difference in values among these resins was 25%. The resins were again ranked according to the values of yield strength as shown in Figure 29. The yield strength values showed virgin PET resin R_6 having the highest value of yield strength (60MPa), while the virgin PET resin R_4 with faster reheat additive had the lowest yield strength. A 41 % difference was observed between the yield strength values of these resins.

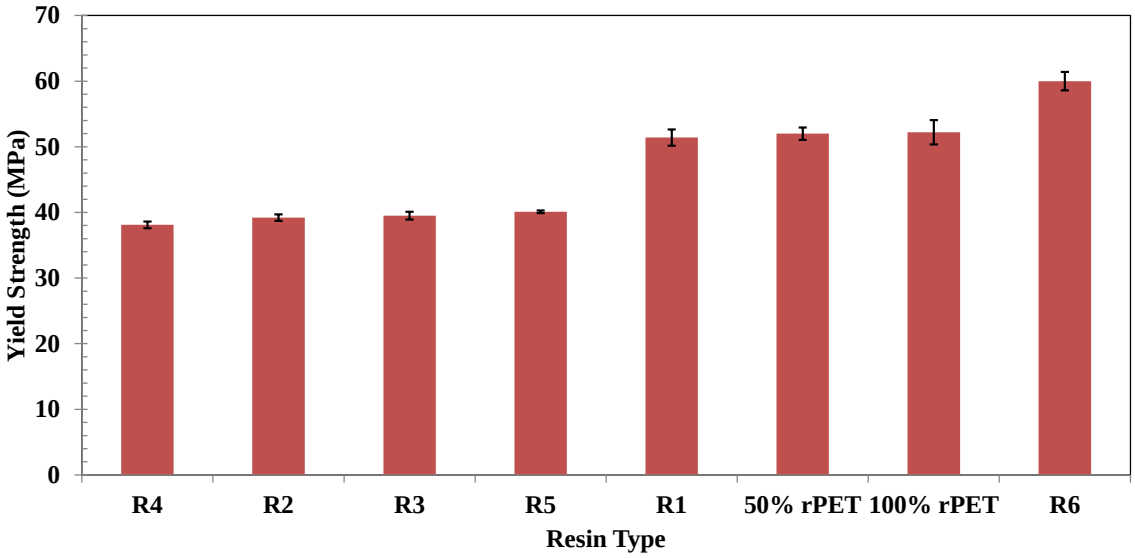

Figure 29: Resins ranked based on lowest to highest value of yield strength.

4.2. Dynamic Mechanical Properties

In order to determine the dynamic properties, tensile testing was performed on 3 types of resins; virgin PET resin R_1 (0.76 I.V., non FRH), 100 % rPET resin, and 50 % rPET resin at higher strain rates. The tests were performed at 7 different strain rates in addition to the quasi static extension rate of 5 mm/min. Figure 30 shows the engineering

stress-strain curve for the 50 % rPET sample for the 3 steady state extension rates used. For the selected gage length of 30 mm, the steady state extension rates were 5, 10, and 50 mm/min. The trend of the stress-strain curve is similar for virgin PET resin R_1 and 100 % rPET as well. However at higher extension rates, the samples have a different failure (Figure 31).

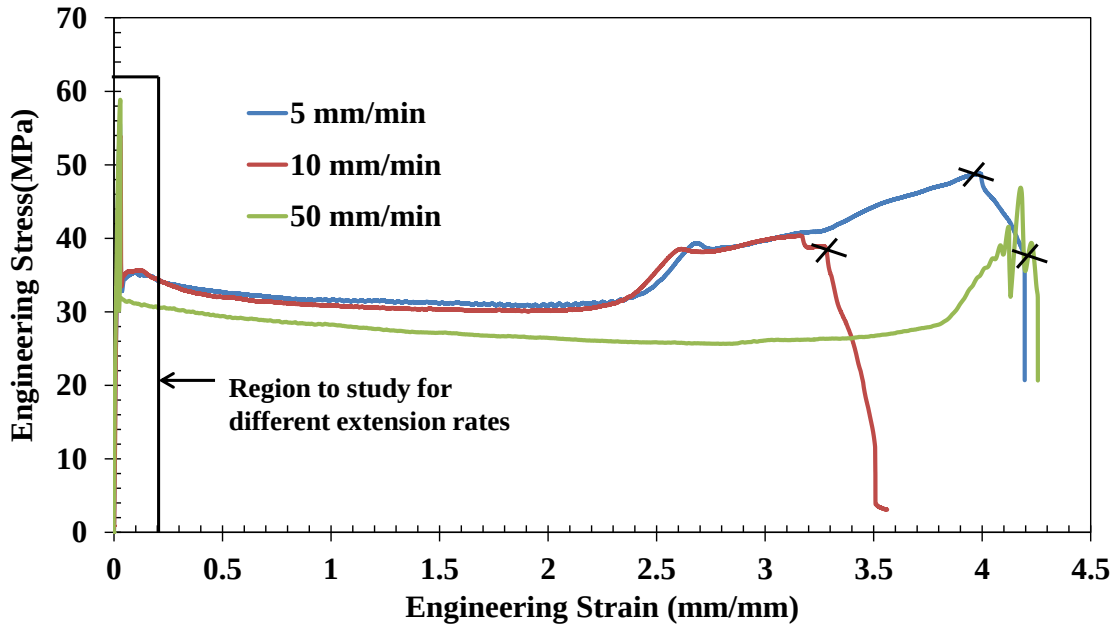

Figure 30: Engineering stress-strain curves for 50 % rPET at lower extension rates.

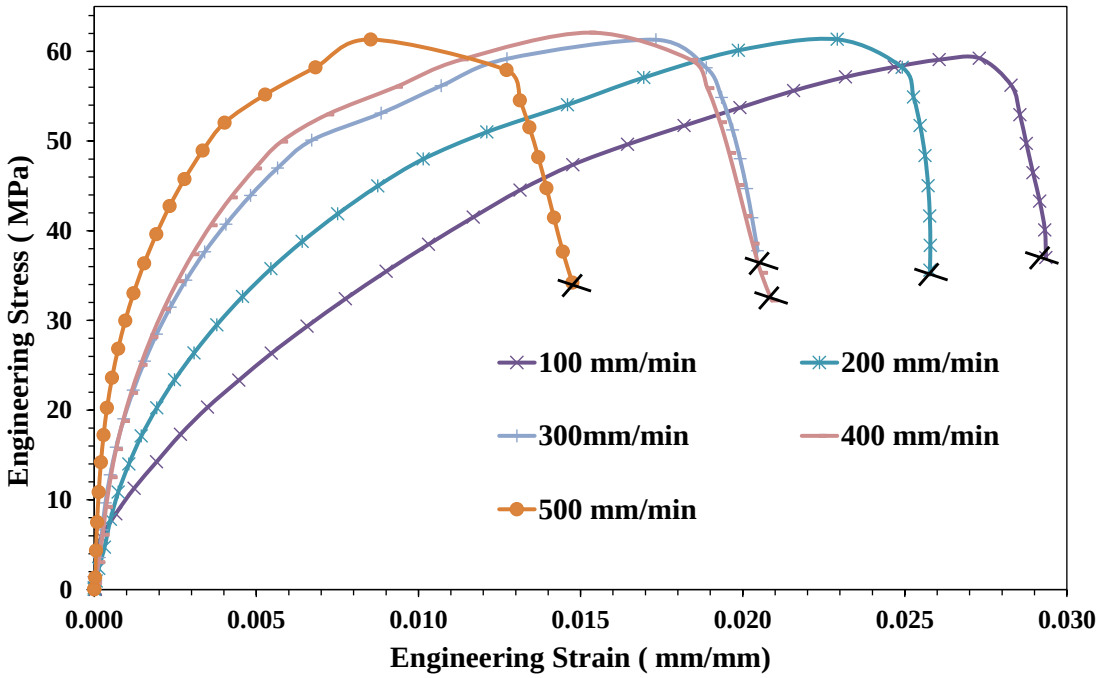

Figure 31: Engineering stress-strain curves for 50% rPET at higher extension rates

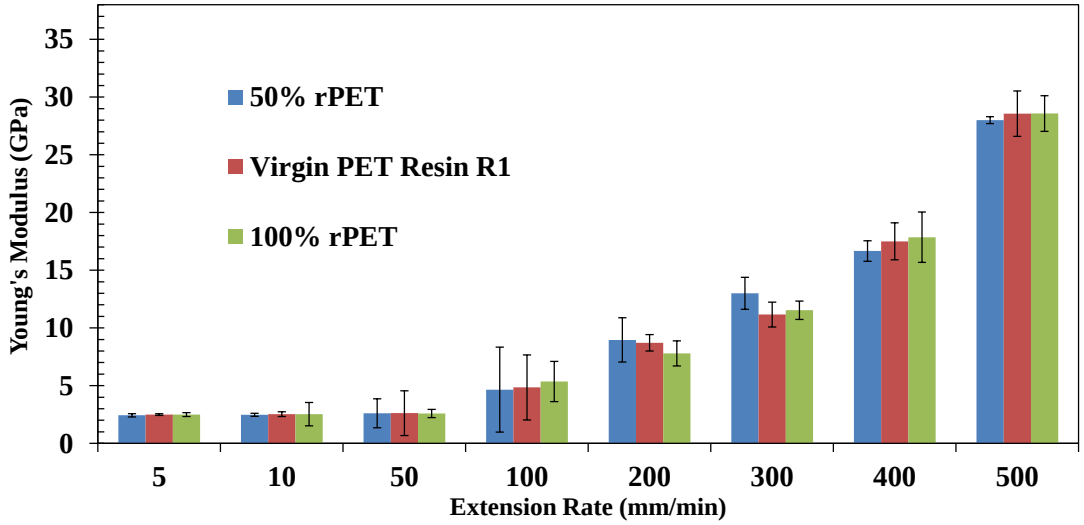

Figure 32: Comparison of Young's modulus with extension rate.

The biggest increase in the values of Young's modulus (Figure 32) was observed for the virgin PET resin R_1 which showed an 11.5 % increase in modulus between the lowest and highest extension rates. The 50 % rPET and 100 % rPET resins showed an

increase of approximately 10 % in the modulus values respectively between lowest and highest extension rates.

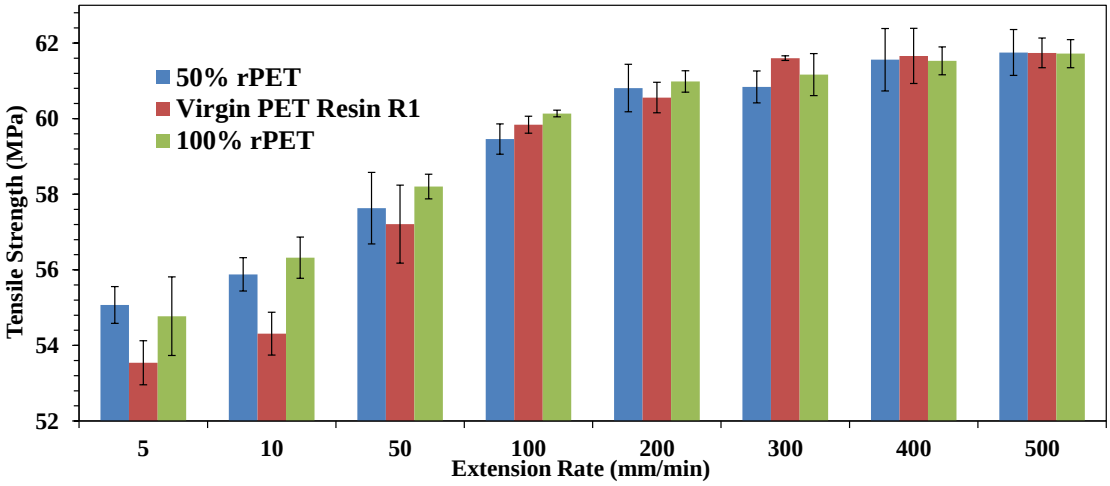

Figure 33: Measured increase of tensile strength with extension rates.

The Tensile strengths of the PET resins were obtained from the engineering stress-strain curves. Tensile strength also increased with an increase in strain rates (Figure 33). This was also evident from the stress-strain plots (see Appendix C). The most significant increase in tensile strength between two successive extension rates was for the virgin PET resin R_1 which had a 5.3 % increase between extension rates of 10 mm/min and 50 mm/min.

Yield strength would be the next important dynamic mechanical property to be observed. The values of yield strength also increased with an increase in extension rate (Figure 34). The yield strength of 100 % rPET and 50 % rPET resin were almost in range with virgin PET resin R_1, the resin R_1 had the highest value for yield strength (59 MPa at 500 mm/min).

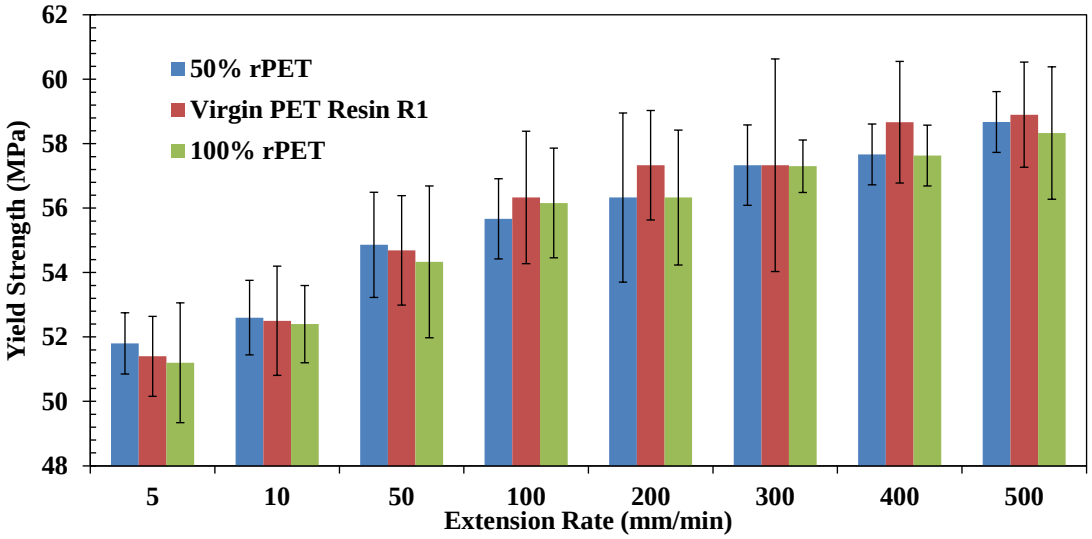

Figure 34: Increase of yield strength with extension rate.

The toughness values were calculated by finding the area under the engineering stress-strain graph. The units for toughness are MJ/m^3. From Figure 35, the results showed a drop in toughness values for all resins for extension rates above 50 mm/min.

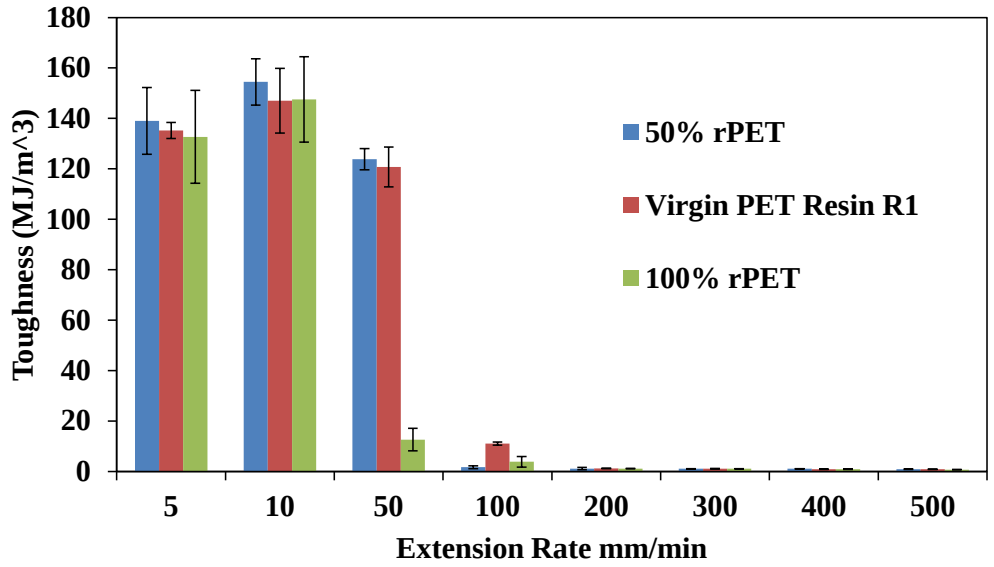

Figure 35: Toughness values for different extension rates.

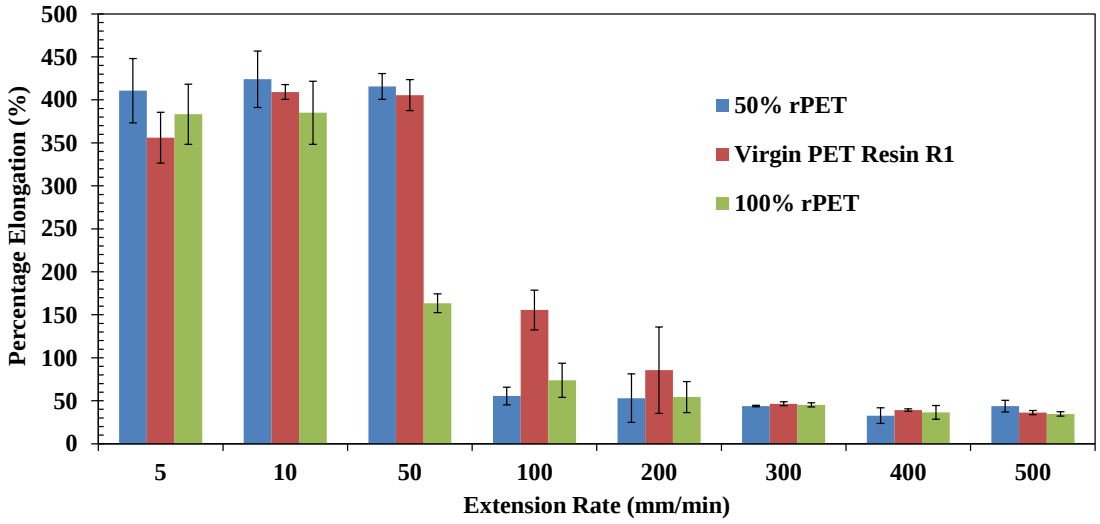

Figure 36: Percentage elongation till break for different extension rates.

The percentage elongation till break was also calculated for all the samples for different extension rates. As explained earlier, the samples tend to fail early at higher strain rates due to lower toughness values. The average sample extension was recorded as 130 mm when stretched at quasi static strain rates, however, this extension value falls drastically for extension rates above 50 mm/min.

4.3. Shear Viscosity and Molecular Weight Measurements

The measurement of the zero-shear viscosity or the melt viscosity helps in understanding the resin processing ability. This is of significance since the resin is subjected to a shearing force inside the screw during melting. Also the molecular weights were obtained from the zero shear viscosity data to relate with mechanical properties. These measurements would also help in choosing the best resin from different suppliers [79].

The shear viscosity results (Figure 37) showed virgin PET resin R_5 having the lowest value; this was in accordance with earlier results for yield strength and Young's modulus where resin R_5 was among the low performing resins. The virgin PET resins; R_1, R_3, R_4, and R_6 had higher values of shear viscosity. 100 % rPET resin showed an average value lying between the other resins. The results for the molecular weight are shown in Figure 38.

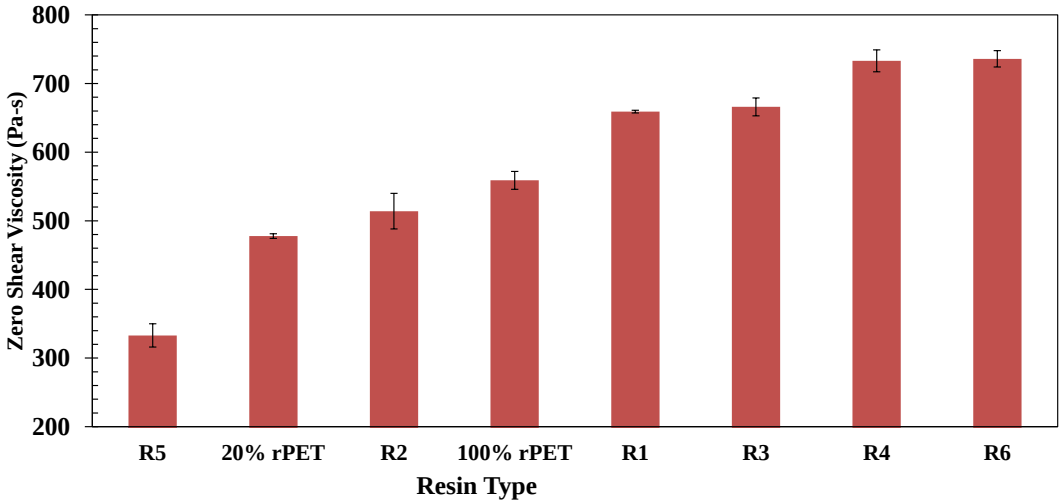

Figure 37: Resins ranked based on increasing zero shear viscosity.

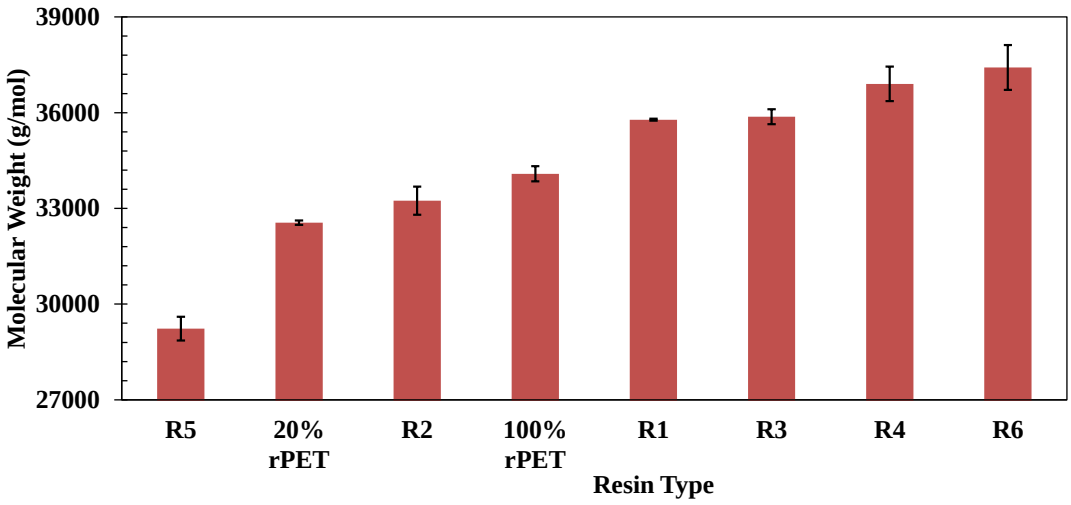

Figure 38: Resins ranked based upon increasing molecular weight

The rheometry results show that the virgin PET resin R_5 and R_6 had the lowest and highest molecular weights respectively. Resin R_6 also had the highest value of yield strength correlating that higher molecular weight to yield strength values. The 100 % rPET resin had molecular weight in range with virgin PET resins. Increase in molecular weight also increases the zero shear viscosity due to increased polymer chain entanglement.

4.4. DSC Results; Crystallinity Measurements

DSC experiments were performed on the pellet and preform samples. For the preforms, DSC was performed on different sections of the preform to study the crystallinity along the preform length. Three stretched samples from each type of resin were analyzed for crystallinity values. The pellet samples were found to have the highest crystallinity (Table 4). This was expected since the pellet samples are hard and also opaque.

Figure 40 shows the DSC curves from the first heating cycle for the pellet samples and the finish portion of the preform samples. The preform samples had similar DSC curves, except for the gate portion which had a smaller peak of cold crystallization (see Appendix D). Crystallization distribution along the length of the preform was studied at 6 different locations as shown in Figure 39.

Table 4: Crystallinity results for all samples

DSC Results First Heating Cycle						
Resin Type	**Sample Type**	**Melting Temperature (T_m)**	**Glass Transition Temperature (T_g) First Heating**	**Heat of Melting of 100% Crystalline PET ΔH_m**	**Difference of Heat of Melting and Crystallization (ΔH_m-ΔH_c)**	**Crystallization**
		˚C	**˚C**	**J/g**	**J/g**	**%**
50% rPET Preform	**Finish**	247.95	75.4	140	1.002	0.72
	Support Ledge	247.53	75.53	140	-2.533	1.81
	Body 1	248.71	75.1	140	-4.907	3.51
	Body 2	247.68	72.83	140	-2.613	1.87
	Base/Nipple	248.19	73.8	140	-4.985	3.56
	Gate	247.51	73.47	140	-16.92	12.09
Virgin PET Resin R1 Preform	**Finish**	248.17	75.41	140	0.1679	0.12
	Support Ledge	248.4	72.87	140	-0.5053	0.36
	Body 1	248.55	75.53	140	-5.961	4.26
	Body 2	248.02	73.34	140	-3.937	2.81
	Base/Nipple	247.85	73.85	140	-2.726	1.95
	Gate	248.4	72.87	140	-16.83	12.02
100% rPET Preform	**Finish**	249.25	75.95	140	-3.359	2.40
	Support Ledge	247.91	73.6	140	-1.574	1.12
	Body 1	251.19	72.66	140	-9.61	6.86
	Body 2	248.71	71.1	140	-2.757	1.97
	Base/Nipple	251.19	72.66	140	0.4201	0.30
	Gate	247.91	73.6	140	-14.96	10.69
Virgin PET Resin R1	**Pellet**	234.98	89.45	140	-59.19	42.28
100% rPET	**Pellet**	229.75	81.26	140	-53.4	38.14

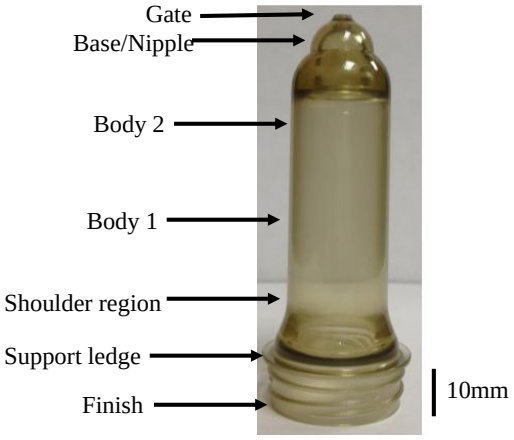

Region on Preform	Distance from Finish Portion (mm)
Finish	2
Support Ledge	10
Body 1	35
Body 2	50
Base/Nipple	65
Gate	70

Figure 39: Preform nomenclature and region distribution.

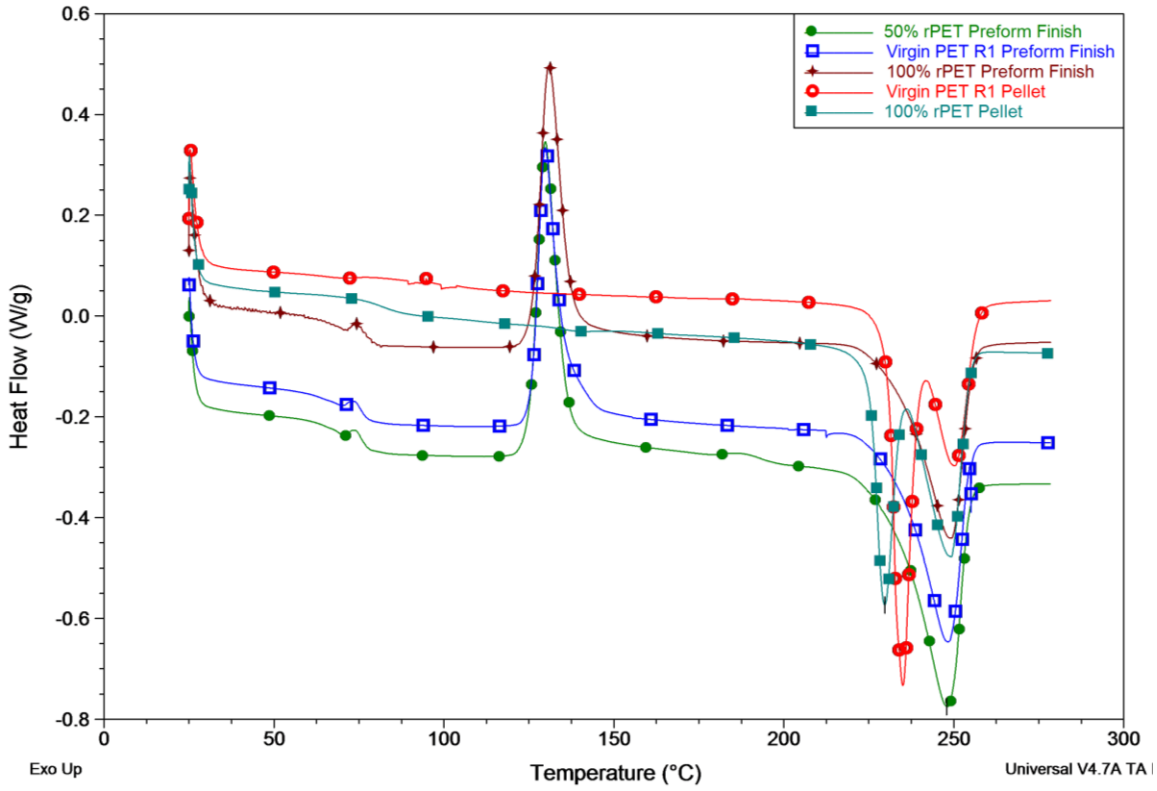

Figure 40: DSC first heating curves for pellet samples and trend for preform samples.

DSC results for 100 % rPET samples also did not show considerable differences in the melting temperatures and glass transition temperatures as compared to virgin PET samples. The only significant difference was for the 100% rPET sample from the central part of the preform which had a melting temperature of 251.1˚C which was around 3˚C higher than other samples for the same region. The portion also showed a crystallinity level of 6.8 % while the resin R1 and 50 % rPET samples showed crystallinity levels of 4.5 % and 3.5 % respectively.

After studying the crystallinity levels in the preform samples right after their production from the injection molding process, it was interesting to study the crystallinity

levels in stretched samples after tensile testing. The samples which were stretched at higher extension rates showed crazing during the stretching process itself. The stretched samples had high crystallinity values.

Table 5: DSC results for stretched preform samples after stretching at 50mm/min extension rate.

Sample	Melting Temperature (T_m)	Heat of Melting of 100% Crystalline PET ΔH_m	Difference of Heat of Melting and Crystallization (ΔH_m-ΔH_c)	Crystallization
	˚C	J/g	J/g	%
50% rPET	249.81	140	-56.59	40.42
Virgin PET Resin R1	251.38	140	-52.28	37.34
100% rPET	250.86	140	-45.75	32.68

4.5. Color Measurement Results

The color measurements were done on 8 different preform samples of different resins. The yellowness index, the percentage transmission and the absorbance values were determined. The Y transmission value is a very good single value indicator of the transmission values obtained over various wavelengths. All the data obtained was normalized based on the wall thickness of each of the preform samples.

The sample description, wall thickness measurements, Y transmission values and the yellowness index (YI) values are shown in Table 6. The Y transmission value was the highest (31.49) for the virgin PET R1 preform since it was completely clear and had maximum clarity. The 50 % rPET preform also showed high Y transmission value. However the addition of rPET content in the sample showed a drop in the transmission value as compared to virgin PET R1. Y transmission value for the 50 % rPET preform

sample had the highest value among the other samples. It is interesting to note that the presence of reheat additive in virgin PET resin R2 reduces the transmission value significantly as compared to virgin PET resin R7 (R2 without reheat additive). The difference in the values between the tensile preform samples (samples 1-4) and production preform samples (samples 5-8) could also be attributed to the fact that the region of the preform which was exposed to the light was higher for the tensile preform though very marginally. The lowest transmission was observed for the rPET preform sample number 7 with toner added to it to mitigate the yellowing.

Table 6: Y Transmission and Yellowness Index values for all samples.

Sample No	Sample Description	Wall Thickness (mm)	Y Transmission	Yellowness Index(YI)
1	Virgin PET Resin R1	1.46	31.49	5.64
2	50% rPET	1.46	25.03	19.03
3	Sample R8	1.46	21.21	7.78
4	100% rPET	1.46	23.47	23.22
5	Virgin PET Resin R2	2.39	15.10	1.93
6	Virgin PET Resin R7	2.32	17.40	2.44
7	Sample R9 (100% rPET with Toner)	3.43	3.15	6.70
8	20% rPET	2.42	12.50	8.84

The yellowness index values (Table 6) was highest for the 100 % rPET preform followed by the 50 % rPET preform because they had the highest content of rPET in them. This was followed by the 20 % rPET preform sample and the rPET preform sample (R9) with toner added to it. However the addition of color agents or toners to the preform can bring down the yellowness levels as shown in the case of sample number 7 which was 100% rPET sample with toner added to it (Table 6).

The values of percentage absorbance and percentage transmittance are shown in Table 7 for four different wavelengths; 355nm, 550nm, 750nm and 1050nm which is scattered over the visible and near infrared spectrum. Figure 41 shows normalized spectral plot for transmission values over different wavelengths. The range of wavelength measured is from 350nm-1150nm. The focus of these measurements was to observe the percentage transmission and absorbance values with varying wave length.

Table 7: Percentage transmittance and absorbance values for different samples.

Sample No/ Wave Length	Percentage Transmittance				Percentage Absorbance			
	355 nm	550 nm	750 nm	1050 nm	355 nm	550 nm	750 nm	1050 nm
1	10.281	31.596	33.897	34.541	0.562	0.233	0.212	0.205
2	1.774	25.342	31.116	33.582	1.089	0.295	0.233	0.212
3	7.610	21.267	23.658	25.349	0.651	0.349	0.315	0.295
4	1.164	23.836	30.644	33.911	1.212	0.315	0.240	0.212
5	1.326	14.916	17.402	17.678	0.628	0.188	0.159	0.155
6	3.974	17.336	18.884	19.026	0.448	0.172	0.155	0.155
7	0.166	2.974	8.848	10.023	0.656	0.289	0.152	0.134
8	0.690	12.417	16.252	16.793	0.736	0.215	0.169	0.161

The normalized absorbance plots are shown in Figure 42. The absorbance values were high for all samples in the ultra violet region (up to 400nm). However, when in the visible light region (390nm-750nm), the samples with rPET content in them showed higher values. The samples R_8 and R_9 (with toner) also showed high values of absorption compared to virgin PET samples like R_1 and R_2. This can be attributed to the darker appearance of these samples. From the spectral graph in Figure 42, the absorption values are initially high and slowly fall on reaching the near infrared spectral region (>750 nm).

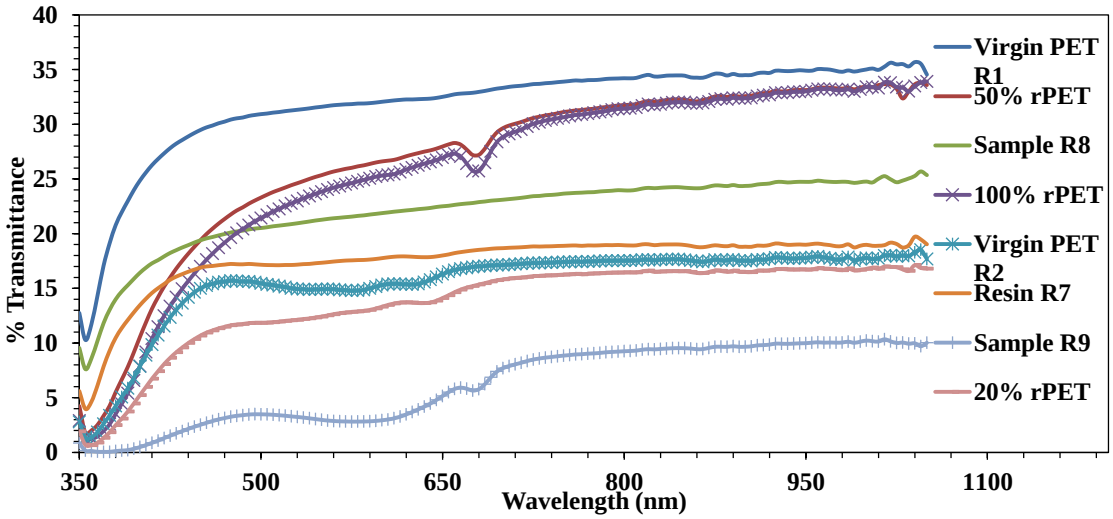

Figure 41: Normalized plot of percentage transmittance.

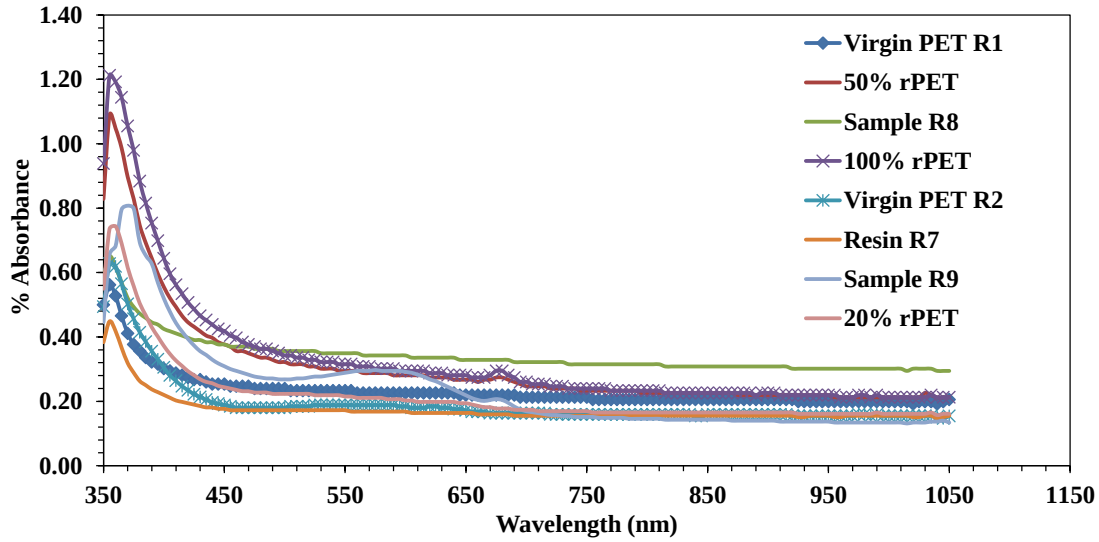

Figure 42: Normalized plot of absorbance.

4.6.Friction Testing Results

The friction tests were performed on 3 types of resin for the bottles and 5 types of resin for the preform samples. The tests were run for 30 seconds for the preform samples

and 60 seconds for the bottle samples. 200 g (1.96 N) normal load was used for the bottles while 100 g (0.981 N) normal load was used for the preforms

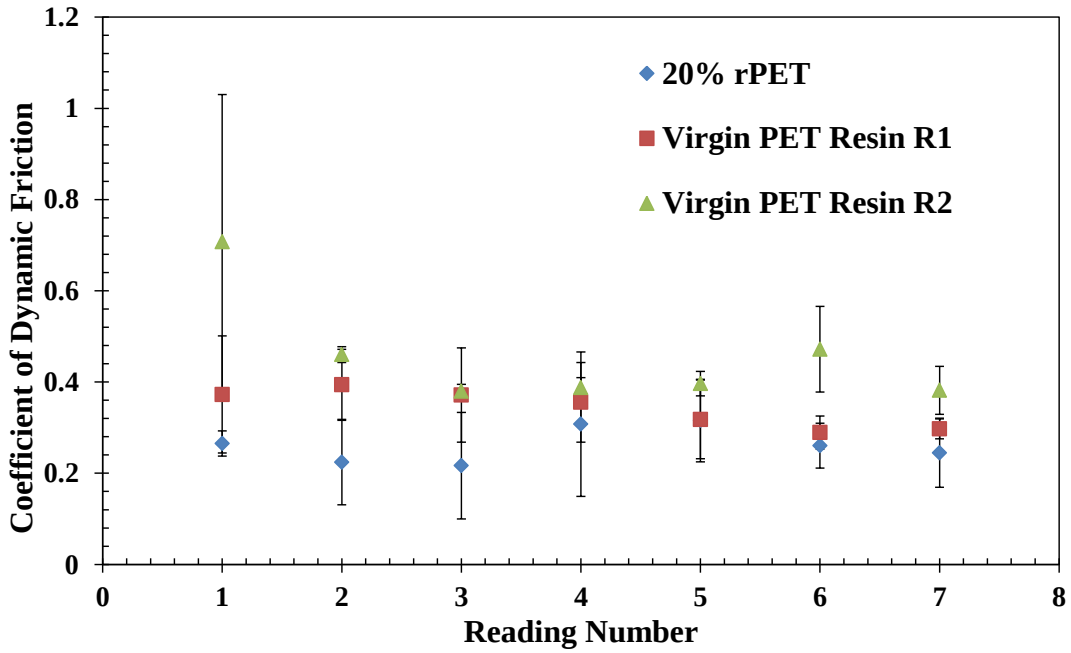

Figure 43: Dynamic friction coefficient for bottles.

The friction results for the bottle samples (Figure 43) showed virgin PET resin R_2 to have the highest values for the friction coefficient followed by the virgin PET resin R_1 and the 20 % rPET bottles. This was an interesting result since the other resin in the 20 % rPET bottle was R_2. For the preform samples (Figure 44), the rPET preform samples showed lowest friction coefficient values while virgin PET resins R_5 and R_1 showed very high friction values.

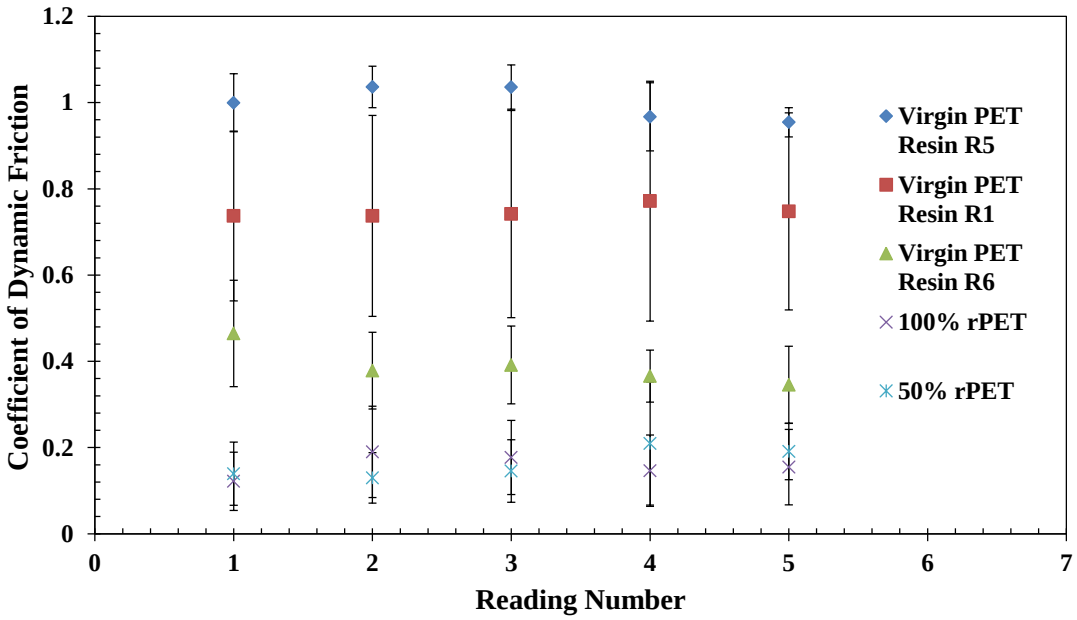

Figure 44: Friction coefficient for preforms.

4.7. Wall Thickness Measurements

Wall thickness measurements (Figure 45) for 20 % rPET bottle have been tabulated (See Appendix G Table 16) and the variation of thickness over the length of the bottle measured from the top has been plotted. Wall thickness measurements show a steady pattern with highest value of thickness near the neck region of the bottle. The thickness near the ribs region of the bottle is almost uniform. The lowest thickness is found near the base of the bottle. A total of 17 bottle samples were tested for wall thickness. The virgin PET resin R1 bottles for the same design did not show any difference. The values of wall thickness were used as input for the FE simulations.

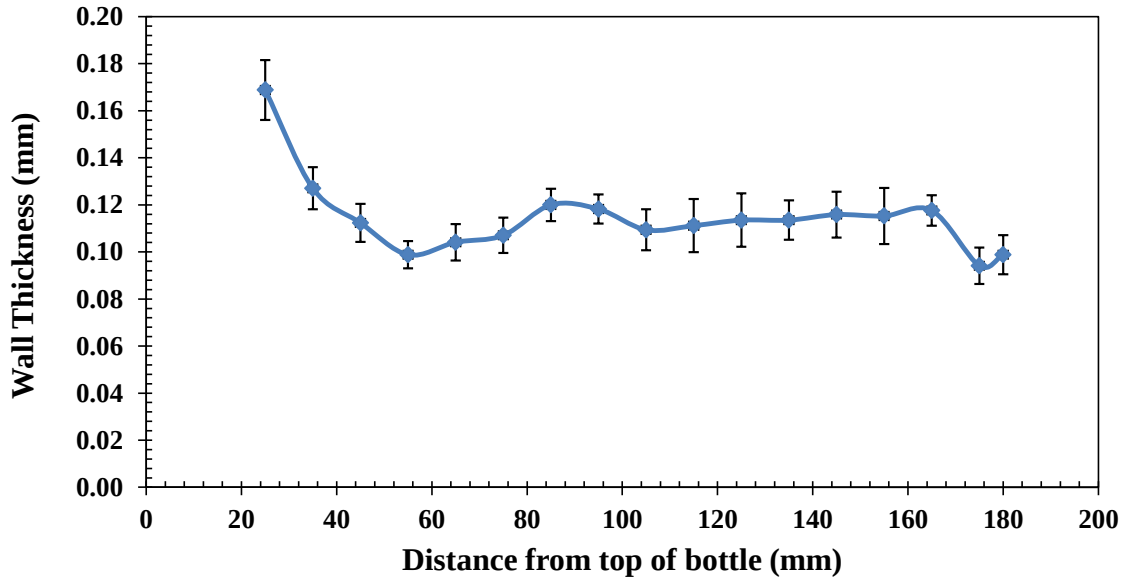

Figure 45: Wall thickness values for 20 % rPET bottle. [137]

4.8. Hoop Strength; Feel Test Results for Bottle Stiffness

Hoop strength was determined for 3 different types of bottles (Figure 46). The virgin PET R_2 bottles had the highest stiffness values followed by the 20 % rPET bottles. The lowest stiffness was found in the virgin PET R_1 bottles. Resin R_2 bottles were the best performers among this set of bottles which achieved high stiffness with a moderate weight. The bottle with rPET content also had stiffness values greater than virgin PET R_1 which further suggests that rPET was performing similar to virgin PET.

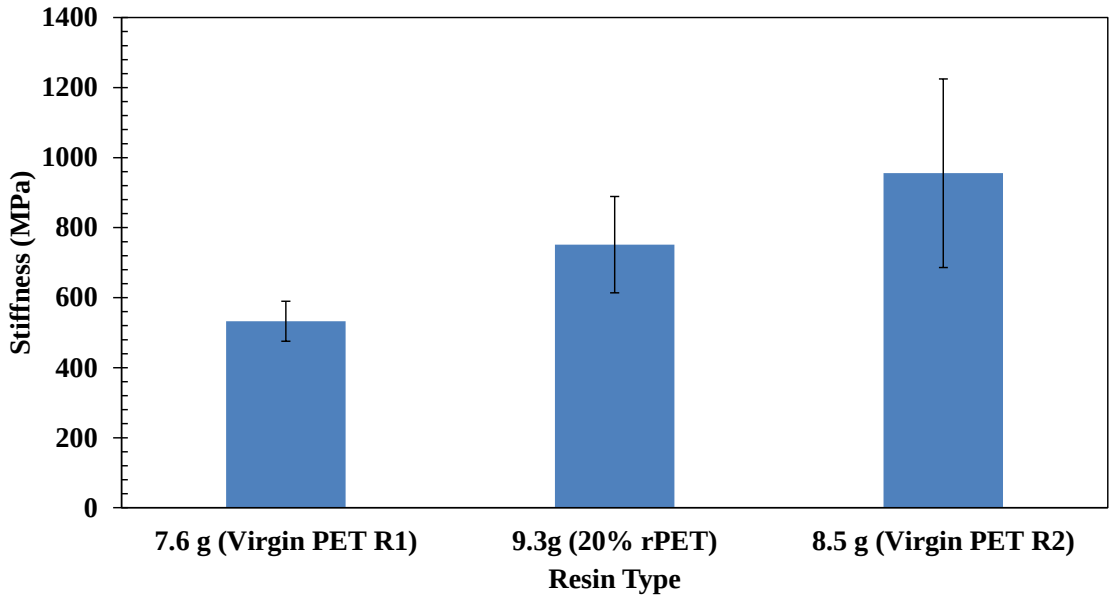

Figure 46: Hoop Strength (Stiffness values) for different bottles.

4.9.Top Load Results

The top load for 0.5L 20 % rPET and virgin PET R_1 bottles of the same design are shown in Figure 47. The 20 % rPET bottles were also tested for empty bottle top load. The top load results for the 20 % rPET bottles are very encouraging since they are above industry standards considered at about 75 lbf [138]. The average top load values for the rPET bottle were actually higher than that measured for the virgin PET R_1 bottle of the same design.

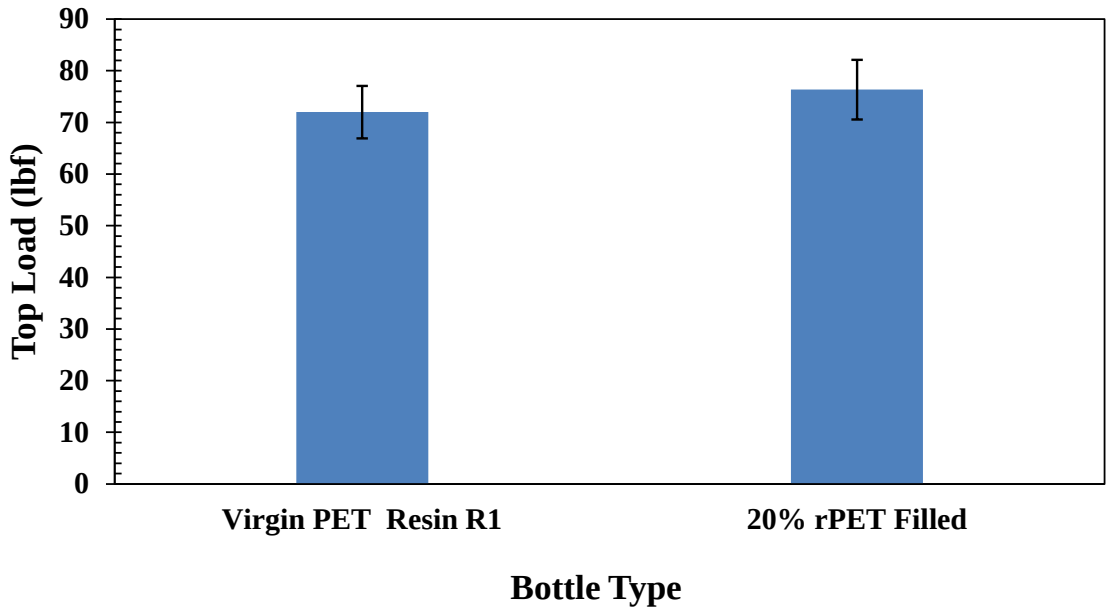

Figure 47: Top load results for bottles.

4.10. Density Measurements

Density measurements from preform samples are listed in Table 8. The density of all the resins did not see considerable differences. 100 % rPET had the highest density among samples measured.

Table 8: Density values for different resins.

Sample Description	Density (g/cc)
Virgin PET Resin R1	1.325
50% rPET	1.278
100% rPET	1.330
Virgin PET Resin R2	1.310
Virgin PET Resin R7	1.323
20% rPET	1.327
Virgin PET Resin R6	1.335

4.11. Energy Cost Results

Table 9: Energy saving data.[141]

Blow Molding Energy (KWh) per 1000 Bottles			
PET Resin	**10.2g Bottle**	**9.65g Bottle**	**9.17g Bottle**
R1	4.75	4.26	-
R7	4.54	4.19	-
R4	-	3.47	2.25
R2	-	3.36	-
20% rPET	-	-	2.14

The energy savings data for different resins are listed in Table 9. The energy savings is calculated from the power consumption readings for the blow molding machines at Niagara Bottling LLC. The machine was found to be running with an average consumption of around 65 amps for the period of May 2012. While running virgin PET resin R1, the consumption was found to reduce to 60 amps and for the 20 % rPET runs, the consumption was found to have lowered to 57 amps which meant a 5 % reduction in energy usage. Also the overall preform temperatures were reduced form 118˚C to 113˚C, thereby reducing the energy consumption of the oven. The heating lamps intensity was also reduced from 100 % to 95 % [142]. The comparison for the blow molding energy required (Table 9) for the same bottle design showed virgin PET (Resin R1) consuming 2.25 KWh energy while the rPET bottle consumed 2.14 KWh which was a 5% energy saving.

4.12. FEM Results for Lean Test

The lean test was performed on a 0.5L bottle design using material properties for the resins; virgin PET resin R_1, R_6, R_3 and 100% rPET. The buckling behavior of the bottle was studied based on inferences from the load vs. displacement curves as well as

the buckling stress values. The values for the Young's modulus and the density were changed for the resins R_1, R_3, R_6 bottle and the 100% rPET bottle.

The lean test results for the virgin PET resin R_6 and 100% rPET 0.5L bottles are shown in Figure 48 and Figure 49. The leaning behavior for the bottle design was similar. Bottles with resins R_6 and R_1 had higher buckling stress values compared to the one with rPET resin, whereas rPET bottle performed better than virgin PET resin R_3 bottle. There was a rise and fall in the loads with the change in the buckling behavior in the ribs near the waist region of the bottle. The deformation and stress distribution was highest near the waist region and no damage was found in the base of the bottle. The bottle design was able to withstand the load applied without significant damage for both the resins. The bottle's behavior can be explained in six different stages,

1. Stage 1 is the maximum load condition when the load first begins to act on the bottle, initial buckling occurs.
2. Stage 2 is a point where there is fall in the load.
3. Stage 3 is where the stress begins to shift to different section of the bottle.
4. Stage 4 is when the buckling begins to occur near the waist region, the load is low, but slowly rises.
5. Stage 5 involves rise in load again and shift in buckling to other ribs.
6. Stage 6 has a fall in load again; the deformation and stress is distributed to the ribs in the waist region and partly near the label panel at the end of bending.

Load Displacement curve from lean test on Virgin PET (R6 Resin) bottle

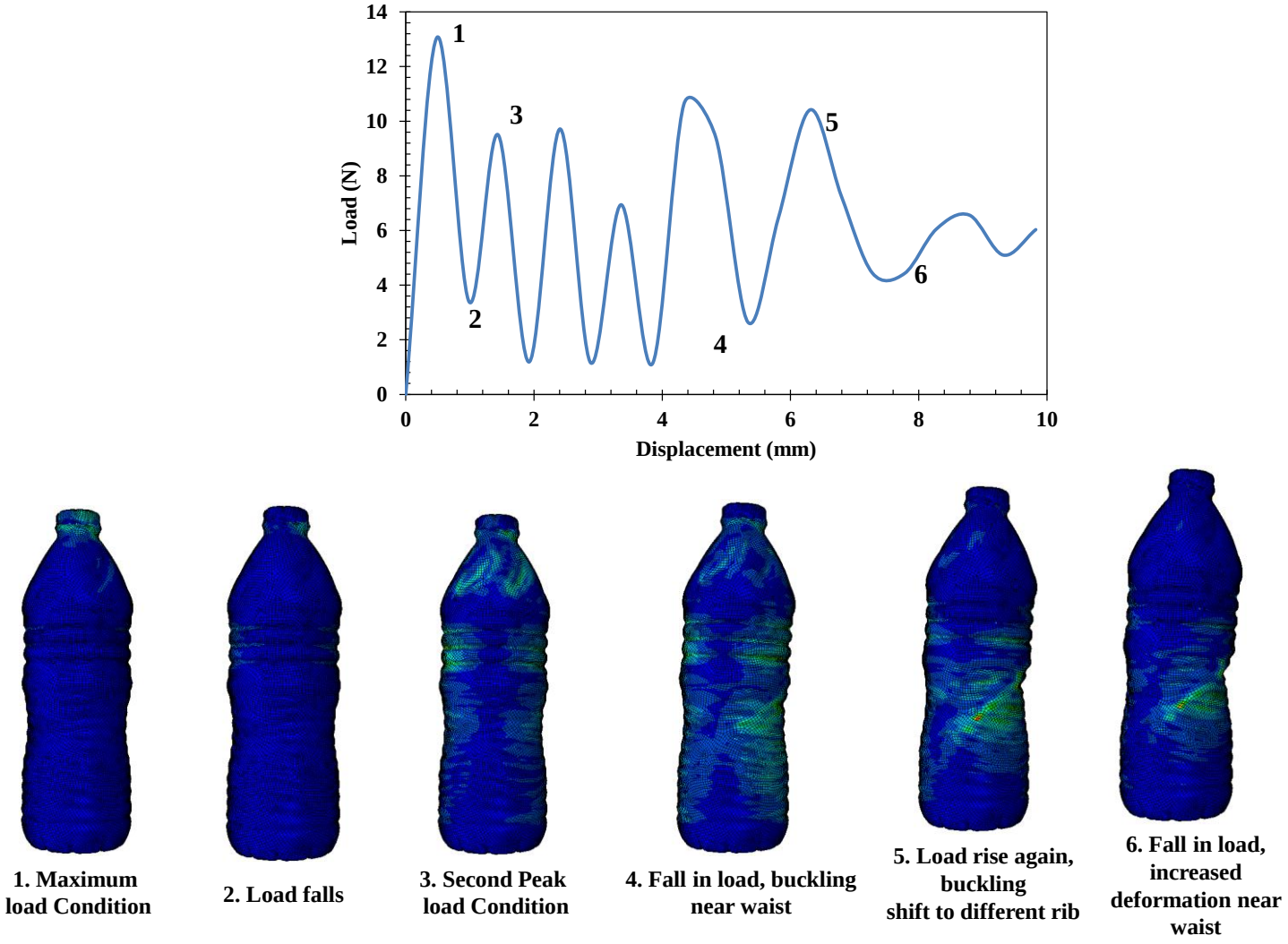

Figure 48: Lean Test FE Simulation results on Virgin PET (Resin R6) 0.5L Bottle

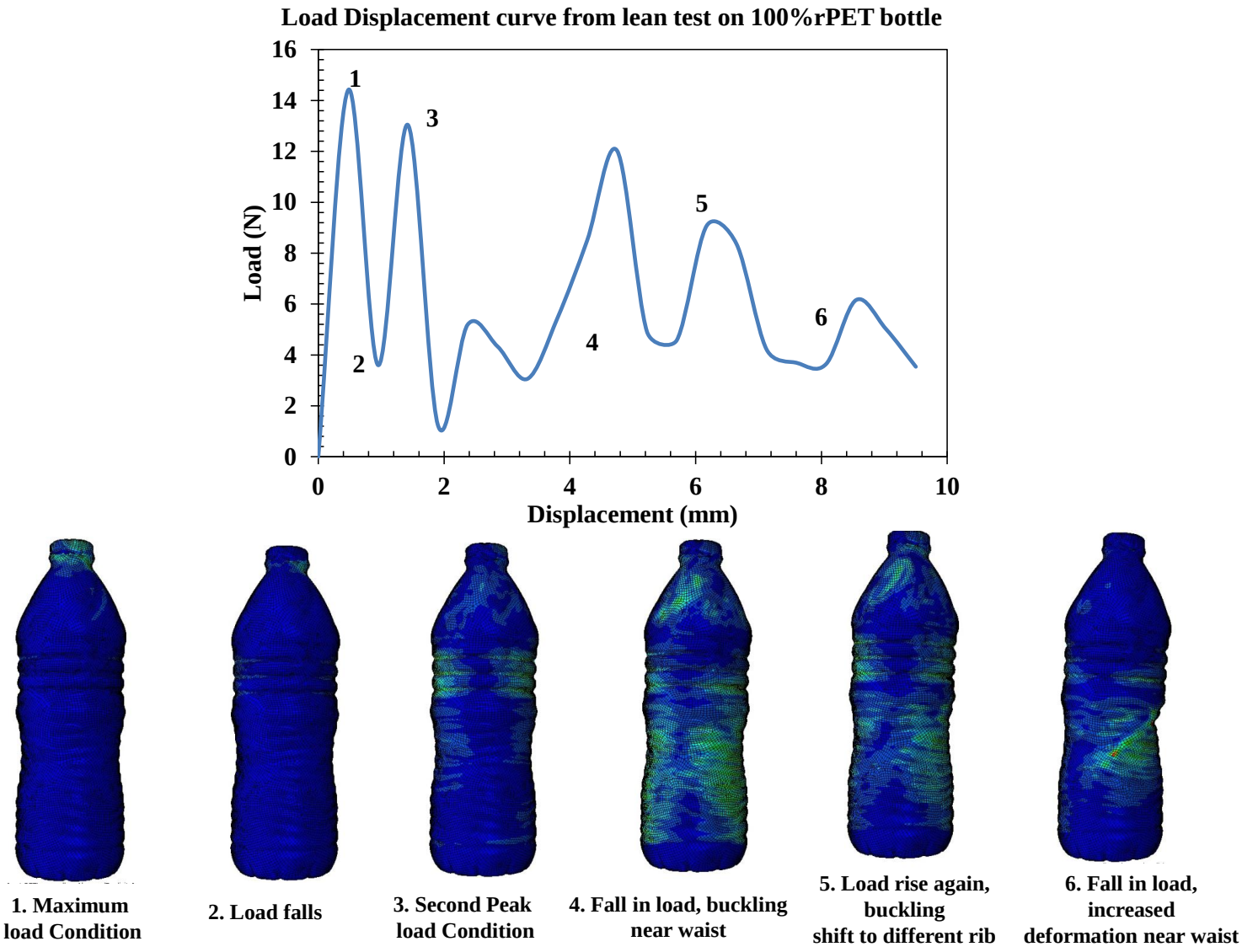

Figure 49: Lean test FE simulation results on 100% rPET 0.5L bottle

CHAPTER V

5. DISCUSSION

While PET recycling is steadily increasing over the years, the percentage of recycled material used for bottling applications has been low compared to other applications. The major focus of this research is to understand the implications w.r.t. the processing, and performance in bottle to bottle PET recycling. Hence studying the mechanical properties and understanding the behavior of rPET for end product applications is very important.

5.1. Mechanical Behavior

The mechanical properties of rPET were found to be similar to virgin PET for the different strain rates tested. Only the toughness values showed difference for strain rates greater than 0.0278 s^{-1}. The resin mixtures and the number of processing cycles are factors which affect their mechanical performance. Among the 8 different resin types which were compared at quasi static strain rate (0.0028 s^{-1}), the Young's modulus (Figure 28) for the 100 % rPET resin and the 50 % rPET resin lies between the other virgin PET resins. This indicate that the values of Young's modulus of the resins with rPET content were within 1-5 % range of next nearest better performing virgin PET resin (See Appendix B).

In case of yield strength of the PET resins (Figure 29), the values range between 38 MPa to 60 MPa. The yield strength values for the rPET resins were near an average of 52 MPa which was among the higher end. Only virgin PET resins R_1 (non FRH) with 0.76 I.V. and resin R_6 with 0.8 I.V. had higher yield strength values. Resin R_2 and R_4 which contained fast reheat additives had lower yield strength; leaving the effect of fast reheat additive on the yield strength values questionable. This was also the case for Young's modulus. One could hypothesize that these values makes sense since the rPET could be a mixture of the resins tested as mentioned earlier. However, it is likely that the rPET resin also comes from heat-set and carbonated soft drink bottles so the mixture of potential properties could be even wider.

At higher extension rates (> 5 mm/min), the deformation behavior for the amorphous preform sample remained the same under steady state conditions (for extension rates 5, 10 and 50 mm/min). However, for extension rates above 100 mm/min, the preforms exhibited very limited plastic deformation. The change in the trend of the stress-strain curves (See Appendix C) could be attributed to the change in the molecular orientations and early crystallization with increasing strain rates which was observed by other researchers as well. [94, 103] .

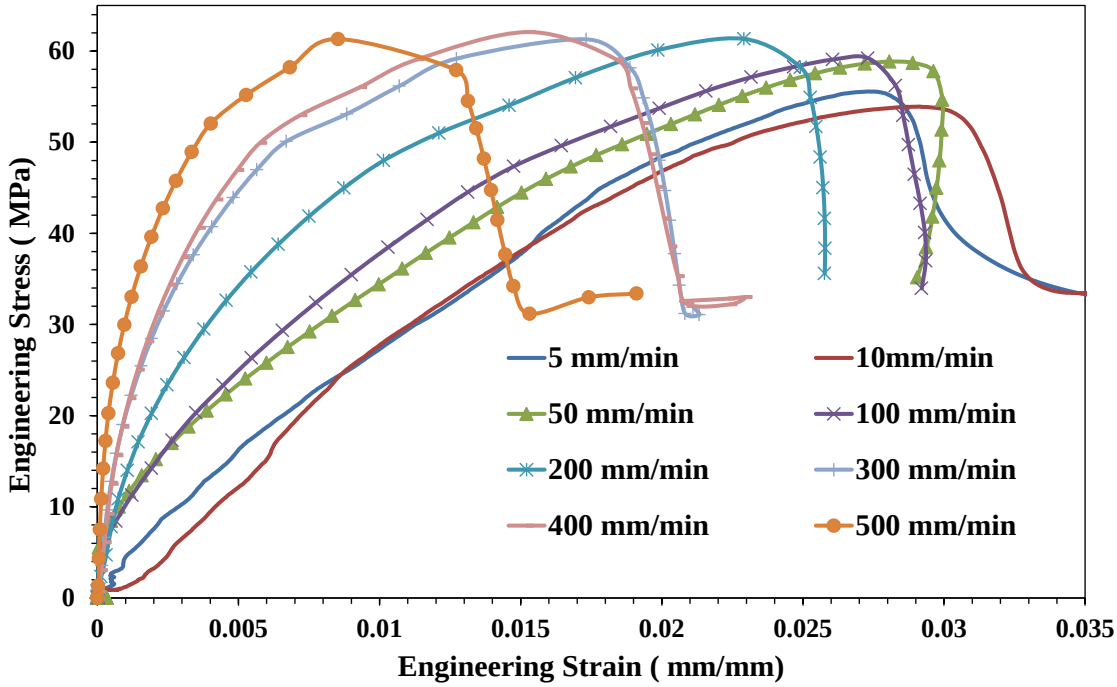

Figure 50: Engineering stress-strain curves up to strain level of 0.03 for 50 % rPET.

The portion of the stress-strain curve for different extension rates up to a stress level of 50 MPa is shown in Figure 50. The values of Young's modulus was found to increase with increasing strain rate, this was evident from the increasing slopes of the stress-strain curves. An exponential curve fit the trend of Young's Modulus (E) vs. strain rate as shown in Figure 51.

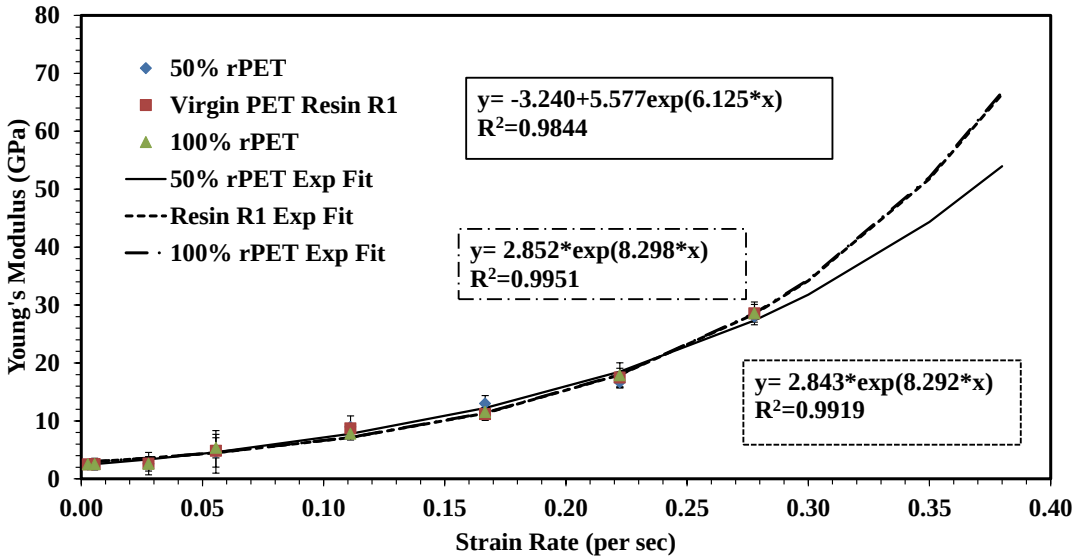

Figure 51: Increase of Young's modulus with strain rates and curve fitted plot.

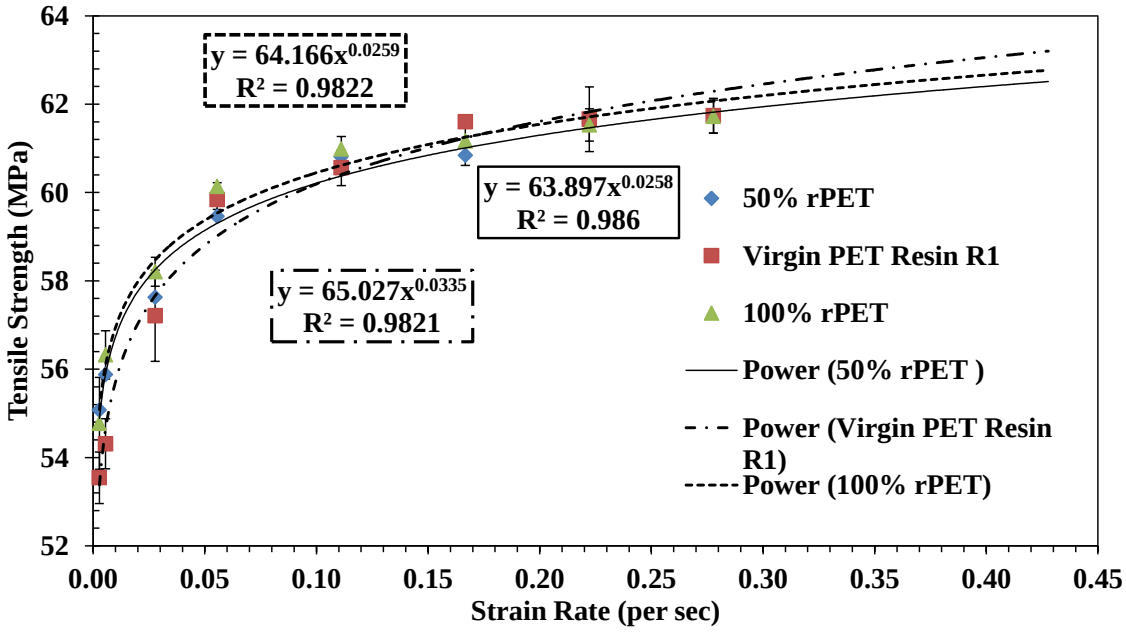

Figure 52: Increase of tensile strength with strain rate and power law curve fits.

A steady increase in the values of the tensile strength for higher strain rates was observed. The trend observed shows the most significant transition for strain rates greater than 0.05 s^{-1}. From the plot of variation of tensile strength with strain rate (Figure

52), the power fit equation provided the best fit with experimental results. However, the values for the tensile strength did not show significant variation at higher strain rates; 200 mm/min and above, the increase was around 1 % for each extension rate in steps of 100 mm/min. This trend is to be investigated further by testing for extension rates between 50mm/min and 100 mm/min to see the behavior at lower strain rates and understand the pattern.

The yield strength is a critical property since it helps understand resin behavior under different processing conditions and at higher stretching rates. It indicates when the material actually begins to deform plastically. On the lab-scale, these tests were performed at room temperature and one would require temperature controlled extension in order to directly relate these results to stretch blow molding.

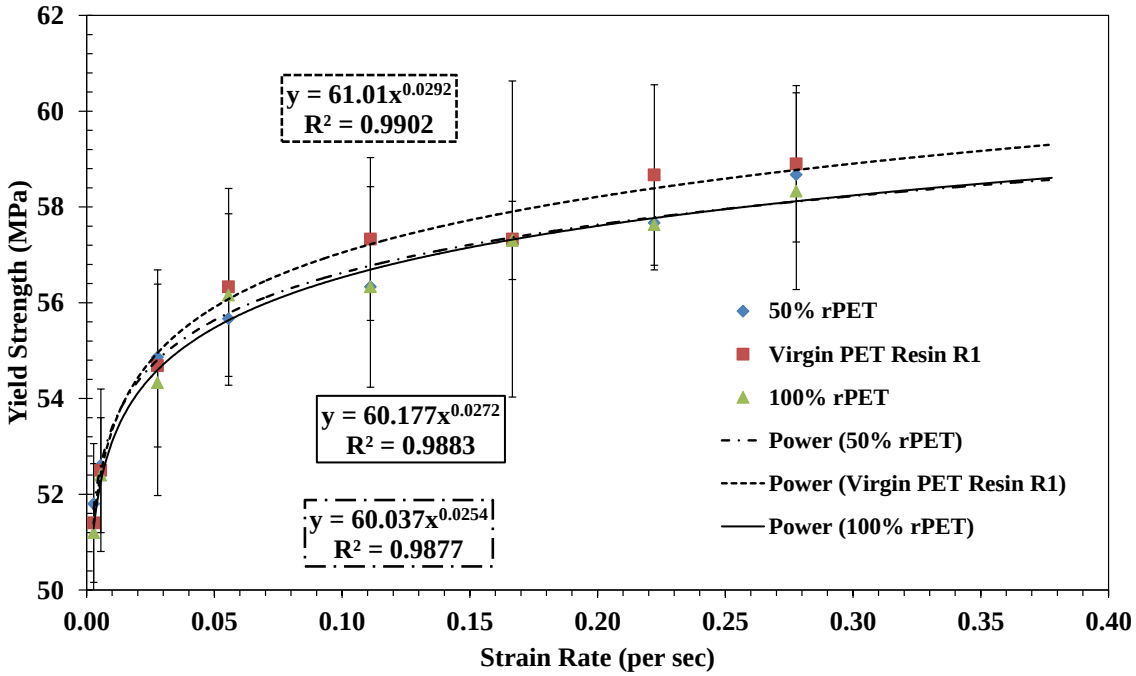

Figure 53: Curve fitting for yield strength vs. strain rate.

The yield strength values also increased with increasing strain rates. This increase also showed a similar trend to the tensile strength values. The closeness of values of (Figure 53) for extension rates higher than 100 mm/min for the yield strength could also be attributed to machine capability and accuracy of stretching at high extension rates. There might also be variations from machine to machine [105]. A Power law equation was the best fit (Figure 53) for yield strength vs. strain rate.

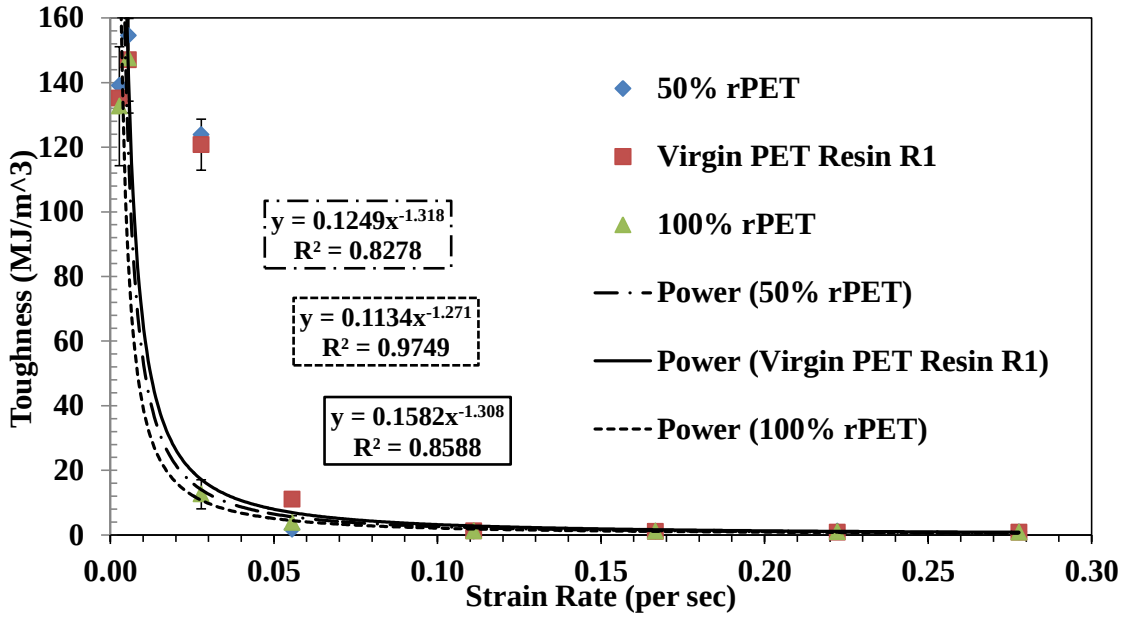

Figure 54: Curve fitting for toughness vs. strain rate.

Off all mechanical properties, the toughness showed the largest sensitivity to strain rate. In general, the toughness is the energy absorbed by the material before it fails. The results obtained were similar to published data [143] which suggests that at dynamic strain rates the ductility and the toughness values decrease. Early failure at higher strain rates is also attributed to the lack of time to allow the molecular chains to align and extend slowly; the fast stretching ends up breaking the molecular chains and causes an

early fracture. These results also relate to decrease in impact resistance for rPET as observed by Zanin and Mancini [84]. 100 % rPET had the largest drop in toughness values from extension rates of 50 mm/min (91.3 % drop) whereas 50 % rPET and virgin PET resin R_1 had the largest fall in toughness for extension rates above 50mm/min. The engineering stress-strain curves for the extension rate of 50 mm/min are shown in Figure 55, where the 100% rPET sample fails much faster at lower strain value compared to 50% rPET and virgin PET resin R_1. This relates to the drastic fall in toughness values. With more data points (Figure 54) at extension rates between 50 mm/min and 100 mm/min, their behavior can be studied further.

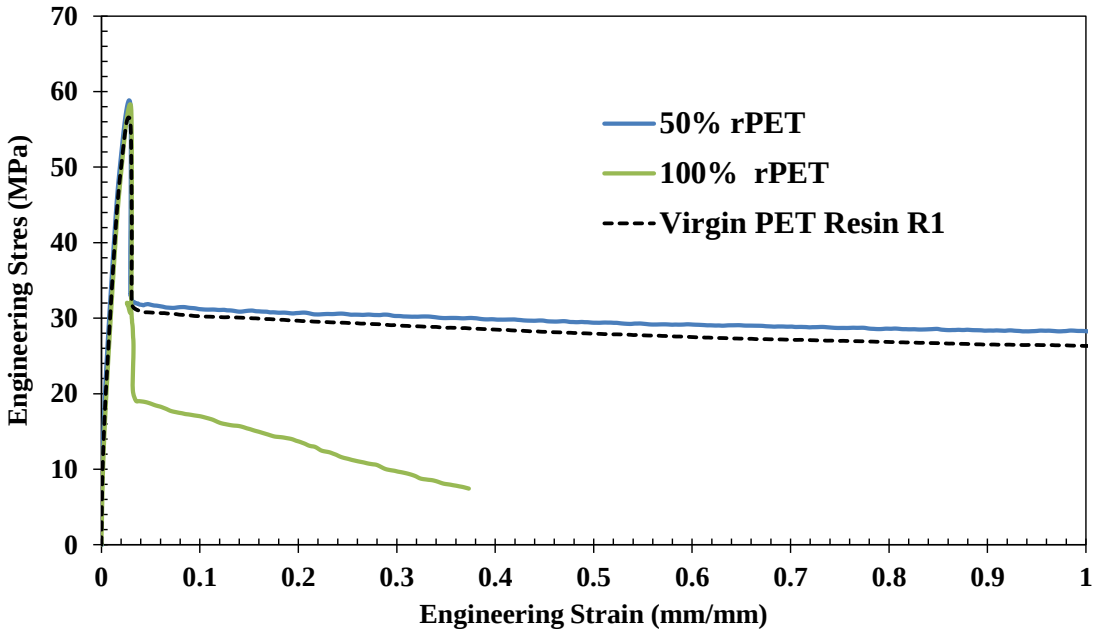

Figure 55: Engineering stress-strain curves for extension rate of 50mm/min. The 50% rPET and virgin PET failed off the scale at 4 mm/mm.

The efficacy of the mathematical equation to calculate toughness would need to be verified especially with respect to the large difference and abrupt drop in toughness

values for high strain rates. A good fit was obtained for the 100 % rPET resin with a power law. Curve fitting into the data will help to predict the sample behavior at intermediate and higher strain rates but other parameters that govern the material behavior at higher strain rates need to be considered.

5.1.1. Failure Behavior

A typical sample failure was close to the bottom end of the gage section (gate end). However, some samples failed near the shoulder (Figure 56). Failure location of the sample is related to stress concentration from defects, fixture design, and preform geometry.

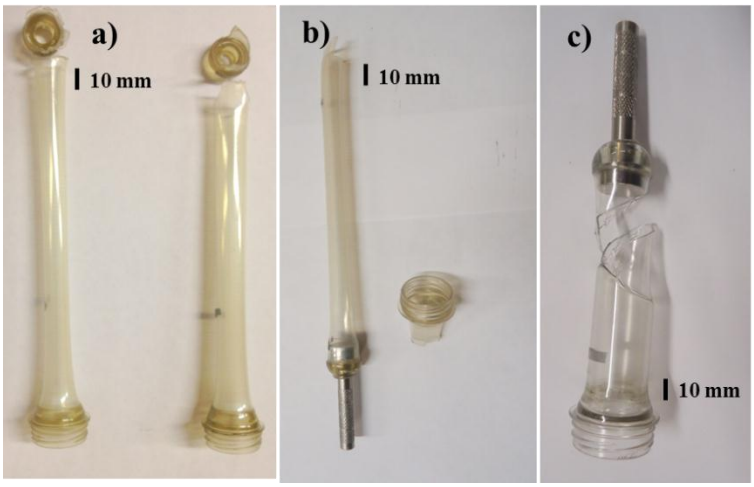

Figure 56: Typical sample failures a) Nipple b) Neck c) Brittle.

Brittle failure was observed in some samples, the samples which failed early at lower strain rates probably were defective samples and these were studied using a Polariscope (Figure 57). Defective samples did not have a uniform fringe distribution and showed blurry images. These fringes are associated with residual stresses. A sample with uniform fringe distribution was found to stretch up to 130 mm for testing under

quasi static strain rates. The samples which failed at higher strain rates had low toughness values. Brittle failure at higher strain rates caused the samples to shatter like glass. The 50% rPET samples had more brittle failure compared to the other resin samples tested. This can be related to mixing of the rPET resin and the virgin PET resin R_1.

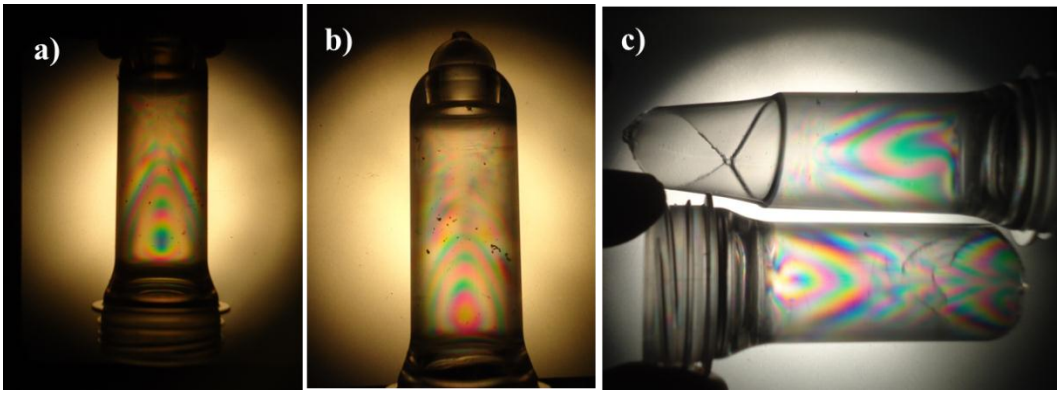

Figure 57: Polariscope images a) Expected fringe pattern b) Defective sample fringe pattern c) Failed sample images.

5.2. Crystallinity

The DSC results (Table 4) showed the pellet samples having a higher glass transition temperature than the preform samples. While the glass transition temperatures for the preform samples lies between 71-75 ˚C, the 100 % rPET pellet showed a T_g of 81.26 ˚C and the virgin PET resin R1 pellet showed T_g of 89.4˚C. The melting temperatures for the pellet samples (229 ˚C -234˚C) were lower than preform samples (247 ˚C -249 ˚C). There were no cold crystallization peaks (Figure 40) in the first heating cycle for the preform samples since the samples already had a high level of crystallinity.

The crystallinity in the preform samples did not exceed 4 % which confirmed that the samples were amorphous [8]. All the samples had similar DSC curves (See Appendix D). No significant rise or fall in melting and glass transition temperatures was observed on addition of rPET content to the virgin PET material. Figure 58 shows the crystallinity distribution for the preform samples at different locations on the preform. A significant rise in crystallinity was observed in the body 1 region which is the central region of the preform.

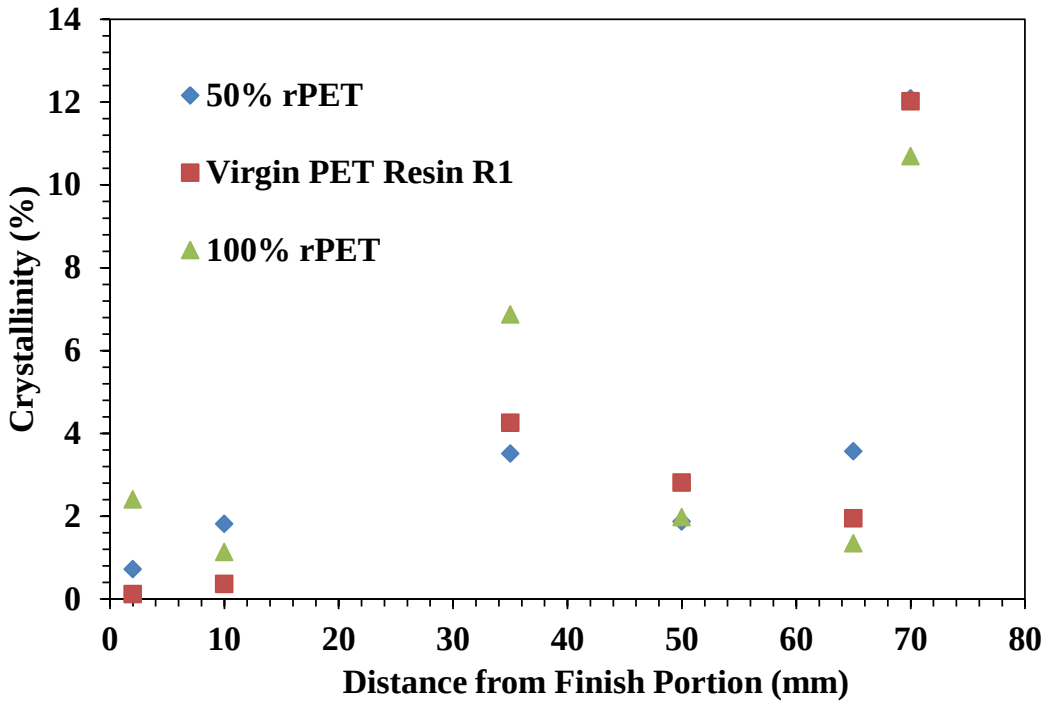

Figure 58: Crystallinity variation along preform for all resins.

However, only the gate region of the preform showed higher values of crystallinity (nearly 12 %). The gate of the preform is harder than the other regions of the preform and it governs the distribution of the material in the base region of the bottle during the stretch blow molding process. The gate of the preform is also white in color which indicates that there is some degree of crystallinity already imparted to it after the

injection molding process. This is due to the slower rate of cooling in this part of the preform with a major difference in the values of heat of melting and crystallization.

The DSC results on the stretched preform samples showed signs of strain induced crystallization which results from sudden temperature increase in the preform at high strain rates. The DSC results on samples taken from this failed portion of the preforms had signs of crazing (Figure 59) confirming effect of strain induced crystallization. There was a significant difference in the values of heat of melting and crystallization. The crystallinity values were close to that of pellet samples (35 %-40 %).

Figure 59: Failed preform samples with crazing after stretching at high extension rate.

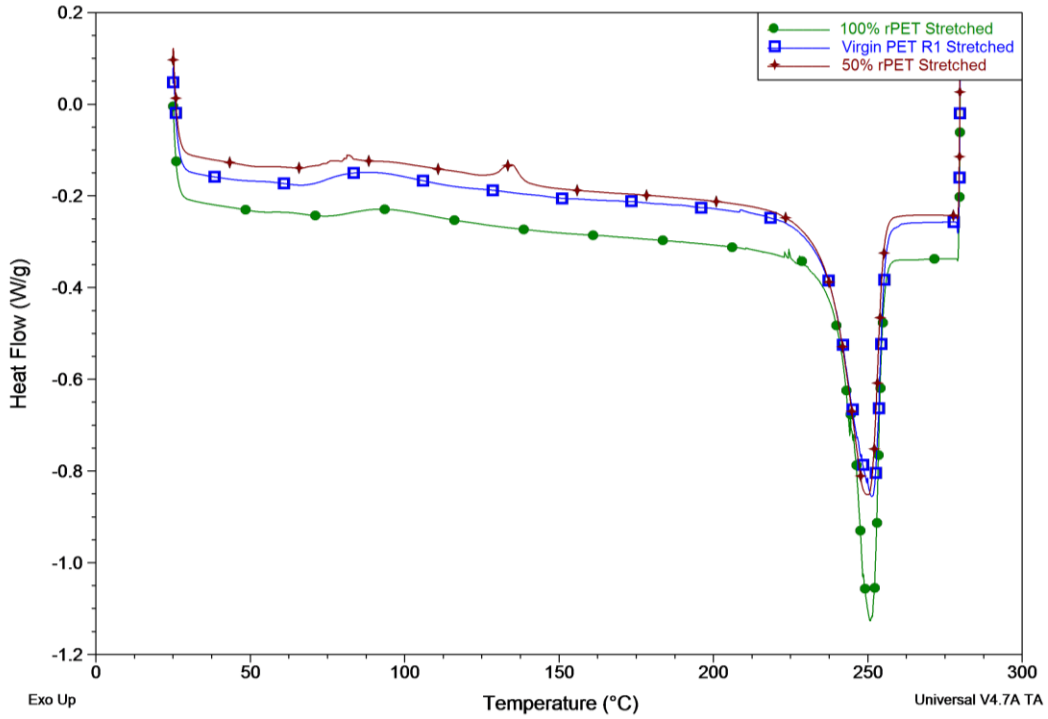

Figure 60: DSC curves for failed preform samples.

No significant cold crystallization peak was observed in the curves (Figure 60). The glass transition temperature zones were also not visible which indicated that the preform sample had already crossed the T_g zone and was now similar to a crystallized pellet sample. The highest crystallinity was observed for the 50 % rPET sample which also had the highest percentage of elongation at the extension rate of 50 mm/min. This can be related to a discussion where rPET is found to have better mechanical behavior when mixed with virgin PET.

5.3. Inferences from Yellowness Measurements

The yellowness index values from the color measurements showed rPET resins having higher values than virgin PET. This was expected since it is known that rPET tends to have higher degree of yellowness compared to virgin PET because of resin

reprocessing. The effect of adding toners to reduce yellowing is a viable option to reduce yellowing as evident from the results for sample number 7 which was a 100% rPET sample with toner added to it. The results showed a 71 % decrease in yellowness index value for the 100% rPET sample on addition of 4.5 % toner, however the value was still 18 % higher compared to virgin PET resin R_1. The yellowness index measurements also helps compare different rPET resins and choose the suitable resin that imparts a minimum yellowing effect. Results from this work also aid in setting a benchmark for accepted color levels.

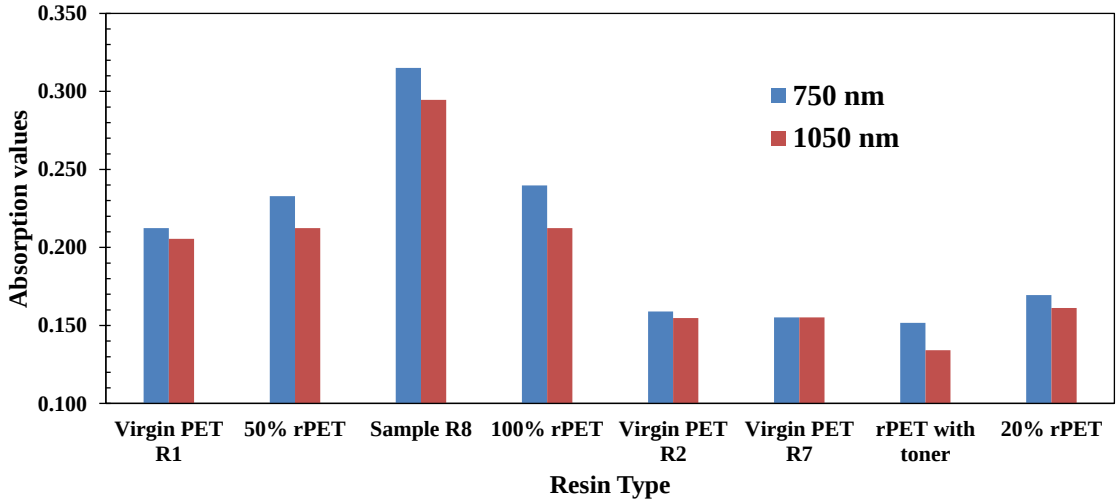

Figure 61: Absorption values for samples in IR region.

The higher absorption values (Table 7) of rPET in the near infrared spectral region (>750 nm) can be related to energy measurements, where the lamp temperatures and power consumption was lower when rPET resin was used, owing to faster absorption of IR light from the heating lamps in the blow molder. However since all the measurement values were normalized based on the wall thickness, samples having higher

wall thickness will bring down the values considerably, hence it would be necessary to perform the experiments on identical samples with same geometry.

5.4. End Product Behavior

After investigating the properties of the preform samples, it is very important to study the mechanical behavior of the end product which is the blow molded bottle. The bottle's friction behavior and its structural performance need to be discussed.

5.4.1. Friction

Results from the friction tests of the bottles showed that the rPET bottle had a lower value of coefficient of friction than the virgin PET bottles. A 55% difference was observed in the average values of coefficient of friction between the rPET bottle and virgin PET resin R_2 bottle which had highest values. In case of the preform samples, the virgin PET resin R5 had the highest friction coefficient values, which was 28% higher than the next nearest PET resin. All the virgin PET resins had higher friction coefficient values than rPET resin samples. The average values of the coefficient of friction are listed in Table 10 and Table 11.

Table 10: Average coefficient of friction values for preforms

Resin Type	R5	R1	R6	100% rPET	50% rPET
Avg Coefficient of Friction	0.999	0.747	0.389	0.158	0.163

Table 11: Average coefficient of friction for bottles

Resin Type	20% rPET	R1	R2
Avg Coefficient of Friction	0.262	0.343	0.455

Figure 62 shows the coefficient of friction with respect to time for the bottle samples. Over a longer period of time and after repeated measurements, it is observed that the friction values begin to decrease. The fluctuations seen in the curves are attributed to the parting line on the bottle which causes the peaks to show up. Also since the same section of the bottle comes in contact with each other after rotation, a periodicity in the trend can be observed. Some of the important factors which affect friction are the time for the test and the age of samples. There could possibly be more change in the values when the test is being run for longer period of time. The age of the samples might also influence the values since preforms which are obtained fresh after injection molding might exhibit more friction as compared to those samples which have been around for some time. The differences in the type of samples; production preform and tensile preform sample are also reasons for differences in values between rPET and virgin PET. The rigidity of the test setup for preform samples and the manufacturing process involved could be contributing parameters.

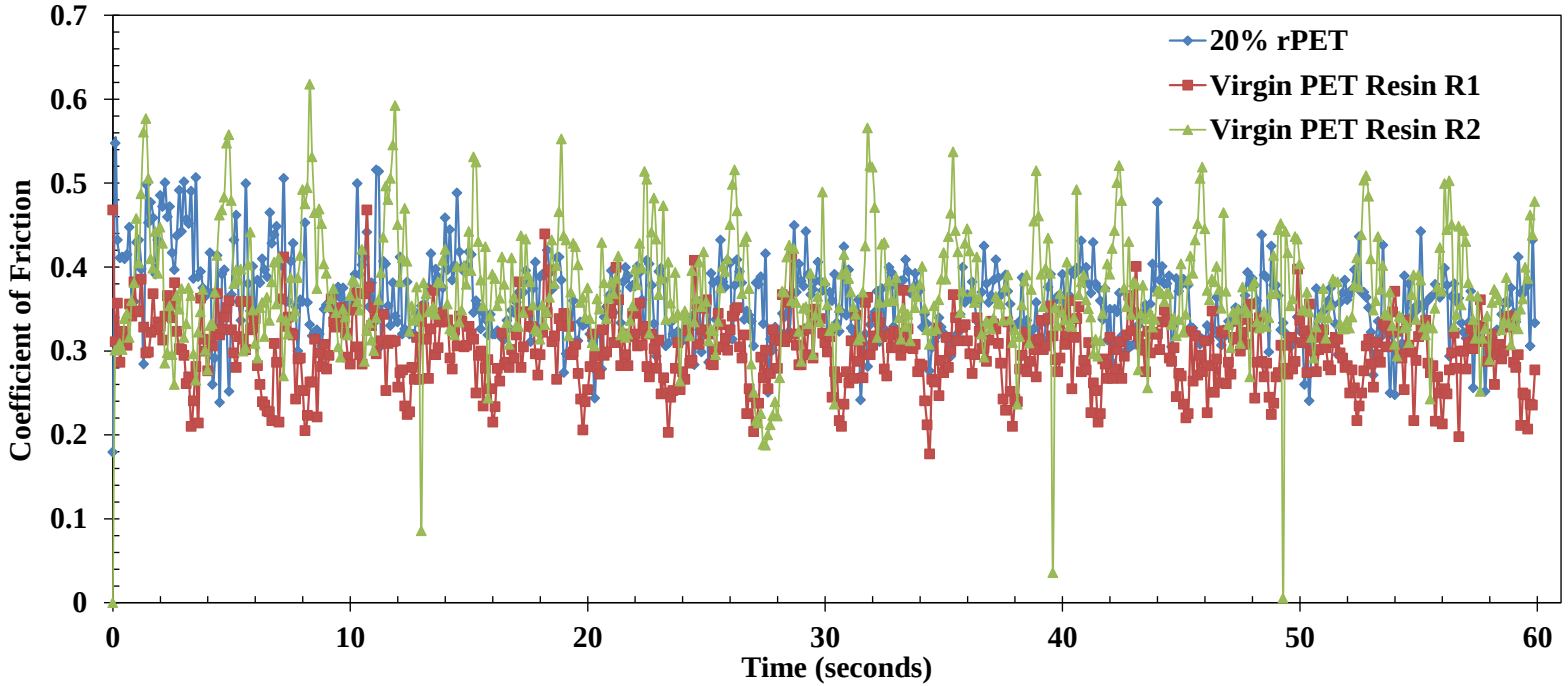

Figure 62: Friction coefficient with time for bottle samples.

The effect of change in bottle design also impacts the friction since the number of contact areas might vary based on the design. These tests help determine how different resins behave with respect to friction and can help in choosing the best resin.

5.4.2. Structural Performance

Variations in wall thickness values can be attributed to the processing conditions. With respect to industry relevance, wall thickness is measured to check the quality of the bottles. For example, if the wall thickness is low at certain regions, the blow molder needs to get adjusted to bring more plastic in that region. Checking the wall thickness helps understand the processing consistency of the blow molders.

The hoop strength (feel test) results have brought about an interesting discussion on the light weighting of bottles. While it is known that light weighting of the bottles tends to reduce its strength and structural performance, in some cases a bottle with lighter weight but a better design can still perform better than a bottle with higher weight because relatively ineffective design. This is seen in the case of the virgin PET resin R_2 bottle which had higher stiffness values while having a lower weight. A 27% increase in stiffness was observed for virgin PET resin R_2 bottle than the rPET bottle for a 9.4% lower weight. Top load results for the same bottle design showed rPET bottles having higher top load capability than virgin PET bottles. This is an encouraging result for rPET since both the bottles had similar wall thickness values and were blown using the same parameters.

5.4.3. Finite Element Simulation of Lean Test

The lean test FEM simulation result did not show variations in the buckling pattern of the bottle. However, there are significant differences observed in the lean stress (buckling stress) values of the bottles. The bottles with higher stiffness required more stress for deformation to occur. In order to obtain a proper ranking for the rPET

bottle, comparison was done on the same bottle design for rPET with other virgin PET resins having stiffness values on the extremes of the properties (Table 13). The difference in the Young's modulus values was highest (8%) between 100% rPET and virgin PET resin R_6. The difference between 100% rPET and virgin PET R_3 which had lower Young's modulus value was 16%.

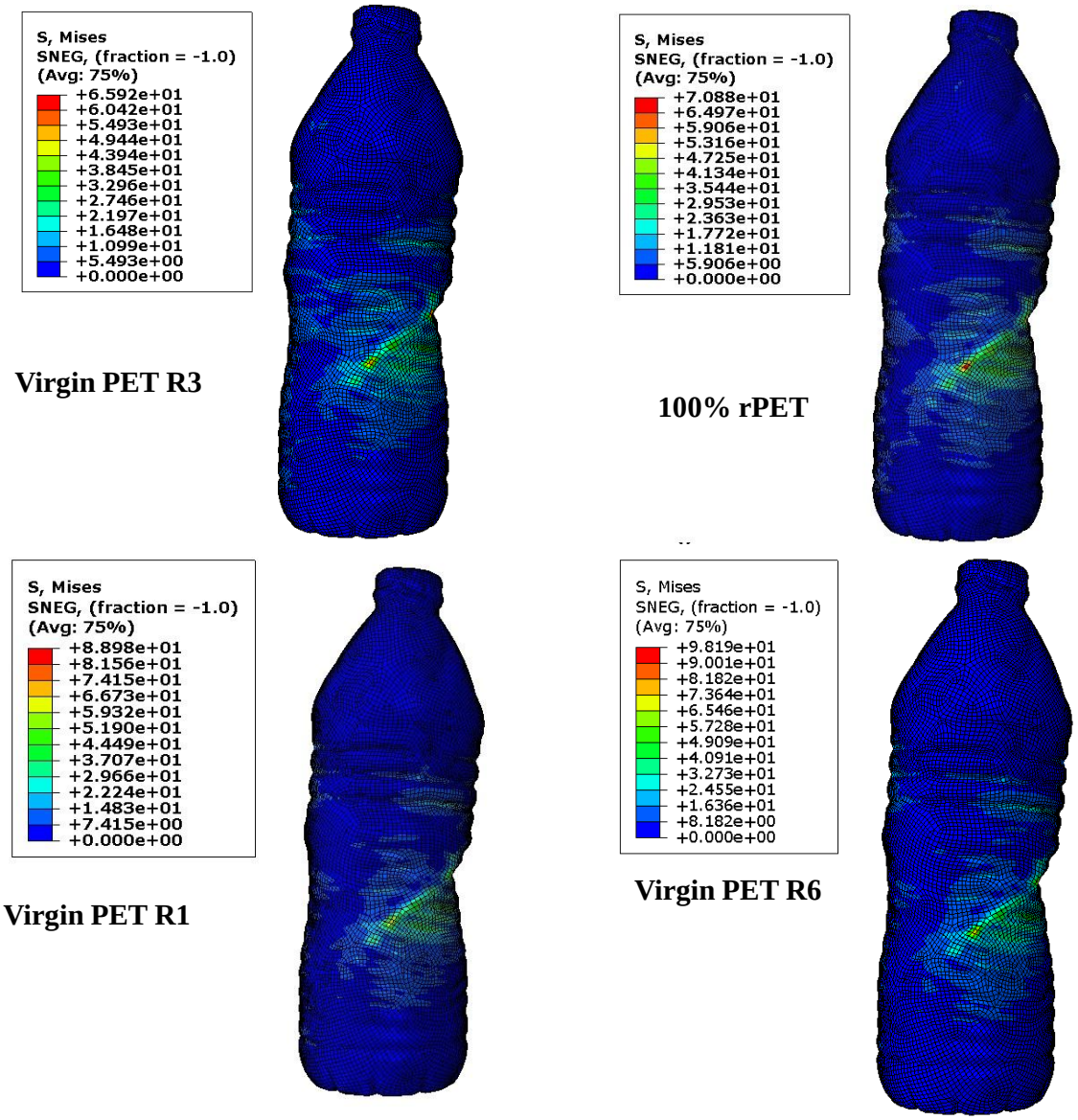

Figure 63: FE lean test simulation results for different resin bottles.

The buckling stresses distribution for different resins in shown in Figure 63. The buckling stress value was least for the virgin PET resin R_3 bottle which meant it required lower load to deform than the bottles from other resins. A 7% increase in buckling stress value was observed for the rPET bottle when compared to resin R_2.

The virgin PET bottle with resin R_6 was the best performing bottle which showed 32% higher buckling stress value than the rPET bottle meaning it would require an higher amount of load to cause an equivalent amount of deformation in that bottle. Since all the bottles were of the same design and processed on similar conditions, the rPET bottle's structural performance indicates that it lies in range with other virgin PET resins as exhibited earlier in case of the Young's modulus.

The load increases up to the initial buckling and the load fluctuation after this point is owing to the stress distribution in different sections of the bottle. The buckling of the bottle gradually progresses through several loading and unloading cycles. The loads to cause buckling fall with time. The critical loading condition is where the load first begins to deform the bottle. The stress is distributed to different sections of the bottle during the fluctuations. The change in material properties causes the difference in the load displacement curves (Figure 64).

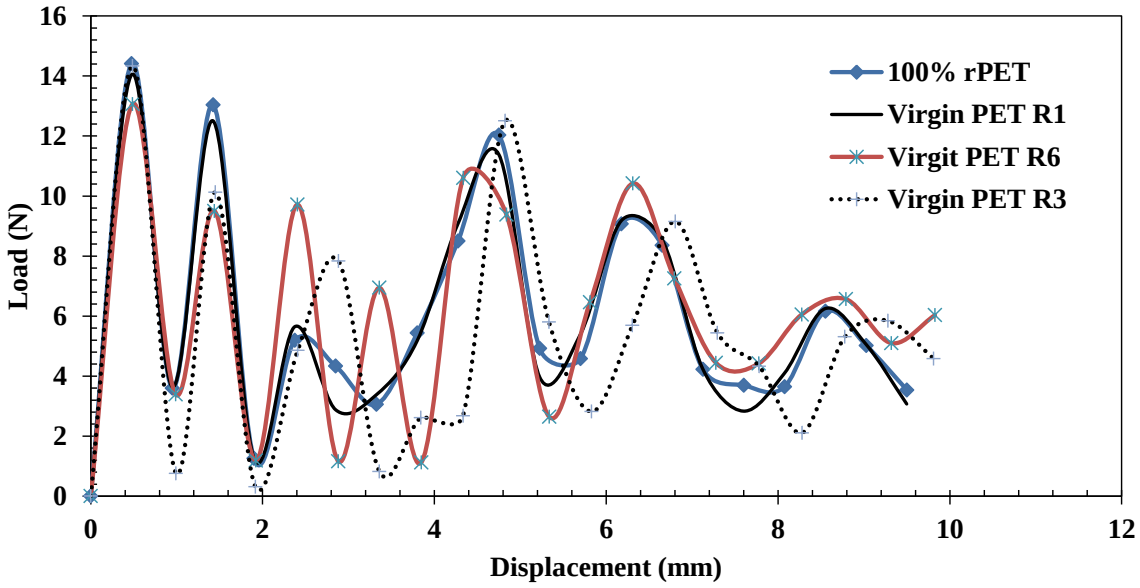

Figure 64: Lean test load-displacement curves for different resins

The bottle design has a significant impact on the leaning behavior, since buckling is distributed near the ribs and having greater rib depth creates stress concentration. The common deformation was observed near the waist and the bottom region of the bottle. There was no deformation to the base of the bottle which indicated that the bottle had a good design. A dynamic explicit analysis was chosen in order to study the behavior of the bottle over time in detail (20 time steps of 0.1 seconds each). A more detailed deformation behavior can be obtained by increasing the time steps.

The effects of change in wall thickness need to be studied further since it can cause significant change to the buckling behavior. An optimum bottle design under bending is expected to have no deformation in the lower region of the bottle and the base since this may cause the bottle to fail quicker.

CHAPTER VI

6. CONCLUSIONS

- This research has provided a clear framework for the comparison of mechanical properties of recycled PET (rPET) with other virgin PET resins. rPET is similar mechanically to virgin PET and bottle mechanical properties were also as good with rPET.
    - Tensile testing using the new tensile preform geometry and fixture on the preform samples was an effective method of determining the mechanical properties of the resin.
        - The results for Young's modulus showed that among 8 different PET resins compared, rPET was within the range of virgin PET resins.
        - Dynamic testing results showed an increase in Young's Modulus, tensile strength and yield strength from which curve fitting could predict behavior for higher strain rates as well as strain rates which were not tested. A fall in toughness values was observed.

    - A change in the trend of the yield properties was observed at a specific transition between 50 and 100 mm/min from steady state to dynamic rate limits.

- The DSC results from the dynamically stretched samples confirmed the effect of strain induced crystallization at room temperature from higher strain rates (>50 mm/min). This was associated with whitening or "crazing" in the polymer and was the same in rPET or virgin PET.
- All the samples used in the study were obtained from industrial injection molding machines, and hence the results were relevant to industrial operations.
- The crystallinity measurements along the length of the preform indicated a sufficient cooling rate, but that there are differences potentially due to cooling, shear, or geometry that impact crystallinity during injection. The preform samples were amorphous as confirmed by the DSC results. Both virgin PET and rPET had similar crystallinity.
- In rPET higher yellowness index values were observed. The effect of adding toners to reduce yellowing is also a viable option since it reduced the yellowness index values; A 71 % decrease in yellowness index value was observed for the 100% rPET sample on addition of 4.5 % toner, however the value was still 18 % higher compared to virgin PET resin R_1.
- Friction testing using the custom setup was an effective method for measuring friction on the preforms and bottles for different types of resins. rPET resin was found to have lower values of friction coefficient than some other virgin PET resins.

- The hoop strength results for the bottle stiffness showed rPET bottles having stiffness values close to virgin PET bottles
- A 5% decrease in total energy consumption was observed when rPET was blow molded compared to other virgin PET resins. This is a very encouraging result which would support using rPET on a larger scale and reducing the impact on the environment. This is supported by the higher IR absorption of rPET.
- Finite element lean test simulations showed similar deformation pattern for the bottles of different resins. The structural performance of rPET bottle was superior compared to some of the virgin PET resins used in industry.

CHAPTER VII

7. FUTURE WORK

The recycling rate for PET was 29 % in 2010. Efforts are being made to increase this recycling rate. However, application of rPET for large scale food grade applications has still not reached competitive levels compared to virgin PET. The difficulties with processing conditions, obtaining the recycled resin, market introduction, and the change in properties needs to be studied further. It will also be useful to study the differences in properties on samples made from rPET pellets and those made from flakes.

The dynamic behavior of rPET for industrial blow molding strain rates (10 s^{-1} to 12 s^{-1}), needs to be investigated further by considering effects of temperature and also with more accurate testing equipment. Comparison of experimental data with existing models and curve fitting would also need more validation with more data points in order to arrive at better dynamic models that can effectively predict the mechanical properties with change in strain rates.

The basis of comparison for rPET with virgin PET must be extended over to a larger number of resins in order to obtain a ranking for the rPET resin in terms of essential mechanical properties.

Comparison with heat-set and carbonated soft drink resins could explain some of the differences seen with resins traditionally used for cold fill applications. The crystallinity measurements need to be extended to different sections of a bottle to study crystallinity over the length of a bottle for different resins. DSC experiments on stretched samples at different extension rates also need to be studied to better understand sample failure and crystallinity at high strain rates. Flake samples would also need to be included in future studies.

Friction testing for different types of resins needs to be performed for better understanding of the friction behavior of bottles and preforms to save production time in industry and provide better solutions to solve problems due to friction. The friction testing procedure needs modifications with respect to the normal load applications and the tests needed to study friction behavior over longer periods of time. Top load testing and hoop strength measurements should be performed on bottles made with different rPET content in them to study differences with virgin PET.

Heating tests by melting rPET as well as virgin PET pellets to study differences in melt viscosity and yellowing imparted on repeated processing cycles needs to be carried out. Performing color measurements on bottle samples in addition to the preform samples would help in understanding the correlation between color measurements before and after the blow molding process. Also samples of the same thickness must be compared for better result inferences. The addition of toners and their effect on yellowness index values is also an area to study further.

FE simulations for top load, hoop strength, and lean tests on different bottle designs, with changes in material properties, wall thickness, and the effects of these on the structural performance will be of great interest. This could then be extended to FE simulations for drop tests and also for pallet packaging using improved meshing and modeling techniques.

REFERENCES

[1] PlasticsNews. (2010, 6/5/2012). Materials World Plastic Resin Consumption. [Online news article].

[2] D. W. Brooks and G. A. Giles, "PET Packaging Technology," ed: Blackwell Publishing.

[3] CMAI. (2010, 5/20/2012). Thermoplastic Market Review. *Global Plastics & Polymers* [Electronic article].

[4] SBA-CCI, "Strategic Consulting and Supply Demand Modeling for the PET Raw Material, Resin and Packaging Industry," in *Packaging Conference*, Las Vegas, 2011.

[5] Rohieb and Wikipedia. (2007, 5/15/2012). Structure formula of polyethylene terephthalate. [Electronic article].

[6] U. o. Bolton. (2012, 6/22/2012). Difference of thermoplastics and thermoset plastics. [Electronic article course topics].

[7] K. Ravindranath and R. A. Mashelkar, "Polyethylene terephthalate—I. Chemistry, thermodynamics and transport properties," *Chemical Engineering Science*, vol. 41, pp. 2197-2214, 1986.

[8] S. Bandla, "Evaluation and stability of PET resin mechanical properties," M.S. 1480967, Oklahoma State University, United States -- Oklahoma, 2010.

[9] H. E. H. Meijer and L. E. Govaert, "Mechanical performance of polymer systems: The relation between structure and properties," *Progress in Polymer Science,* vol. 30, pp. 915-938, 2005.

[10] KenPlas. (2012, 5/10/2012). What is PET (PolyEthylene Terephthalate). *Plastics Projects* [Electronic article].

[11] M. Tarr. (2011, 5/20/2012). Polymer materials and properties. *Course Topics Polymers* [Electronic article].

[12] J. Markarian. (2009, Additives and New Processes Improve rPET Properties. *SpecialChem*.

[13] D. A. Hannemann, "The Gneuss Online Viscometer," Gneuss Kunststofftechnik, Germany2012.

[14] W. J. Sichina. (2000, 5/20/2012). DSC as an Effective Tool: Measurement of Percent Crystallinity of Thermoplastics. [Electronic Resource Article].

[15] S. Venkataraman, *Orientation and Structure Development of Highly Crystalline and Clear Polyethylene Terephthalate (PET)*: University of Toledo., 1997.

[16] J. C. Viana, N. M. Alves, and J. F. Mano, "Morphology and mechanical properties of injection molded poly(ethylene terephthalate)," *Polymer Engineering & Science,* vol. 44, pp. 2174-2184, 2004.

[17] A. K. Oultache, X. Kong, C. Pellerin, J. Brisson, M. Pézolet, and R. E. Prud'homme, "Orientation and relaxation of orientation of amorphous poly(ethylene terephthalate)," *Polymer,* vol. 42, pp. 9051-9058, 2001.

[18] Y. Maruhashi, "Structure and physical properties of biaxially stretched polyethylene terephthalate sheets under different heat-set and stretch conditions," *Polymer Engineering & Science,* vol. 41, pp. 2194-2199, 2001.

[19] S. Nikolov, R. A. Lebensohn, and D. Raabe, "Self-consistent modeling of large plastic deformation, texture and morphology evolution in semi-crystalline

polymers," *Journal of the Mechanics and Physics of Solids,* vol. 54, pp. 1350-1375, 2006.
[20] C. D. Papaspyrides and S. N. Vouyiouka, *Solid State Polymerization*: John Wiley & Sons, INC., 2009.
[21] P. P. LLC. (2009, 4/1/2012). Solid State Polymerization. [Online Report].
[22] S. N. Vouyiouka, E. K. Karakatsani, and C. D. Papaspyrides, "Solid state polymerization," *Progress in Polymer Science,* vol. 30, pp. 10-37, 2005.
[23] F. Mallon, K. Beers, A. Ives, and W. H. Ray, "The effect of the type of purge gas on the solid-state polymerization of polyethylene terephthalate," *Journal of Applied Polymer Science,* vol. 69, pp. 1789-1791, 1998.
[24] T. M. Chang, "Kinetics of thermally induced solid state polycondensation of poly(ethylene terephthalate)," *Polymer Engineering & Science,* vol. 10, pp. 364-368, 1970.
[25] J. Gaymans R and J. Schuijer, "Polyamidation in the Solid Phase," in *Polymerization Reactors and Processes*. vol. 104, ed: AMERICAN CHEMICAL SOCIETY, 1979, pp. 137-148.
[26] P. V. Katsikopoulos and C. D. Papaspyrides, "Solid-state polyamidation of hexamethylenediammonium adipate. II. The influence of acid catalysts," *Journal of Polymer Science Part A: Polymer Chemistry,* vol. 32, pp. 451-456, 1994.
[27] D. N. Bikiaris, D. S. Achilias, D. J. Giliopoulos, and G. P. Karayannidis, "Effect of activated carbon black nanoparticles on solid state polymerization of poly(ethylene terephthalate)," *European Polymer Journal,* vol. 42, pp. 3190-3201, 2006.
[28] Y. Ma, U. S. Agarwal, D. J. Sikkema, and P. J. Lemstra, "Solid-state polymerization of PET: influence of nitrogen sweep and high vacuum," *Polymer,* vol. 44, pp. 4085-4096, 2003.
[29] F. J. Medellin-Rodriguez, R. Lopez-Guillen, and M. A. Waldo-Mendoza, "Solid-state polymerization and bulk crystallization behavior of poly(ethylene terephthalate) (PET)," *Journal of Applied Polymer Science,* vol. 75, pp. 78-86, 2000.
[30] S. A. Cruz and M. Zanin, "PET recycling: Evaluation of the solid state polymerization process," *Journal of Applied Polymer Science,* vol. 99, pp. 2117-2123, 2006.
[31] R. Vaidya, "Structural Analysis of Poly Ethylene Terephthalate Bottles using the Finite Element Method " Masters Thesis, Mechanical and Aersopace Engineering, Oklahoma State University, Stillwater, OK, 2011.
[32] J. Hanan, "OSU Niagara Capstone Design Project Preliminary Report," 2012.
[33] H. Ben Daly, B. Sanschagrin, K. T. Nguyen, and K. C. Cole, "Effect of polymer properties on the structure of injection-molded parts," *Polymer Engineering & Science,* vol. 39, pp. 1736-1751, 1999.
[34] D. J. Blundell, D. H. MacKerron, W. Fuller, A. Mahendrasingam, C. Martin, R. J. Oldman, R. J. Rule, and C. Riekel, "Characterization of strain-induced crystallization of poly(ethylene terephthalate) at fast draw rates using synchrotron radiation," *Polymer,* vol. 37, pp. 3303-3311, 1996.
[35] N. C. Lee, *Practical Guide to Blow Moulding*: Rapra Technology Limited, 2006.
[36] NAPCOR, "2010 Report on Post Consumer PET Container Recycling Activity,"

2010.
[37] J. Hopewell, R. Dvorak, and E. Kosior, "Plastics recycling: challenges and opportunities," *Philosophical Transactions of the Royal Society B: Biological Sciences*, vol. 364, pp. 2115-2126, July 27, 2009 2009.
[38] N. B. LLC, "Executive Summary Report on rPET," Report2012.
[39] E. P. News. (2012, 5/10/2012). Europe's 100% plastics waste goal. [Online news article].
[40] M. Edge, M. Hayes, M. Mohammadian, N. S. Allen, T. S. Jewitt, K. Brems, and K. Jones, "Aspects of poly(ethylene terephthalate) degradation for archival life and environmental degradation," *Polymer Degradation and Stability*, vol. 32, pp. 131-153, 1991.
[41] F. Awaja and D. Pavel, "Recycling of PET," *European Polymer Journal*, vol. 41, pp. 1453-1477, 2005.
[42] F. Welle, "Twenty years of PET bottle to bottle recycling—An overview," *Resources, Conservation and Recycling*, vol. 55, pp. 865-875, 2011.
[43] ngplasticscorp. (2012, 5/10/2012). Green PET Reduce, Reuse, Recycle. [Electronic article].
[44] T. Chilton, S. Burnley, and S. Nesaratnam, "A life cycle assessment of the closed-loop recycling and thermal recovery of post-consumer PET," *Resources, Conservation and Recycling*, vol. 54, pp. 1241-1249, 2010.
[45] E. P. Agency, "Reducing Greenhouse Gas Emissions through Recycling and Composting," Seattle, WA2011.
[46] B. Barbosa, "Recycled PET: The Whole Story," Niagara Bottling LLC. , Report2012.
[47] G. Churchward, A. Ebel, E. Kosior, O. Tait, A. J. Boots, and S. O. Boots, "WRAP, Closed Loop: Final Report: Large-scale Demonstration of rPET in Retail Packaging," WRAP, Closed Loop, United Kingdom2006.
[48] K. S. Rebeiz, "Time-temperature properties of polymer concrete using recycled PET," *Cement and Concrete Composites*, vol. 17, pp. 119-124, 1995.
[49] D. J. White, "Microstructure of Composite Material from High-Lime Fly Ash and RPET," *Journal of Materials in Civil Engineering*, vol. 12, pp. 60-65, 2000.
[50] H. NABIL, H. ISMAIL, and A. R. AZURA, "Recycled Polyethylene Terephthalate Filled Natural Rubber Compounds: Effects of Filler Loading and Types of Matrix," *Journal of Elastomers and Plastics*, June 1, 2011 2011.
[51] F. Ronkay and T. Czigány, "Development of composites with recycled PET matrix," *Polymers for Advanced Technologies*, vol. 17, pp. 830-834, 2006.
[52] P. Santos and S. H. Pezzin, "Mechanical properties of polypropylene reinforced with recycled-pet fibres," *Journal of Materials Processing Technology*, vol. 143–144, pp. 517-520, 2003.
[53] M. T. M. Bizarria, A. L. F. d. M. Giraldi, C. M. de Carvalho, J. I. Velasco, M. A. d'Ávila, and L. H. I. Mei, "Morphology and thermomechanical properties of recycled PET–organoclay nanocomposites," *Journal of Applied Polymer Science*, vol. 104, pp. 1839-1844, 2007.
[54] A. F. Ávila and M. V. Duarte, "A mechanical analysis on recycled PET/HDPE composites," *Polymer Degradation and Stability*, vol. 80, pp. 373-382, 2003.
[55] J. Scheirs, *Polymer recycling: science, technology, and applications*: Wiley,

1998.
[56] Bepex, "BePET Recycling Technology for rPET Report," Electronic report2011.
[57] K. S. Seo and J. D. Cloyd, "Kinetics of hydrolysis and thermal degradation of polyester melts," *Journal of Applied Polymer Science,* vol. 42, pp. 845-850, 1991.
[58] F. Samperi, C. Puglisi, R. Alicata, and G. Montaudo, "Thermal degradation of poly(ethylene terephthalate) at the processing temperature," *Polymer Degradation and Stability,* vol. 83, pp. 3-10, 2004.
[59] K. Breyer, K. Regel, and W. Michaeli, "Reprocessing of post-consumer PET by reactive extrusion " *Polymer Recycling (UK).* vol. 2, pp. 251-255, 1996.
[60] J.-M. Charrier, *Polymeric Materials and Processing: Plastics, Elastomers, and Composites*: Hanser Publishers, 1991.
[61] H. Inata and S. Matsumura, "Chain extenders for polyesters. IV. Properties of the polyesters chain-extended by 2,2′-bis(2-oxazoline)," *Journal of Applied Polymer Science,* vol. 33, pp. 3069-3079, 1987.
[62] H. Inata and S. Matsumura, "Chain extenders for polyester. II. Reactivities of carboxyl-addition-type chain extenders; bis cyclic-imino-ethers," *Journal of Applied Polymer Science,* vol. 32, pp. 5193-5202, 1986.
[63] M. Paci and F. P. La Mantia, "Influence of small amounts of polyvinylchloride on the recycling of polyethyleneterephthalate," *Polymer Degradation and Stability,* vol. 63, pp. 11-14, 1999.
[64] N. Cardi, R. Po, G. Giannotta, E. Occhiello, F. Garbassi, and G. Messina, "Chain extension of recycled poly(ethylene terephthalate) with 2,2′-Bis(2-oxazoline)," *Journal of Applied Polymer Science,* vol. 50, pp. 1501-1509, 1993.
[65] M. Paci and F. P. La Mantia, "Competition between degradation and chain extension during processing of reclaimed poly(ethylene terephthalate)," *Polymer Degradation and Stability,* vol. 61, pp. 417-420, 1998.
[66] F. Villain, J. Coudane, and M. Vert, "Thermal degradation of polyethylene terephthalate: study of polymer stabilization," *Polymer Degradation and Stability,* vol. 49, pp. 393-397, 1995.
[67] F. M. Schloss, "Decontamination of RPET by steam distillation," US Patent 5824196, 1998.
[68] L. R. Deardurff and D. W. Hayward, "Method for Optimization of RPET Decontamination," US Patent Application Publication US 2009/0093557 A1, 2009.
[69] D. W. Hayward, A. S. Martin, and F. M. Schloss, "Decontamination of RPET through particle size reduction," US Patent 5899392, 1999.
[70] D. W. Hayward and D. L. Witham, "Method for treating recycled polyethylene terephthalate " US Patent Application Publication US 2006/0189789 A1, 2006.
[71] H. A. Al-Ghatta, "Method for recycling polyethylene terephthalate (PET) beverage bottles by treating with carbon dioxide " US Patent 5073203, 1991.
[72] X-Rite, "A Guide to Understanding Color Communication," Michigan, USA, Report2007.
[73] CIE, "CIE Color Space," in *Commission internationale de l'Eclairage Proceedings*, 1932.
[74] TAPPI, "Indices for whiteness, yellowness, brightness, and luminous reflectance factor(Revision of T1216 sp-03)," in *T 1216*, ed, 2007.

[75] R. S. Hunter and R. W. Harold, *The measurement of appearance*, 2nd ed.: Wiley-Interscience, 1987.
[76] H. Labs, "Insight on Color, Yellowness Indices," Hunter Labs, Applications Note2008.
[77] ASTM, "E313 – 10 Standard Practice for Calculating Yellowness and Whiteness Indices from Instrumentally Measured Color Coordinates," ed. West Conshohocken, PA: ASTM International, 2010.
[78] Phoenix Technologies International, "rPET Resin Technical Processing Guide," 2011.
[79] T.-C. E. Tseng and J. C. Hanan, "Rheological Characterization of Poly(ethylene terephthalate) Resins Used in the Bottling Industry," presented at the ANTEC Boston, 2011.
[80] E. Tseng, "Resin Ranking Parameters," Personal communication/Presentation ed, 2012.
[81] N. Torres, J. J. Robin, and B. Boutevin, "Study of thermal and mechanical properties of virgin and recycled poly(ethylene terephthalate) before and after injection molding," *European Polymer Journal*, vol. 36, pp. 2075-2080, 2000.
[82] A. Pawlak, M. a. Pluta, J. Morawiec, A. Galeski, and M. Pracella, "Characterization of scrap poly(ethylene terephthalate)," *European Polymer Journal*, vol. 36, pp. 1875-1884, 2000.
[83] A. Oromiehie and A. Mamizadeh, "Recycling PET beverage bottles and improving properties," *Polymer International*, vol. 53, pp. 728-732, 2004.
[84] S. D. Mancini and M. Zanin, "Consecutive steps of PET recycling by injection: evaluation of the procedure and of the mechanical properties," *Journal of Applied Polymer Science*, vol. 76, pp. 266-275, 2000.
[85] E. Kosior, P. Pattabiraman, I. Sbarski, and T. H. Spurling, "Thermal and mechanical properties of recycled PET and its blends," ed, 2005.
[86] M. Kegel, I. Sbarski, P. G. Iovenitti, S. H. Masood, and E. Kosior, "Effect of additives on processing and physical properties of recycled polyethylene terephthalate (RPET)," ed, 2002.
[87] Y. Srithep, A. Javadi, S. Pilla, L.-S. Turng, S. Gong, C. Clemons, and J. Peng, "Processing and characterization of recycled poly(ethylene terephthalate) blends with chain extenders, thermoplastic elastomer, and/or poly(butylene adipate-co-terephthalate)," *Polymer Engineering & Science*, vol. 51, pp. 1023-1032, 2011.
[88] L. Incarnato, P. Scarfato, L. Di Maio, and D. Acierno, "Structure and rheology of recycled PET modified by reactive extrusion," *Polymer*, vol. 41, pp. 6825-6831, 2000.
[89] M. Kráčalík, L. Pospíšil, M. Šlouf, J. Mikešová, A. Sikora, J. Šimoník, and I. Fortelný, "Effect of glass fibers on rheology, thermal and mechanical properties of recycled PET," *Polymer Composites*, vol. 29, pp. 915-921, 2008.
[90] I. Rezaeian, S. H. Jafari, P. Zahedi, and S. Nouri, "An investigation on the rheology, morphology, thermal and mechanical properties of recycled poly (ethylene terephthalate) reinforced with modified short glass fibers," *Polymer Composites*, vol. 30, pp. 993-999, 2009.
[91] F. Fraïsse, V. Verney, S. Commereuc, and M. Obadal, "Recycling of poly(ethylene terephthalate)/polycarbonate blends," *Polymer Degradation and*

Stability, vol. 90, pp. 250-255, 2005.
[92] M. kh.Abunawas, "A Suitable Mathematical Model of PET for FEA Drop-Test Analysis," *International Journal of Computer Science and Network Security,* vol. 10, pp. 215-219, 2010.
[93] A. Mahendrasingam, C. Martin, W. Fuller, D. J. Blundell, R. J. Oldman, D. H. MacKerron, J. L. Harvie, and C. Riekel, "Observation of a transient structure prior to strain-induced crystallization in poly(ethylene terephthalate)," *Polymer,* vol. 41, pp. 1217-1221, 2000.
[94] G. H. Menary, C. W. Tan, E. M. A. Harkin-Jones, C. G. Armstrong, and P. J. Martin, "Biaxial deformation and experimental study of PET at conditions applicable to stretch blow molding," *Polymer Engineering & Science,* vol. 52, pp. 671-688, 2012.
[95] P. G. Llana and M. C. Boyce, "Finite strain behavior of poly(ethylene terephthalate) above the glass transition temperature," *Polymer,* vol. 40, pp. 6729-6751, 1999.
[96] A. M. Ghanem and R. S. Porter, "Cold crystallization and thermal shrinkage of uniaxially drawn poly(ethylene 2,6-naphthalate) by solid-state coextrusion," *Journal of Polymer Science Part B: Polymer Physics,* vol. 27, pp. 2587-2603, 1989.
[97] J. Y. Guan, L.-H. Wang, and R. S. Porter, "Planar deformation of amorphous poly(ethylene terephthalate) by stretching and forging," *Journal of Polymer Science Part B: Polymer Physics,* vol. 30, pp. 687-691, 1992.
[98] C. P. Buckley, D. C. Jones, and D. P. Jones, "Hot-drawing of poly(ethylene terephthalate) under biaxial stress: application of a three-dimensional glass—rubber constitutive model," *Polymer,* vol. 37, pp. 2403-2414, 1996.
[99] D. R. Salem, "Development of crystalline order during hot-drawing of poly(ethylene terephthalate) film: influence of strain rate," *Polymer,* vol. 33, pp. 3182-3188, 1992.
[100] E. D. Morrison, M. W. Malvey, R. D. Johnson, and J. S. Hutchison, "Mechanism of stress cracking of poly(ethylene terephthalate) beverage bottles: A method for the prevention of stress cracking based on water hardness," *Polymer Degradation and Stability,* vol. 95, pp. 656-665, 2010.
[101] J. S. Zaroulis and M. C. Boyce, "Temperature, strain rate, and strain state dependence of the evolution in mechanical behaviour and structure of poly(ethylene terephthalate) with finite strain deformation," *Polymer,* vol. 38, pp. 1303-1315, 1997.
[102] S. A. Jabarin, "Strain-induced crystallization of poly(ethylene terephthalate)," *Polymer Engineering & Science,* vol. 32, pp. 1341-1349, 1992.
[103] F. Chaari and M. Chaouche, "Rheooptical investigation of the crystallization of poly(ethylene terephthalate) under tensile strain," *Journal of Polymer Science Part B: Polymer Physics,* vol. 42, pp. 1915-1927, 2004.
[104] E. Gorlier, J. M. Haudin, and N. Billon, "Strain-induced crystallisation in bulk amorphous PET under uni-axial loading," *Polymer,* vol. 42, pp. 9541-9549, 2001.
[105] G. Dean and B. Read, "Modelling the behaviour of plastics for design under impact," *Polymer Testing,* vol. 20, pp. 677-683, 2001.
[106] G. M. Swallowe, *Mechanical Properties and Testing of Polymers: An A-Z*

Reference: Kluwer Academic, 1999.
[107] Q. Li, S.-l. Liu, and S.-y. Zheng, "Rate-dependent constitutive model of poly(ethylene terephthalate) for dynamic analysis," *Journal of Zhejiang University - Science A*, vol. 11, pp. 811-816, 2010.
[108] C. v. Dongen and R. D. E. Kosior, "Design Guide for PET Bottle Recyclability," EFBW, UNESDA2011.
[109] PETCORE, "Guidelines on Acceptability of Additives and Barrier Materials in the PET Waste Stream for an Effective Recycling of PET," PETCORE2003.
[110] D. H. Kang, R. Auras, K. Vorst, and J. Singh, "An exploratory model for predicting post-consumer recycled PET content in PET sheets," *Polymer Testing*, vol. 30, pp. 60-68, 2011.
[111] M. Edge, N. S. Allen, R. Wiles, W. McDonald, and S. V. Mortlock, "Identification of luminescent species contributing to the yellowing of poly(ethyleneterephthalate) on degradation," *Polymer*, vol. 36, pp. 227-234, 1995.
[112] D. E. James and L. G. Packer, "Effect of Reaction Time on Poly(ethylene terephthalate) Properties," *Industrial & Engineering Chemistry Research*, vol. 34, pp. 4049-4057, 1995/11/01 1995.
[113] G. J. M. Fechine, R. M. Souto-Maior, and M. S. Rabello, "Structural changes during photodegradation of poly(ethylene terephthalate)," *Journal of Materials Science*, vol. 37, pp. 4979-4984, 2002.
[114] C. Reynolds, "Color change in flake," J. Hanan, Ed., Personal communication ed. Husky, 2012.
[115] M. Edge, R. Wiles, N. S. Allen, W. A. McDonald, and S. V. Mortlock, "Characterisation of the species responsible for yellowing in melt degraded aromatic polyesters—I: Yellowing of poly(ethylene terephthalate)," *Polymer Degradation and Stability*, vol. 53, pp. 141-151, 1996.
[116] M. Software. (2008, Accelerating Time to Market with Bottle Simulation Event Automation.
[117] N. Dusunceli and O. U. Colak, "The effects of manufacturing techniques on viscoelastic and viscoplastic behavior of high density polyethylene (HDPE)," *Materials & Design*, vol. 29, pp. 1117-1124, 2008.
[118] M. Vigny, A. Aubert, J. M. Hiver, M. Aboulfaraj, and C. G'Sell, "Constitutive viscoplastic behavior of amorphous PET during plane-strain tensile stretching," *Polymer Engineering & Science*, vol. 39, pp. 2366-2376, 1999.
[119] J. Dees, "Preform Optimization using Non-linear Finite Element Simulations," in *ANTEC 2003*, 2003, pp. 842-849.
[120] S. Bagherzadeh, F. R. Biglari, and K. Nikbin, "Parameter study of stretch—blow moulding process of polyethylene terephthalate bottles using finite element simulation," *Proceedings of the Institution of Mechanical Engineers, Part B: Journal of Engineering Manufacture*, vol. 224, pp. 1217-1227, August 1, 2010 2010.
[121] G. H. Menary, C. W. Tan, C. G. Armstrong, Y. Salomeia, M. Picard, N. Billon, and E. M. A. Harkin-Jones, "Validating injection stretch-blow molding simulation through free blow trials," *Polymer Engineering & Science*, vol. 50, pp. 1047-1057, 2010.
[122] B. Demirel and F. Daver, "The effects on the properties of PET bottles of changes

to bottle-base geometry," *Journal of Applied Polymer Science,* vol. 114, pp. 3811-3818, 2009.
[123] R. van Dijk, J. C. Sterk, D. Sgorbani, and F. van Keulen, "Lateral deformation of plastic bottles: experiments, simulations and prevention," *Packaging Technology and Science,* vol. 11, pp. 91-117, 1998.
[124] J. Rowson, A. Yoxall, and J. H. Hart, "Modelling capping of 28 mm beverage closures using finite element analysis," *Packaging Technology and Science,* vol. 21, pp. 287-296, 2008.
[125] S. Mukherjee, "Virtual Simulation of Top Load Performance of Plastic Bottles," in *ANTEC*, 2010.
[126] B. Graham, K. Guinn, M. Guinn, and C. Young, "Bottle Friction Tester Senior Design Final Report," Oklahoma State University, Tulsa2012.
[127] ASTM, "D638-10 Standard Test Method for Tensile Properties of Plastics," ed. West Conshohocken, PA, USA: ASTM International, 2010.
[128] R. B. Dupaix and M. C. Boyce, "Finite strain behavior of poly(ethylene terephthalate) (PET) and poly(ethylene terephthalate)-glycol (PETG)," *Polymer,* vol. 46, pp. 4827-4838, 2005.
[129] ASTM, "E8/E8M Standard Test Methods for Tension Testing of Metallic Materials," ed. West Conshohocken, PA: ASTM International, 2011.
[130] J. R. Davis, *Tensile Testing*: Asm International, 2004.
[131] wikipedia. (2012, 5/24/2012). Rheology.
[132] E. Tseng, "Rheology Measurements for Niagara Resins," Report2012.
[133] TAInstruments. (2000, 5/20/2012). Thermal Analysis. [Online Resource Presentation].
[134] K. T. Academy, "Blow Molding Process Training Slides," 2012.
[135] T. I. Thermal Support, "DSC Curves Data Analysis," A. Rajakutty, Ed., Personal communication/email ed, 2012.
[136] S. Johnson and P. Bischof, "Color Measurements for OSU," Hunter Labs, Virginia, USA2012.
[137] R. Ahmed, "Wall Thickness Measurements for rPET," A. Rajakutty, Ed., Personal communication/email ed, 2012.
[138] E. Tseng and J. Fuhst, "rPET Top Load Trial Results," A. Rajakutty, Ed., Personal communication/email ed, 2012.
[139] K. Yamazaki, R. Itoh, M. Watanabe, J. Han, and S. Nishiyama, "Applications of structural optimization techniques in light weighting of aluminum beverage can ends," *Journal of Food Engineering,* vol. 81, pp. 341-346, 2007.
[140] D. Ing and E. h. W. Michaeli, "Modelling The Structural Performance of Stretch Blow Molded PET Bottles," in *ANTEC*, 2010.
[141] E. Tseng and B. Barbosa, "Energy Saving Data for rPET," Niagara Bottling LLC. , Report2012.
[142] B. Barbosa, "Energy Measurements for rPET," A. Rajakutty, Ed., Personal communication/email ed, 2012.
[143] N. D. T. R. Center. (2012, 5/27/2012). Toughness. [Electronic Report].

APPENDICES

APPENDIX A: Virgin PET Resins Classification

Table 12: Virgin PET resin classification

Resin Type	Code Name
R1 (0.76 I.V.)	R1
R2 (0.75 I.V.)	R2
R1 (non FRH) (0.82 I.V.)	R3
R1 with FRH	R4
R5 (0.75 I.V.)	R5
R6 (0.8 I.V.)	R6
R2 (non FRH)	R7
R7 (additive)	R8
100% rPET with 4.5% Toner	R9

APPENDIX B: Young's Modulus and Yield Strength Values for PET Resins

The Young's modulus and yield strength values for the 8 different PET resins are tabulated in Table 13.

Table 13: Young's Modulus and yield strength values of PET resins

Resin Type	Young's Modulus (GPa)		Yield Strength (MPa)	
	Avg	Stnd Dev	Avg	Stnd Dev
R3	2.10	0.13	39.50	0.60
R4	2.13	0.09	38.10	0.50
R5	2.26	0.07	40.10	0.20
R2	2.28	0.09	39.20	0.50
50% rPET	2.43	0.15	52.00	0.95
100% rPET	2.49	0.16	52.20	1.86
R1	2.52	0.07	51.40	1.24
R6	2.70	0.15	60.00	1.40

APPENDIX C: Engineering Stress-Strain Curves for different Extension Rates.

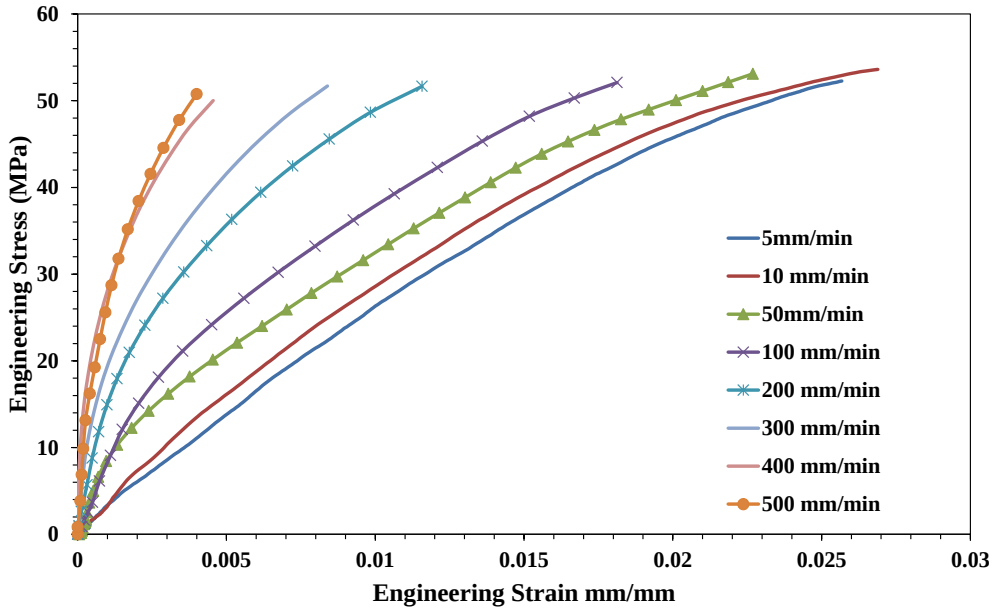

Figure 65: Engineering stress-strain curves for virgin PET R_1 up to stress level of 50 MPa.

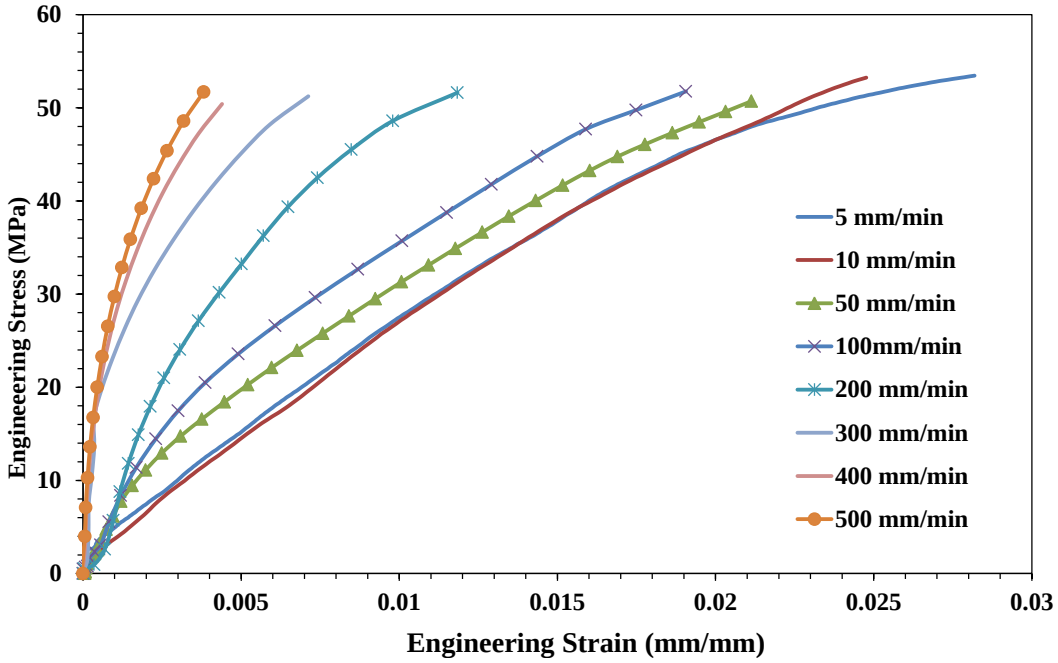

Figure 66: Engineering stress-strain curves for 100% rPET up to stress level of 50 MPa.

Table 14: Efficiency and limits of Instron machine for extension rates

Summary of Efficiency of Extension in INSTRON 5582 Machine for different Extension Rates		
Extension Rate	**Average Extension**	**Standard Deviation**
mm/min	**mm**	**-**
5	5.000	0.000
10	10.008	0.005
50	50.045	0.033
100	101.177	0.149
200	204.739	4.539
300	307.980	6.650
400	406.473	11.150
500	502.800	22.963

APPENDIX D: DSC First Heating Curves for all Preform Samples

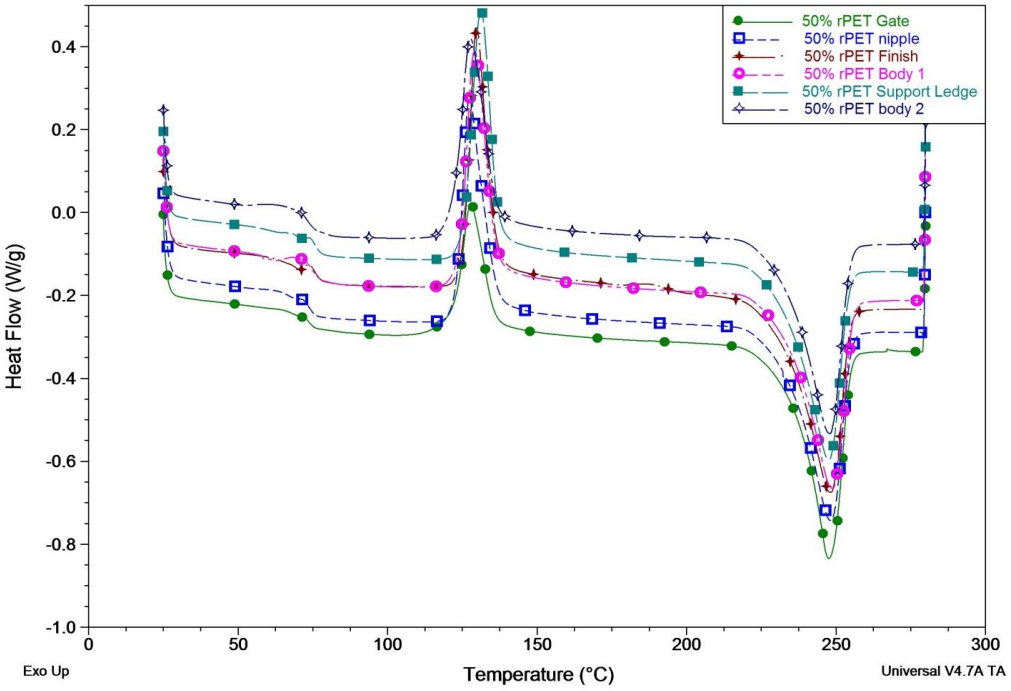

Figure 67: DSC first heating curves for 50% rPET preform samples

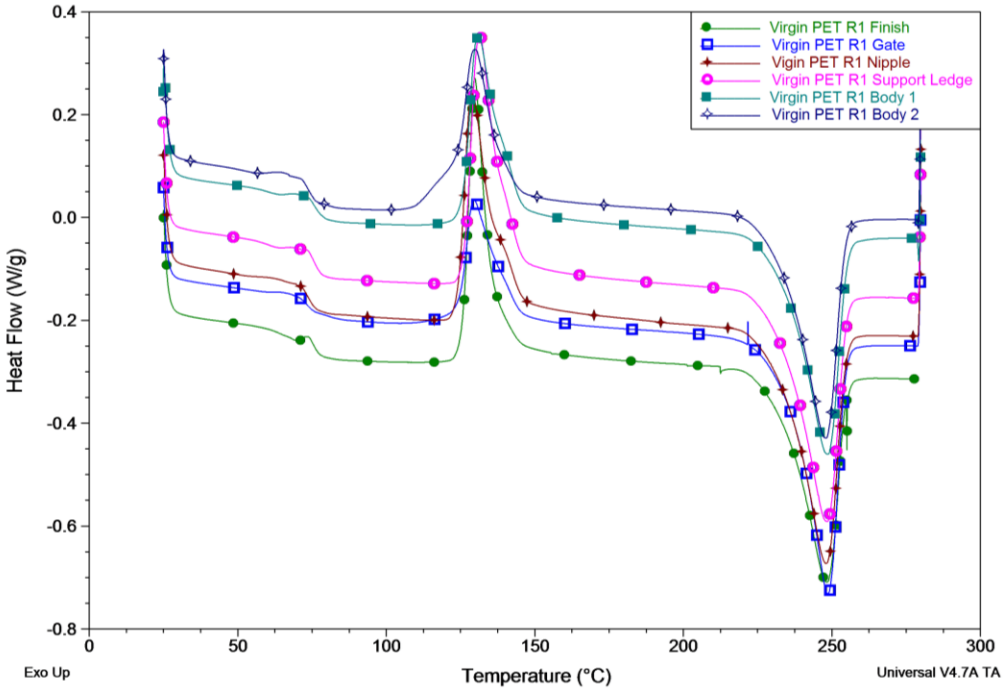

Figure 68: DSC first heating curves for 100% Jade virgin PET preform samples

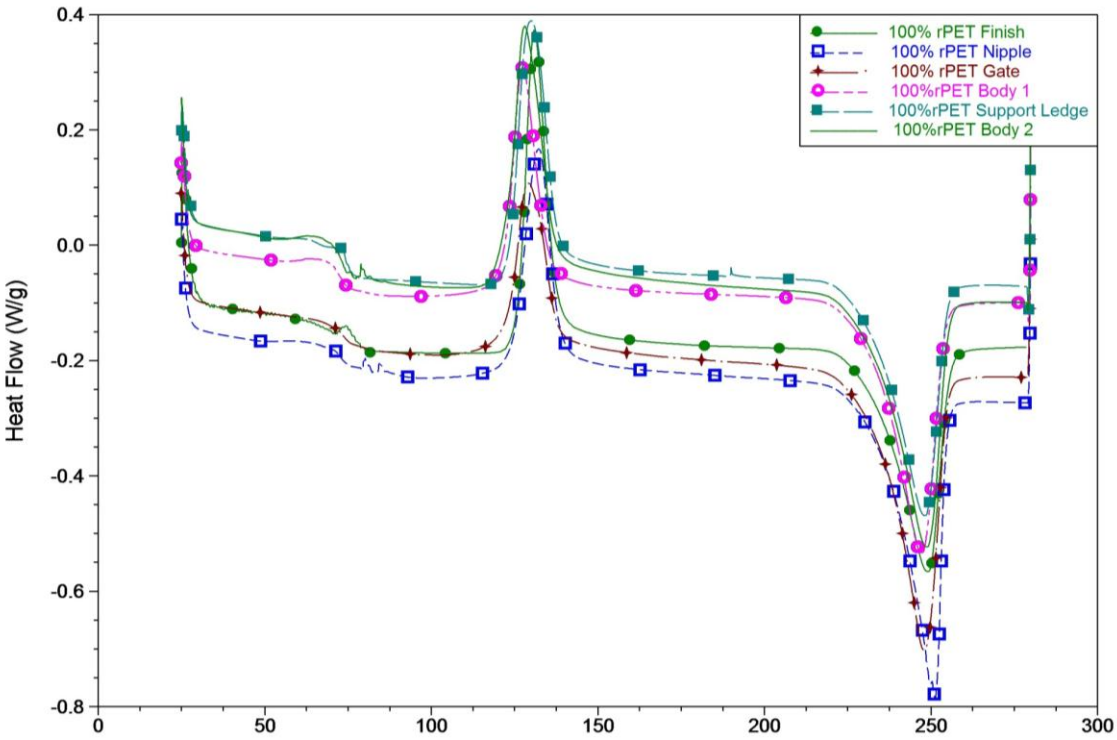

Figure 69: DSC first heating curves for 100%rPET preform samples

APPENDIX E: Melt Viscosity and Molecular Weight Summary

Table 15: Melt viscosity and molecular weight measurements for different resins.[132]

Resin Type	Zeo-shear Viscosity (η_0) (Pa-s)		Molecular Weight (g/mol)	
	Avg	Stnd Dev	Avg	Stnd Dev
R5	332.00	17.00	29234.00	372.00
20% rPET	477.80	3.39	32549.69	68.01
R2	514.00	26.00	33242.00	443.00
100% rPET	558.90	13.15	34084.84	235.93
R1	659.10	1.98	35779.76	31.61
R3	666.00	13.00	35874.00	235.00
R4	733.00	16.00	36902.00	542.00
R6	736.00	12.00	37415.00	704.00

APPENDIX F: Effect of Toner Addition to rPET Preform Samples

Figure 70 shows difference in color for a sample with 100% rPET content and a recycled PET sample with toner added to it.

Figure 70: Color difference in rPET preforms without and with toner

APPENDIX G: Wall Thickness Measurements & FEM Top Load Boundary Conditions

Table 16: Wall thickness measurements for 20%rPET bottle [137]

Height From Top (mm)	Avg Wall Thickness (mm)	Std Dev
25	0.169	0.013
35	0.127	0.009
45	0.112	0.008
55	0.099	0.006
65	0.104	0.008
75	0.107	0.007
85	0.120	0.007
95	0.118	0.006
105	0.109	0.009
115	0.111	0.011
125	0.114	0.011
135	0.114	0.008
145	0.116	0.010
155	0.115	0.012
165	0.118	0.006
175	0.094	0.008
180	0.099	0.008

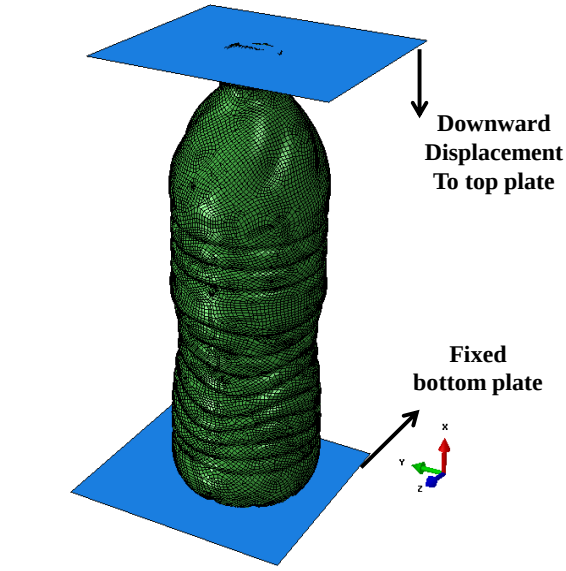

Figure 71: Boundary conditions for Top load simulation.

VITA

ARJUN RAJAKUTTY

Candidate for the Degree of

Master of Science

Thesis: STATIC AND DYNAMIC MECHANICAL PROPERTIES OF AMORPHOUS RECYCLED POLY (ETHYLENE TEREPTHALATE)

Major Field: Mechanical and Aerospace Engineering

Biographical: Born on the 24th of September, 1988 in Secunderabad, Andhra Pradesh, India to Dr. Rajakutty Sadhasivam and Mrs. Malini Rajakutty.

Education: Completed the requirements for the Master of Science Degree in Mechanical and Aerospace Engineering at Oklahoma State University, Stillwater, Oklahoma, July 2012.

Received the Bachelor of Engineering Degree in Mechanical Engineering from Anna University, Chennai, India, May 2010.

Experience: Graduate Research Assistant in Mechanical and Aerospace Engineering Department, Oklahoma State University, May 2011-July 2012.

Graduate Teaching Assistant in Mechanical and Aerospace Engineering Department, Oklahoma State University, August 2010-May 2012.

Mechanical Engineering Project Intern at KRR Engineering Pvt. Ltd., Chennai, India, June 2009-April 2010.

Professional Memberships: American Society of Mechanical Engineers (ASME)
Society of Plastic Engineers (SPE)

Name: Arjun Rajakutty Date of Degree: July, 2012

Institution: Oklahoma State University Location: Stillwater, Oklahoma

Title of Study: STATIC AND DYNAMIC MECHANICAL PROPERTIES OF AMORPHOUS RECYCLED POLY (ETHYLENE TEREPTHALATE)

Pages in Study: 142 Candidate for the Degree of Master of Science

Major Field: Mechanical and Aerospace Engineering

Scope and Method of Study:

Polymers are among the largest used materials today in the world. PET has a significant market share among all the other polymers. More than 90% of plastic bottles made in the world are from PET. With this huge amount of material being used, the impact on the environment in the form of increasing landfills and carbon dioxide emissions has also been high. Hence the need to recycle PET and reuse it has been a topic of interest over the last few years. However, loss in properties of recycled PET (rPET) has been a concern and it is still considered secondary to virgin PET. This work was aimed at studying the mechanical properties of rPET and comparing these properties with those from virgin PET. The dynamic behavior of PET was part of this study. Apart from studying the mechanical properties of rPET, several other tests were performed to study thermal properties, crystallinity, color measurements (yellowing), friction behavior and also to determine structural performance of blow molded bottles. Material properties obtained from experimental results were used as input for Finite Element simulations.

Findings and Conclusions:

The findings and results from this research have provided a framework to understand the mechanical properties of rPET. The method of tensile testing using the custom fixture was an efficient means of determining bulk mechanical properties. rPET was found to have properties similar to virgin PET resins with dynamic measurements showing the greatest differences near 100 mm/min. The dynamic properties with increasing strain rates generally fit power law or exponential curves. DSC measurements along the preform helped to understand the crystallinity distribution and validate the new tensile sample injection method. Strain induced crystallization was also observed. Color measurements provided a good indication of the yellowness index values in rPET and changes in these values on addition of coloring agents. Top load and hoop strength measurements on bottles showed rPET performing similar to virgin PET resins. Using rPET was found to give considerable energy savings. All these results provided encouragement for rPET to be considered for industrial applications on a large scale, and that it will have a positive impact on the environment in the long run.

ADVISER'S APPROVAL: Dr. Jay C. Hanan